2-9-2010

Throughput optimization in MPR-capable multi-hop wireless networks

Jorge Crichigno

Jorge Crichigno
Candidate

Electrical and Computer Engineering
Department

This dissertation is approved, and it is acceptable in quality
and form for publication:

Approved by the Dissertation Committee:

_____ , Chairperson

_____

_____

_____

_____

_____

_____

Throughput Optimization in MPR-Capable Multi-Hop Wireless Networks

by

Jorge Crichigno

B.Sc., Electrical Engineering, Universidad Catolica, Paraguay, 2004

M.Sc., Computer Engineering, University of New Mexico, 2008

DISSERTATION

Submitted in Partial Fulfillment of the

Requirements for the Degree of

Doctor of Philosophy

Engineering

The University of New Mexico

Albuquerque, New Mexico

August, 2009

Dedication

To my mom, for the infinite love she has provided us through our lives; to my dad, my brothers and my sister, for the support and emotional fortitude they provided me during these years.

Acknowledgments

I am fortunate to have been advised by Dr. Wennie Shu. She has been a mentor and the person who has supported me with no reserves at ECE for the last four years. None of this work would have been possible without her expertise on how to approach research problems. She was also responsible for my visit to Shanghai along with Dr. Min-You Wu, where I spent five wonderful months.

My sincere thanks to Dr. Min-You Wu, who supported me in Shanghai and co-advised this work. His wisdom has been a priceless source of knowledge. He has proposed the topic of this dissertation and deserves credits for it.

Special thanks to Dr. Ramiro Jordan for unconditionally supporting us *latinos* at ISTEC Lab and being member of my thesis committee. Many thanks also to Dr. Nasir Ghani for being part of the committee.

I am grateful to Dr. Sudharman Jayaweera for very fruitful discussions on multi-access channels and convex sets. I am also indebted to ECE Professors Marios Pattichis, Chaouki Abdallah, Greg Heileman, Ed Graham, Peter Dorato, and Professor Xinbing Wang from SJTU. Many thanks also to all my friends from ECE at UNM, and from Wireless and Sensor Networks Lab at SJTU.

Special thanks go out to Bel, Jeremy, and Pablo. They opened the door of their house and treated me as a family member.

Finally, thanks dad, Juan, Pipo, and Carla for your emotional fortitude and support during these years. Thanks mom for the infinite love you have provided us through our entire lives.

Acronyms

AS Approximation-based Scheduler

AWGN Additive White Gaussian Noise

CDMA Code Division Multiple Access

DCF Distributed Coordination Function

FDMA Frequency Division Multiple Access

GSI Greedy Scheduler I

GSII Greedy Scheduler II

HD Half-Duplex

IETF Internet Engineering Task Force

ILP Integer Linear Program

JRS Joint Routing and Scheduling algorithms

LP Linear Program

MAC Medium Access Control

MANET Mobile Ad Hoc Network

MMSP Minimum Makespan Scheduling Problem

MPR Multi-Packet Reception

MUD Multi-User Detection

RT-LP Routing Linear Program

RTSCH-LP Routing and Scheduling Linear Program

SIC Successive Interference Cancelation

SINR Signal to Interference Plus Noise Ratio

TDMA Time Division Multiple Access

WMN Wireless Mesh Network

Throughput Optimization in MPR-Capable Multi-Hop Wireless Networks

by

Jorge Crichigno

ABSTRACT OF DISSERTATION

Submitted in Partial Fulfillment of the
Requirements for the Degree of

Doctor of Philosophy

Engineering

The University of New Mexico

Albuquerque, New Mexico

August, 2009

Throughput Optimization in MPR-Capable Multi-Hop Wireless Networks

by

Jorge Crichigno

B.Sc., Electrical Engineering, Universidad Catolica, Paraguay, 2004

M.Sc., Computer Engineering, University of New Mexico, 2008

Ph.D, Computer Engineering, University of New Mexico, 2009

Abstract

Recent advances in the physical layer have enabled the simultaneous reception of multiple packets by a node in wireless networks. This capability has the potential of improving the performance of multi-hop wireless networks by a logarithmic factor with respect to current technologies. However, to fully exploit multiple packet reception (MPR) capability, new routing and scheduling schemes must be designed. These schemes need to reformulate a historically underlying assumption in wireless networks which states that any concurrent transmission of two or more packets results in a collision and failure of all packet receptions. In this work, we present a generalized model for the throughput optimization problem in MPR-capable multi-hop wireless networks. The formulation incorporates not only the MPR protocol model to quantify interference, but also the multi-access channel. The former is related with the MAC and routing layers, and considers a packet as the unit of transmission.

The latter accounts for the achievable capacity of links used by simultaneous packet transmissions. The problem is modeled as a joint routing and scheduling problem. The scheduling subproblem deals with finding the optimal *schedulable sets*, which are defined as subsets of links that can be scheduled or activated simultaneously. Among other results, we demonstrate that any solution of the scheduling subproblem can be built with $|E| + 1$ or fewer schedulable sets, where $|E|$ is the number of links of the network. This result contrasts with a conjecture that states that a solution of the scheduling subproblem, in general, is composed of an exponential number of schedulable sets. The model can be applied to a wide range of networks, such as half and full duplex systems, networks with directional and omni-directional antennas with one or multiple transmit antennas per node. Due to the hardness of the problem, we propose several polynomial time schemes based on a combination of linear programming, approximation algorithm and greedy paradigms. We illustrate the use of the proposed schemes to study the impact of several design parameters such as decoding capability and number of transmit antennas on the performance of MPR-capable networks.

Contents

Contents

Contents

Contents

List of Figures

List of Figures

List of Figures

Chapter 1

Introduction

1.1 Wireless Networks

A wireless network consists of *wireless nodes* and *wireless links*. A wireless node, or simply node in the context of this work, is equipped with one or more wireless interfaces. A wireless link from a node u to a node v exists if node v can correctly receive packets from node u.

A special type of wireless network, which is self-organized and configured, and can operate without the support of any infrastructure, is known as an ad hoc wireless network. In the last years, there has been a tremendous interest in ad hoc wireless networks, driven by their potential, by new advances at the physical layer, by the low cost of the wireless devices, and by their robustness [1].

Generally, ad hoc networks are multi-hop networks; a node can operate not only as a source of data but also as a router, forwarding packets on behalf of other nodes that may not be within direct wireless transmission range of their destinations. Certainly, the absent of central coordinator or base station may require more complex routing
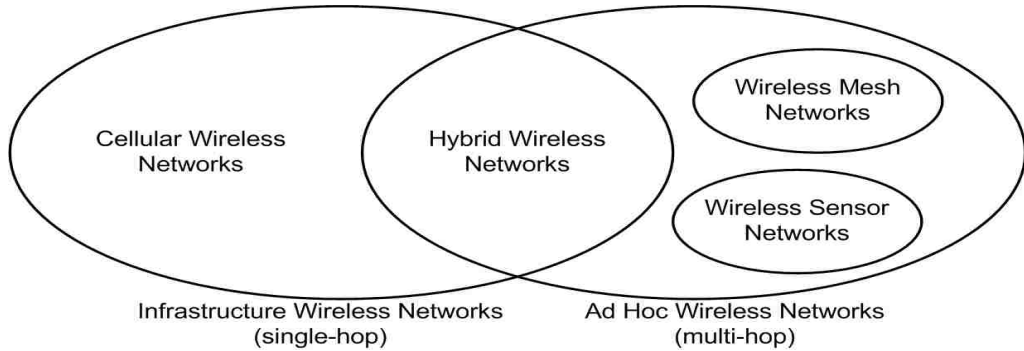
Figure 1.1: Classification of wireless networks.

and scheduling schemes with respect to *cellular networks*. However, this is also the main advantage of ad hoc networks, since there is no central point of failure [2].

A broad but typical classification of ad hoc networks is illustrated in Figure 1.1. They are further divided in more than one type of network, including wireless sensor networks and *wireless mesh networks* (WMNs). The former is composed of a large number of sensor nodes that are densely deployed in a specific area of interest. Nodes are generally limited in processing capability, and subject to power constraints. Additionally, nodes may have mobility, and the size of the network can be much larger than other types of ad hoc networks [1].

On the other hand, nodes in WMNs are mostly static, have no power constraint and more data processing capability. Nodes serve as routers and provide to final users (clients) access to other networks such as the Internet. Each node has a point-to-point and point-to-multipoint connectivity with other nodes (thereby forming a mesh). Features such as self-establishment and maintenances of the mesh connectivity brings many advantages including low up-front cost and reliable service coverage. In this work, we will mainly focus on wireless mesh networks, i.e., networks where nodes have power processing capability, no power consumption restriction, may decode multiple packets at a time, and may be endowed with multiple transmit antennas.

Thus, when referring to wireless networks, we will actually refer to networks with these characteristics.

A fundamental issue in wireless networks is that performance degrades sharply as the number of hops traversed increases. For example, in a network of nodes with identical and omnidirectional transmission ranges, going from a single hop to two hops away halves the throughput of a flow, because wireless interference dictates that only one of the two hops can be active at a time. The seminal work by Gupta et al. [3] formalized this observation, and showed that the throughput capacity of random wireless ad hoc networks is $\Theta\left(\frac{1}{\sqrt{|V|\log|V|}}\right)$, where $|\cdot|$ denotes cardinality and V is the set of nodes of the network. The reason of this result is the fact that transmitting nodes exclusively consume spatial resource, which is proportional to the area involving the transmission. Nodes close to the intended receiver require to be idle to avoid collisions, which cause the loss of packets.

To overcome the spatial limitation, possible approaches include: (i) the increment of the amount of information a transmitting node relays in each transmission; (ii) the reduction of interference through directional transmissions; (iii) the increment of reception capability, so that a receiver can decode multiple concurrent transmissions within its receiver range. The latter permits the reception of multiple packets simultaneously through the use of *multi-user detection* (MUD) techniques at the physical layer. Work has been carried out in the three fronts. Liu et al. [4] showed that the first approach does not increase the throughput capacity order. Similarly, Yi [5] et al. demonstrated that directional antennas improve the throughput by a constant factor with respect to the work by Gupta et al. [3]. Finally, Garcia-Luna-Aceves et al. [6] demonstrated that the increment of reception capability is the more appealing approach, since the throughput capacity can be increased by a logarithmic factor with respect to the work in [3]. However, the little research currently done is this area has mostly focused on theoretical work to find asymptotic bounds on

the throughput capacity. Furthermore, the combination of directional antennas and *multi-packet reception* (MPR) has not been addressed yet.

From the above, it is clear that using MPR is an attractive approach for making wireless networks scale. However, as promising as the above theoretical recent results on the use of multi-packet reception are, there is much work to be done before MPR-capable networks can be reduced to practice. The transmissions that are to be decoded at a receiver node need to be sent synchronously, and the number of concurrent transmissions allowed around a receiver cannot exceed the number of concurrent transmissions that the receiver can decode, which may be smaller than the number of neighbors near the receiver if the network is densely connected. Furthermore, the protocols used to date in ad hoc networks have been designed to avoid multi-access, and are derivatives of protocols and architectures originally designed for wired networks based on point-to-point links. For example, the IEEE 802.11 *Distributed Coordination Function* (DCF) adopts a similar back-off strategy to Ethernet when more than one transmission occurs around a receiver [7]. Similarly, the IETF MANET routing protocols work independently of the channel access method, even though it is not true that routing in ad hoc networks occurs over a pre-existing network topology and the transmission over one link does not impact the transmissions over other links, as it can be done in a wired network [8].

Motivated by the potential of multi-packet reception, this work presents a generalized model for the throughput optimization problem in MPR-capable multi-hop wireless networks. The formulation incorporates not only the MPR protocol model [6] to quantify interference, but also the multi-access channel model [9]. The former models wireless interference from MAC and routing layer perspectives, and considers a packet as the unit of transmission. The latter accurately accounts for the physical layer rates in bits per second used by simultaneous transmissions. The problem is modeled as a joint routing and scheduling problem. The scheduling subproblem deals

with finding the optimal *schedulable sets*, which are defined as subsets of links that can be scheduled or activated simultaneously. Among other results, we demonstrate that any solution of the scheduling subproblem can be built with $|E| + 1$ or fewer schedulable sets, where $|E|$ is the number of links of the network. This result contrasts with a conjecture that states that a solution of the scheduling subproblem, in general, is composed of an exponential number of schedulable sets [10]. The model can be applied to a wide range of networks, such as half and full duplex systems, networks with directional and omni-directional antennas with one or multiple transmit antennas per node. Due to the hardness of the problem, we propose several polynomial time schemes based on combinations of linear programming, approximation algorithms and greedy paradigms, which are referred as *Joint Routing and Scheduling* (JRS) algorithms. We illustrate the use of the proposed schemes to study the impact of several design parameters such as decoding capability and number of transmit antennas on the performance of MPR-capable networks, and the relation of them with topological network properties.

1.2   Goals and Contribution

In this dissertation, we introduce a novel model for throughput optimization in multi-hop wireless networks with MPR-capability. The model incorporate several features not included in previous works, such as the use of directional antennas and multi-access channel. In summary, the dissertation includes the following contributions:

1. Provide a novel model for the throughput optimization problem in MPR networks. The formulation incorporates not only the MPR protocol model to quantify interference, but also the multi-access channel. To the best of our knowledge, the application of multi-access channel in an MPR-capable network has not been previously considered.

2. Characterize the throughput optimization in multi-hop wireless as a convex optimization problem. The advantages of casting the problem as a convex optimization include the application of well-known techniques and theorems for this kind of problem.

3. As a main result from item 2, we demonstrate that any solution of the scheduling subproblem can be built with $|E| + 1$ or fewer schedulable sets, which contradicts previous work. This theoretical result is valid for single-hop and multi-hop networks, with directional and omnidirectional antennas, with multi-packet and single-packet reception.

4. Provide efficient schemes to solve the proposed optimization model. By efficient schemes we mean polynomial time optimization schemes, since the throughput optimization problem under any model of interference is known to be NP-hard [10].

5. Study the fundamental limitations of MPR networks, and how to overcome those eventual limitations.

6. Study the impact of directional antennas in MPR networks. There is no previous work considering the use of directional antennas with multi-packet reception. A reason may be the fact that MPR capability, intuitively, mitigates the inefficient spatial reuse of omni-directional antennas. However, the impact of directional antennas in MPR networks is a very important open research issue, which is analyzed in this work.

7. Study the use of multiple transmit interfaces. Previous work attempted to improve the throughput in MPR network by increasing the MPR capability *only*, assuming a single half-duplex interface and neglecting the potential benefits of multiple interfaces.

1.3 Organization

The present chapter presented an overview and motivation of the research work, and exposed the goals and novel contributions of this doctoral dissertation. Chapter 2 presents background information about wireless networks, models of interference and radiation patterns, and convex optimization. Chapter 3 provides a literature survey on previous work regarding throughput optimization in wireless networks. Chapter 4 presents a mathematical generalized model for the throughput optimization problem in multi-hop wireless networks that support multi-packet reception capability. The problem is further characterized as a convex optimization, and some important theorems are derived from this model. Chapter 5 presents the JRS schemes to solve the joint routing and scheduling problem in MPR-capable wireless networks. The schemes decouple the problem into two subproblems: routing and scheduling. The routing subproblem is solved by using linear programming. For the scheduling subproblem, multiple algorithms based on greedy heuristic and approximation algorithm paradigms are presented. Chapter 6 shows performance studies of numerical examples, and Chapter 7 concludes the dissertation and discusses future work.

Chapter 2

Background

This chapter is not intended to provide a comprehensive exposition of background topics needed for this work, but a review of concepts which will be extensively used in next chapters. The chapter is organized as follows: Section 2.1 presents the fundamental properties of antennas for wireless networks. Section 2.2 provides an overview of the classical models of interference for single packet reception, namely, protocol model, physical model and generalized physical model. Section 2.3 presents the models of interference used in MPR-capable networks, which include the MPR protocol model and the multi-access channel model. Section 2.4 introduces the conflict graph, a graph theoretic approach to model interference. Finally, Section 2.5 presents main concepts of convex analysis, which are used in Chapter 4 to characterize the throughput optimization problem.

From here on, we represent a wireless network as a graph $G = (V, E)$, where V is the set of nodes and E the set of links. Let r_{ij} be the distance between two nodes i and j. There exists a link $e = (i, j) \in E$ from node $i \in V$ to node $j \in V$ if $r_{ij} \leq R$, where R is the receiver range. For an active link (i, j), we say that node i transmits to node j. The capacity of link (i, j) (i.e., the rate at which node i transmits to node

j) will be denoted as c_{ij}. Let $S \in E$ be a set of links simultaneously activated at a time. If c_{ij} is affected by such set, we will denote the capacity of the link (i, j) as $c_{ij}(S)$. We will use the notations (i, j) and e in an interchangeable manner.

2.1 Antenna Models

2.1.1 Fundamental Properties of Antennas

Antenna Gain

The antenna radiates the time-averaged power in all directions. The gain of an antenna is defined as

$$G(\theta, \phi) = \varepsilon \frac{U(\theta, \phi)}{U_{avg}}, \tag{2.1}$$

where $U(\theta, \phi)$ is the power density in direction (θ, ϕ), U_{avg} is the average power density over all directions and ε is the efficiency of the antenna. $U(\theta, \phi)$ is a function of the space coordinates, with θ and ϕ being the elevation and azimuth angles. If the antenna transmits power equally in all directions, then $U(\theta, \phi)$ will be equal to U_{avg}, and the antenna is called *isotropic* or *omnidirectional*. An isotropic antenna has a spherical pattern. If no direction is specified, the gain usually means the maximum gain value over all directions. Due to reciprocity, the gain and radiation pattern characteristics are the same for both transmission and reception [11].

Radiation Pattern and Beamwidth

An antenna pattern is the specification of the gain values in each direction in space, described as projections on the elevation and azimuth planes. It typically has a

main lobe of peak gain and *side lobes* of smaller gains, which affect the normal transmission. In most cases, the more directional the antenna is, the higher the gain and the smaller the *beamwidth* will be. The beamwidth of an antenna is a measure of the angle that contains two points on the patterns with a 3 dB power on the main lobe. Gain and beamwidth are related. Typically, the more directional the antenna is, the higher the gain and the smaller the beamwidth are. However, two antennas with the same gain could have different beamwidths. In general, radiation patterns may be very complex for networking analysis purposes. In order to simply and to make the analysis more tractable, two models are commonly used: flat-top and cone+sphere radiation patterns [12].

1. Flat-top

   This model assumes that the gain is constant within the beamwidth and there are no side lobes. The antenna beam can be seen as a slice of a pie in shape. For throughput analysis purposes, the assumption that nodes lie in a two-dimension plane is used, so that the gain of the antenna is a function of the azimuth angle only. Based on this model, a flap-top radiation pattern example is shown in Figure 2.1 (a), where β is the beamwidth of the antenna. Although this model simplifies the radiation pattern, the sidelobes are generally small enough. Moreover, the gain of the main lobe of typical directional antennas is more than 100 times the gain of sidelobes. Additionally, smart antennas often have null capability that mitigates the sidelobes and backlobes. The interference region of an antenna is principally determined by its main lobe and simplifying the radiation pattern does not lead to a fundamental change on the result of the throughput analysis [5].

2. Cone+sphere

   In this model, the main lobe is also represented as a cone of uniform gain. In addition, sidelobes are aggregated to a single *bulb* at the base of the cone with a
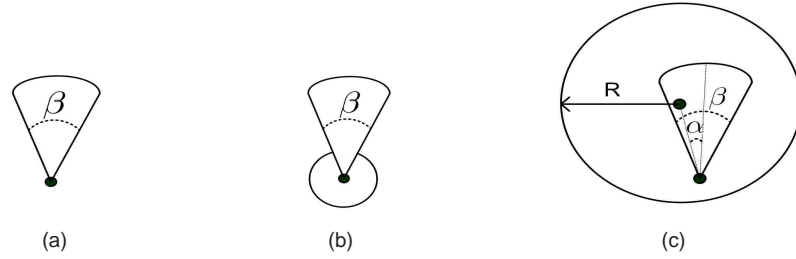
Figure 2.1: (a) Flap-top and (b) cone+sphere radiation patterns. (c) MPR flap-top model.

smaller gain than the mainlobe. Figure 2.1 (b) shows the cone+sphere model.

Figure 2.1 (c) shows the *MPR Flap-top*, which is derived from the flap-top radiation pattern model and the MPR protocol model. As we shall see, this interference model states that a reception of *all transmissions* is achievable if the the number of simultaneous transmissions in the receiver range R is less than or equal to K, where K is the *decoding capability*. The model of Figure 2.1 (c) also includes the angle α, which is defined as the angle between the the axis of the main lobe of the transmit antenna and the direction of an arbitrary node which we would like to analyze.

To account for the case where a node transmits to multiple receivers at the same time through multiple antennas [13], we will denote the number of transmit antennas as M.

Let $S \subseteq E$ be a *schedulable set* (the formal definition of a schedulable set will be given in Section 4.2.2) consisting of links which are scheduled at a time. Thus, if

$$\mathcal{R}_i = \{j | (i, j) \in S\} \qquad (2.2)$$

denotes the set of nodes receiving from node i, then we will require that $|\mathcal{R}_i| \leq M$.

2.1.2 Transmission and Reception Modes

Every antenna has four transmission and reception modes: omnidirectional transmission, omnidirectional reception, directional transmission and directional reception. If a receiver listens in directional mode, the maximum reception gain will be reached. Similarly, if a sender transmits in directional mode, the maximum transmission gain will be reached. Thus, when a receiver listens in directional mode and a transmitter sends data also in directional mode, according to the path loss model, the required transmit power can be further reduced. Moreover, in that case, the communication range can be maximized and the interferences minimized, which leads to an increased wireless network capacity. However, depending on the directivity of the beams, scheduling antenna beams to face each other at the same time is still challenging [12].

2.2 Wireless Models of Interference for Single Packet Reception

An interference model describes the conditions for a successful reception of a packet over a wireless channel. The basic models described in the seminal work Gupta and Kumar [3] are known as *protocol* and *physical* models. More complex models such as *MPR protocol* can be derived from them. These models are discussed in this section.

2.2.1 Protocol Model

Assume nodes transmit omni-directionally. Let r_{ij} be the distance between nodes i and j. A (direct) communication from node i to node j is successful if

$$r_{i'j} \geq (1 + \Delta)r_{ij} \tag{2.3}$$

for every other node i' simultaneously transmitting over the channel. Once Equation (2.3) is satisfied, it is assumed that the data rate over the link is constant (fixed) and greater than zero. The quantity $\Delta \geq 0$ is a parameter that depends on the characteristic of the physical layer. It models situations where a guard zone is specified by the protocol to prevent a neighboring node from transmitting on the same channel at the same time. It also allows for imprecision in the achieved range of transmissions. The protocol model inherently implies that disk areas centered at concurrent receivers are disjoint.

A common assumption is the fact that nodes are homogeneous, i.e., all transmissions employ the same transmission power, which leads to definition of the *transmission range*. Under the assumption of homogeneous transmission power, the transmission range R_{tx} is defined as the maximum distance from which a receiver node can successfully receive a packet.

Based on the definition of transmission range and assuming that all nodes employ the same transmission power, the conditions for successful transmission under the protocol model can be restated as follows. A transmission from node i to node j is successful if:

$$r_{ij} \leq R_{tx}, \tag{2.4}$$
$$r_{i'j} \geq (1 + \Delta)R_{tx}, \tag{2.5}$$

for every other node i' simultaneously transmitting over the same channel. When referring to the protocol model, we will refer to the model under the homogeneous transmission range assumption, unless otherwise is explicitly specified.

2.2.2 Physical Model

Assume nodes transmit omni-directionally. Let $\{i'|i' \in T\}$ be the subset of nodes simultaneously transmitting over a common *Additive White Gaussian Noise* (AWGN) channel, with zero mean Gaussian noise and variance η. Let P_{ij} be the power level of the signal received at node j from node i. Then, the transmission from node $i \in T$ is successfully received by node j if:

$$\frac{P_{ij}}{\eta + \sum_{\forall i' \in T; i' \neq i} P_{i'j}} \geq \delta. \tag{2.6}$$

Once this constraint is satisfied, it is assumed that the data rate over the link is constant (fixed) and greater than zero. Equation (2.6) models a situation where a minimum *signal to interference plus noise ratio* (SINR) of δ is necessary for successful receptions, when a set T of nodes simultaneously transmit. In radio transmissions, a signal power transmitted from node i to node j is reduced in proportion to the distance between them:

$$P_{ij} = \zeta \cdot r_{ij}^{-\gamma}. \tag{2.7}$$

Equation (2.7) states that the signal power decays exponentially according to the distance r_{ij} between nodes i and j. ζ and γ depend on the path loss model. The latter is known as *pass loss exponent*, while the former is the term accounting for other factors such as the gain of transmitter and receiver antennas.

2.2.3   Generalized Physical Model

The physical model assumes that a transmission can only occur at a constant (fixed) rate if Equation (2.2.2) is satisfied. Based on the Shannon's formula for AWGN channel, the data rate of the physical model can be generalized as follows:

$$
c_{ij} = W \log_2 \left(1 + \frac{P_{ij}}{\eta + \sum_{\forall i' \in T; i' \neq i} P_{i'j}} \right),
\tag{2.8}
$$

where W is the bandwidth of the channel in Hertz. To achieve this data rate, however, nodes must adapt the modulation or coding scheme dynamically according to current SINR, a fact that entails complex coordination between the nodes.

2.3   Wireless Models of Interference for MPR-capable Networks

The protocol and physical models do not model wireless networks where nodes are endowed with technologies such as CDMA transceivers and/or multiple antennas. In these networks, nodes may be capable of receiving multiple packets simultaneously, and there may be unexpected reception errors due to channel time variation. In this section, we present two models of interference for MPR-capable networks: MPR protocol Model [6] and multi-access channel [9]. The former is more related with the MAC and routing layers, and considers a packet as the unit of transmission. The latter accurately accounts for the physical layer rates in bits per second used by simultaneous transmissions.

2.3.1   MPR Protocol Model

Ghez et al. [14] proposed a model where a node can correctly receive a fraction of the number of transmissions from nodes located inside its receiver range R. The reception probabilities of a node b are specified by its receiver matrix H_b. The entry $h_{i,j}$ of H_b is given by:

$$
\begin{aligned}
h_{i,j} \;\; = \;\; & \mathrm{Pr}\{\, j \text{ packets are correctly received} \mid i \text{ packets} \\
& \text{are transmitted by nodes within a radius } R \\
& \text{from node } b\},
\end{aligned}
$$

where $i \geq 1$ and $j \geq 0$. The MPR matrix H_b at receiver node b is then defined as:

$$
H_b = \begin{pmatrix}
h_{1,0} & h_{1,1} & 0 & \ldots & & 0 \\
h_{2,0} & h_{2,1} & h_{2,2} & 0 & \ldots & 0 \\
\vdots & \vdots & \vdots & \ddots & &
\end{pmatrix}. \tag{2.9}
$$

A variety of physical layers has been modeled using MPR, including the MPR protocol model proposed by Garcia-Luna-Aceves et al. [6]. In this model, a node can simultaneously decode up to K packets sent inside its receiver range R; if more than K packets are transmitted, then none of them can be correctly received. Thus, K denotes the decoding capability of a receiver node. The entries of the receiver matrix H_b are then given by:

$$
h_{i,j} = \begin{cases}
1 & ;\, i \leq K \text{ and } j = i \\
1 & ;\, j = 0 \text{ and } i > K \\
0 & ;\, \text{otherwise.}
\end{cases} \tag{2.10}
$$
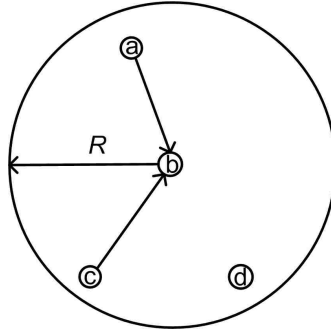
Figure 2.2: Simultaneous transmissions to node b.

Example 2.1. Consider the receiver node b shown in Figure 2.2 and assume a decoding capability of $K = 2$. The channel matrix of node b is then given by:

$$H_b = \begin{pmatrix} 0 & 1 & 0 & \dots & & 0 \\ 0 & 0 & 1 & 0 & \dots & 0 \\ 1 & 0 & \dots & & & \\ \vdots & \vdots & \ddots & & & \\ 1 & 0 & \dots & & & 0 \end{pmatrix}. \tag{2.11}$$

The channel matrix states that node b can simultaneously decode packets from two nodes, say nodes a and c. However, if node d attempts to simultaneously transmit while a and c are active, then none of the packets can be received, since $h_{3,0} = 1$.

The MPR protocol model can be considered as a simplified model of the multi-access channel [9], which describes a system where multiple senders can simultaneously transmit to a single receiver. Although the problem of finding the capacity region of a single multi-access channel was already solved, its application in a multi-hop networking context is very complex, since the overall network should be modeled as multiple multi-access channels. The complexity arises because a single multi-access channel affects the capacity region of the remaining multi-access channels. Moreover, for each multi-access channel, the number of inequalities to be satisfied is exponential

in K, the decoding capability. For these reasons, the MPR protocol model simply assumes an homogeneous capacity value to any link [6, 15, 16, 17, 18] (e.g., a unit link capacity [16]).

In this work, we use a more general approach. Assume nodes transmit directionally according to the MPR flap-top model presented in Section 2.1 and illustrated in Figure 2.1(c). Assume also an AWGN channel with bandwidth W, where the capacity of a link (i, j) is modeled by the following two equations:

$$SINR_{ij} = \begin{cases} \zeta \cdot r_{ij}^{-\gamma} & \text{if } \frac{-\beta}{2} \leq \alpha_{ij} \leq \frac{\beta}{2} \\ 0 & \text{otherwise,} \end{cases} \tag{2.12}$$

$$c_{ij} = W \log_2(1 + SINR_{ij}). \tag{2.13}$$

Equation (2.12) states that the signal to interference plus noise ratio ($SINR_{ij}$) decays exponentially according to the distance r_{ij} between nodes i and j, and it is zero if receiver node j is outside of the main lobe of the radiation pattern of the transmit antenna. For a graphical interpretation of the angle α_{ij}, please refer to Figure 2.1(c). As explained in Equation (2.7), γ is the path loss exponent, and ζ is a term that depends on multiple factors such as path loss model and decoding technology. In a point-to-point model where all transmitters transmit at the same power P, this term is computed as:

$$\zeta = \frac{P}{\eta + \sum_{i' \neq i} P r_{i'j}^{-\gamma}}, \tag{2.14}$$

where η is the variance of the AWGN channel, and the sum is over all node $i' \neq i$ transmitting simultaneously with node i, such that $\frac{-\beta}{2} \leq \alpha_{i'j} \leq \frac{\beta}{2}$. In multi-access channels, Equation (2.14) does not necessarily hold, since technologies such as *Code Division Multiple Access* (CDMA) and *Successive Interference Cancelation* (SIC) permit to achieve improved values of ζ [9]. Equation (2.13) is the Shannon capacity. A similar capacity model is frequently used for omni-directional antennas

[19]. Equations (2.12) and (2.13) model the case where shorter transmission distance implies higher link capacity [19], and the capacity follows a logarithmic dependence on $SINR$. In the MPR protocol model, ζ is an opaque *fixed value*, which can be computed as desired. As a consequence, the capacity of link (i, j) is constant, independently of the links simultaneously activated with link (i, j) [6, 16]. On the other hand, in the multi-access channel model, this value is accurately computed, as we shall see in next section.

The MPR protocol model given by Equation (2.10) has been the most widely used model for MPR-capable networks. We will use it in Chapter 4 to model multi-hop wireless networks with MPR capability.

2.3.2   Multi-Access Channel

Denote P_0 as the uniform fixed power level used for any transmission. For an active link (i, j), the received power P_{ij} at node j decays exponentially with r_{ij}:

$$P_{ij} = P_0 r_{ij}^{-\gamma}, \tag{2.15}$$

where γ is the path loss exponent. This equation is similar to Equation (2.7) and follows the same path loss model.

Consider the following scenario: let $S \subseteq E$ be a schedulable set consisting of links simultaneously activated, and $\mathcal{T}_j$ be the set of nodes transmitting to a receiver node j:

$$\mathcal{T}_j = \{i | (i, j) \in S\}. \tag{2.16}$$

Similarly, let Ψ_j be the set of simultaneous transmitters interfering with node j, which point out their transmit antenna such that node j lies inside the main lobe of

them:

$$\Psi_j = \left\{ i' | (i', j') \in S, j \neq j', \text{ and } \tfrac{-\beta}{2} \leq \alpha_{i'j} \leq \tfrac{\beta}{2} \right\}. \tag{2.17}$$

Then, assuming an AWGN channel, the total noise at receiver node j is:

$$\eta_j = \eta + \sum_{i' \in \Psi_j} P_{i'j}, \tag{2.18}$$

where η is the variance of the channel noise. η_j is referred as *destructive interference* [20]. We define the channel capacity function of a single user of an AWGN channel with bandwidth W and signal to interference plus noise ratio $SINR$ as:

$$\varphi(SINR) = W \log_2(1 + SINR). \tag{2.19}$$

Let $c_{ij}(S)$ be the capacity in bits per second (bps) of a link $(i, j) \in S$, when all links in S are activated. For receiver node j, the capacity region of the multi-access channel is the closure of the convex hull of link capacity vectors satisfying:

$$\sum_{i \in T} c_{ij}(S) \ \leq \ \varphi\left(\frac{\sum_{i \in T} P_{ij}}{\eta_j} \right), \tag{2.20}$$

for all $T \subseteq \mathcal{T}_j$ [9]. The region given by Equation (2.20) is characterized by $2^{|\mathcal{T}_j|} - 1$ constraints, each corresponding to a nonempty subset of transmitters. The capacity region has precisely $|\mathcal{T}_j|!$ vertices in the positive quadrant, each achievable by SIC using one of the $|\mathcal{T}_j|!$ possible orderings. The following example illustrates the case for $|\mathcal{T}_j| = 2$.

Example 2.2. Consider the scenario in Figure 2.3(a), where the schedulable set $S = \{(a, b), (c, b), (e, d), (f, d)\}$, nodes a and c transmit to node b ($\mathcal{T}_b = \{a, c\}$), and
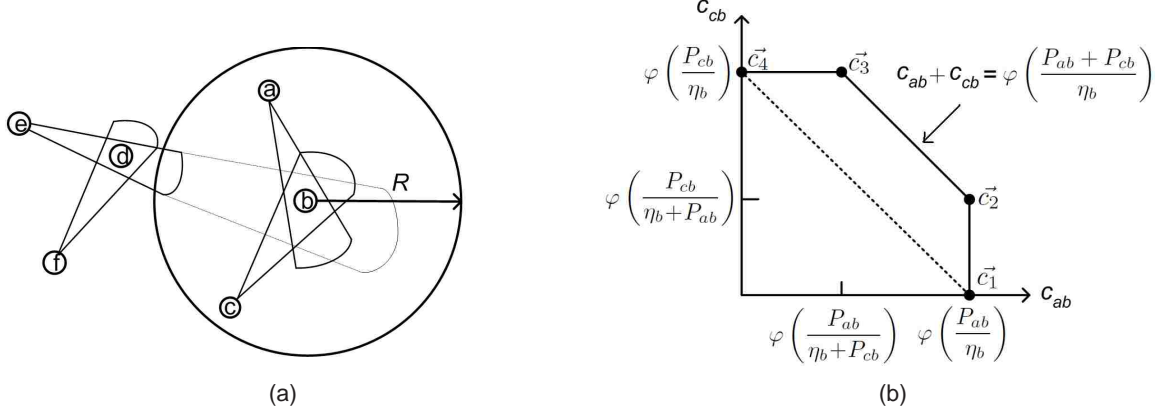
Figure 2.3: (a)Nodes a and c simultaneously transmit to node b, while node e interferers with node b. (b) Corresponding capacity region. For the multi-access channel model, the capacity region is upper bounded by the solid lines. For the single user channel model, the capacity region is upper bounded by the dashed line, which is achieved by using time-sharing.

node e interferers with node b ($\Psi_b = \{e\}$ and $\eta_b = \eta + P_{eb}$). The capacity region for node b is reduced to the following 3 constraints and shown in Figure 2.3(b):

$$
\begin{aligned}
c_{ab}(S) &\leq \varphi\left(\frac{P_{ab}}{\eta_b}\right), \\
c_{cb}(S) &\leq \varphi\left(\frac{P_{cb}}{\eta_b}\right), \\
c_{ab}(S) + c_{cb}(S) &\leq \varphi\left(\frac{P_{ab} + P_{cb}}{\eta_b}\right).
\end{aligned}
$$

The vertices in the positive quadrant are labeled with vector notations, $\vec{c}_i = (c_{ab}(S), c_{cb}(S)), i \in \{1, ..., 4\}$. The aggregate capacity, $c_{ab}(S) + c_{cb}(S)$, is maximized when a link capacity vector lies in the segment line between $\vec{c}_2$ and $\vec{c}_3$. The points $\vec{c}_2$ and $\vec{c}_3$ can be achieved by using SIC and CDMA. For example, $\vec{c}_2$ can be obtained in a two-stage SIC decoding process. In the first stage, node b decodes packet p_1 from node c, considering the transmission from node a as part of noise. Therefore, the link capacity can be $\varphi\left(\frac{P_{cb}}{\eta_b + P_{ab}}\right)$. In the second stage, after packet p_1 has been decoded, it

can be subtracted out, thereafter packet p_2 from node a can be decoded. Thus, the link capacity can be $\varphi\left(\frac{P_{ab}}{\eta_b}\right)$. The packets are sent using different codes (CDMA). In general, the capacity region achieved with CDMA and SIC is larger than that achieved with TDMA, which is bounded by the dashed line in Figure 2.3(b) [9].

For a general number of transmitters, the points in the capacity region that maximize the sum of the capacity of the links are defined as follows.

Definition 2.1 *Max-capacity operation. Let* $\mathcal{T}_j = \{i_1, i_2, ..., i_{|\mathcal{T}_j|}\}$ *be a set of nodes transmitting to a receiver node j. The corresponding links* $(i_1, j), (i_2, j), ..., (i_{|\mathcal{T}_j|}, j)$ *are said to operate at max-capacity if* $\sum_{i_h \in \mathcal{T}_j} c_{i_h j} = \varphi\left(\frac{\sum_{i_h \in \mathcal{T}_j} P_{i_h j}}{\eta_j}\right).$

To maximize the throughput of a network and fully exploit the multi-access channel, any strategy should try to schedule links such that they operate at max-capacity. At the same time, increasing the number of transmitters clearly increases throughput. However, in practice, a receiver node can decode only a finite number of packets [6, 15]. Complexity and energy consumed by decoders are main limitations that restrict the decoding capability. To account for these limitations, interference models for MPR-capable networks [6] restrict the number of transmissions inside the disk of radio R centered at a receiver node j (independently of whether transmissions are intended for node j or not) to a certain value K. Mathematically, this requirement is given by Equation (2.22):

$$\mathcal{T}_j' \;=\; \mathcal{T}_j \cup \{i | i \in \Psi_j \text{ and } r_{ij} \leq R\}, \tag{2.21}$$
$$|\mathcal{T}_j'| \;\leq\; K. \tag{2.22}$$

To be consistent with practical issues and previous works [6, 15, 16, 21], we will assume that Equation (2.22) is satisfied for a receiver node j to successfully decode packets. We will refer to K as the decoding capability. For analysis purposes, this value will be parameterized as needed.
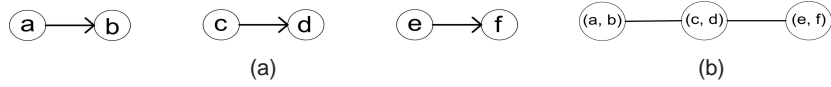
Figure 2.4: (a)A wireless network. Links (a, b) and (c, d) contend with each other, as well as (c, d) and (e, f). (b) The corresponding conflict graph.

2.4   Conflict Graph

The conflict graph [10], also known as contention graph, permits to capture the interaction among wireless links by using graph-theoretic concepts. The conflict graph is a graph $G_c = (V_c, E_c)$, where a vertex $v_{ij} \in V_c$ corresponds to a wireless link of the network topology. There exists an edge between two vertices if the transmissions along these two links conflict with each other according to the protocol model (i.e., they cannot be activated or scheduled simultaneously). We associate the terms node and link with the network topology graph, and the terms vertex and edge with the conflict graph. Thus, an edge between two vertices in the conflict graph is drawn if Equation (2.5) does not hold when the corresponding links are active at the same time (i.e., for two directed links denoted as (i, j) and (p, q), $r_{iq} < (1 + \Delta)R$ or $r_{pj} < (1 + \Delta)R$). Figure 2.4 illustrates the use of conflict graph for a network with three links. Assuming that links (a, b) and (c, d) contend with each other, as well as (c, d) and (e, f), the corresponding conflict graph is shown in Figure 2.4 (b). The edge between vertices (in the conflict graph) (a, b) and (c, d) indicates that they cannot be scheduled simultaneously. A similar relation holds for vertices (c, d) and (e, f).

2.5 Convex Sets and Convex Combinations

2.5.1 Convex Sets

A set $C \subseteq \Re^n$ is called convex if it contains line segments between each pair of its point, that is, if $\lambda_1 x_1 + \lambda_2 x_2 \in C$ whenever $x_1, x_2 \in C$ and $\lambda_1, \lambda_2 \geq 0$ satisfy $\lambda_1 + \lambda_2 = 1$. Equivalently, C is convex if and only if $(1 - \lambda)C + \lambda C \subseteq C$ for every $\lambda \in [0, 1]$ [22].

Roughly speaking, a set is convex if every point in the set can be seen by every other point, along an unobstructed straight path between them, where unobstructed means lying in the set. Figure 2.5 illustrates some simple convex and non-convex sets in $\Re^2$.
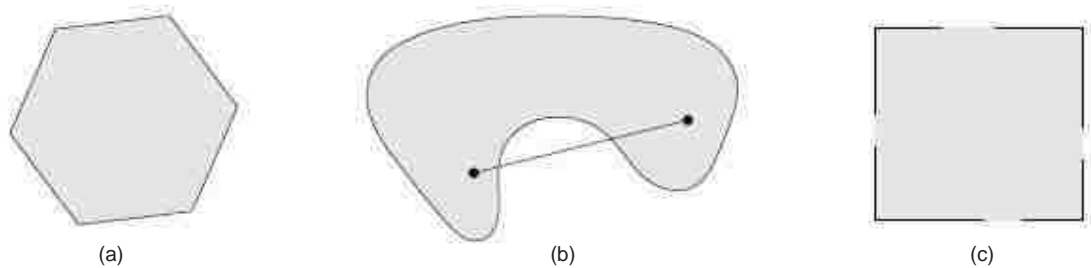
Figure 2.5: (a) The hexagon, which includes its boundary (shown darker), is convex. (b) The kidney shaped set is not convex, since the line segment between the two points in the set shown as dots is not contained in the set. (c) The square contains some boundary points but not others, and is not convex.

2.5.2 Convex Combinations

As we shall see in Chapter 4, the scheduling problem in wireless networks we are interested in has certain special linear combinations of vectors that represent *mix-*

tures of points. When $x_1, x_2, ..., x_m \in \Re^n$ and numbers (*weights*) $\lambda_1, \lambda_2, ..., \lambda_m \geq 0$ satisfy $\sum_{j=1}^{m} \lambda_j = 1$, we say that $x = \sum_{j=1}^{m} \lambda_j x_j$ is a convex combination of the points $x_1, x_2, ..., x_m$. Thus, a set is convex if and only if (iff) it contains each convex combination of any two of its points.

The convex hull of a set C, denoted $Co(C)$, is the set of all convex combinations of points in C:

$$Co(C) = \{\lambda_1 x_1 + \lambda_2 x_2 + ... + \lambda_m x_m | x_i \in C, \lambda_i \geq 0, \lambda_1 + \lambda_2 + ... + \lambda_m = 1\}. (2.23)$$

As the name suggests, the convex hull $Co(C)$ is always convex. It is the smallest convex set that contains C; if B is any convex set that contains C, then $Co(C) \subseteq B$. In the plane, intuitively, if we were to surround the points of C by a large, stretched rubber band, the convex hull is the (convex) polygonal shape that would be enclosed by the band when released. Figure 2.6 illustrates the definition of convex hull.

(a)   (b)
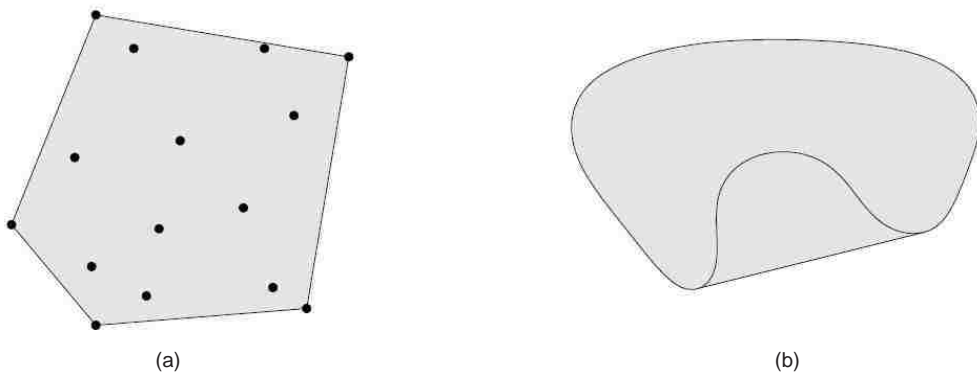
Figure 2.6: (a) The convex hulls of two sets in $\Re^2$. (a) The convex hull of a set of fifteen points (shown as dots) is the pentagon (shown shaded). (b) The convex hull of the kidney shaped set is the shaded set.

2.6 Summary

In this chapter, we have presented the antenna and interference models as well as fundamental concepts of convex analysis. Among the the above topics, we should highlight the importance and relevance of multi-access channel and convex analysis. The former is generally used in information theory to analyze single hop MPR-capable networks, while the latter is commonly applied to optimization theory to demonstrate fundamental results and devise optimization algorithms. In Chapter 4, we will merge these two areas to obtain a novel formulation and characterization of the throughput optimization in MPR-capable networks.

Chapter 3

Related Work

In this chapter, we provide a literature survey regarding the throughput optimization problem in wireless networks. According to the surveyed works, the problem can be casted as a i) pure scheduling problem (when routing is independently performed), ii) joint scheduling and routing problem, iii) joint scheduling, routing and channel assignment. The latter corresponds to systems with multiple narrow-band channels, such as 802.11-based networks. In MPR-capable networks, however, we are interested on the performance over a single channel only. MPR is also compatible with multi-channel networks, where MPR technology can be applied over the different orthogonal channels.

We classify related work according to how the throughput optimization problem is casted. The classification is not an exclusive one. The chapter starts by surveying pure scheduling schemes in Section 3.1. Then, Sections 3.2 and 3.3 discuss related work on joint routing and scheduling, and joint channel assignment, routing and scheduling respectively. Section 3.4 focuses on directional antennas, and Sections 3.5 and 3.6 present related work on theoretical and practical schemes exploiting MPR-capability.

3.1 Scheduling

The scheduling problem in wireless networks has been extensively studied in the literature. Contention-free scheduling schemes are often shown to solve certain maximum weight matching or graph coloring problems, or maximum and maximal independent set problems in the conflict graph. The general approach is to find maximal link sets and optimal allocation of time for those sets such that the performance metric is optimized. The rationale for *time-sharing* scheduling over WMNs can be derived from the very general approach for multi-hop wireless networks where the purpose of a schedule is to prevent interference among transmissions from *neighboring* links. From the fact that finding the optimal schedule (or even finding an approximation) is an NP-hard problem [10], many heuristics have been proposed. Some relevant works are discussed as follows.

Brar et al. [23] presented a centralized greedy algorithm for computing a feasible schedule under the physical model of interference. By using this interference model, they claimed that a significant throughput improvement can be obtained compared to scheduling schemes based on the protocol model of interference.

Moscibroda et al. [24] proposed a heuristic centralized scheduling algorithm for scenarios where the traffic demands are the same on every network link. Although this assumption simplifies the problem, it is not representative of a typical wireless network scenario, where traffic on different links may be very different.

In [25, 26], the scheduling problem was investigated from a theoretical point of view. A lower bound for optimal throughput under the protocol model of interference is given in [25], while an upper bound and a fair scheduling mechanism is presented in [26].

Salonidis et al. [27] proposed a distributed scheduling scheme where a flow model

is used to quantify link activations under the protocol model. The fairness issue is also discussed. Djukic et al. [28] presented a distributed scheduler based on the Bellman-Ford algorithm running on the conflict graph, and Björklund et al. [29] presented an *integer linear program* (ILP) for scheduling under the physical model, and a heuristic *column generation* algorithm.

3.2   Routing and Scheduling

Joint routing and scheduling schemes not only schedule link sets but also compute a path or set of paths between sources and destinations. Relevant schemes are discussed below.

In [10], Jain et al. presented a linear programming scheme for computing upper and lower bounds on the optimal throughput for the joint routing and scheduling problem, where an omnipresent centralized entity performs routing and scheduling. The formulation, however, is computationally intractable because it requires finding all possible sets of non-conflicting transmissions, which takes exponential time.

Kodialam et al. [30] proposed a polynomial time approximation algorithm for the routing problem, and a *graph-coloring* approach for the scheduling problem. In the graph coloring problem, the objective is to assign a color to each link such that links with the same color do not conflict (i.e., they can be simultaneously scheduled) and the number of colors (sets) is minimized.

Zhang et al. [31] formulated the routing and scheduling problem as a joint optimization problem, where end-to-end traffic flows are satisfied (i.e., the authors assumed that the traffic demand is given. On the other hand, max-flow models attempt to maximize the aggregated flow). Due to the NP-hardness of the problem, they developed a column generation approach, which decomposes the original

problem into sub-problems and solves them iteratively.

Wu et al. [32] presented two centralized algorithms for the max-flow problem, which perform joint routing and scheduling: i) link scheduling with shortest hop path, and ii) link scheduling with bandwidth-aware routing. The main idea of the algorithms is to schedule links such that the flow demand on each link is satisfied (similar assumption to the work in [31]). The conflict among links is minimized by requiring a sender node transmit if it is free of interference under the protocol model.

3.3 Channel Assignment, Routing, and Scheduling

In the presence of multiple narrow-band channels, the throughput can be improved by efficiently using the available channels. Schemes considering this dimension are specially designed to exploit the multiple channels.

Kodialam et al. [33] presented a max-flow model for the joint channel assignment, routing and scheduling problem in WMNs, which results into an ILP. To efficiently solve the problem, a centralized greedy algorithm for each, routing, scheduling and channel assignment is presented. Alicherry et al. [34] formulated the joint scheduling, channel assignment and routing for networks with multiple interfaces per node. They devised a constant approximation algorithm which was used to empirically demonstrate the impact of multiple channel on throughput.

Distributed schemes for channel assignment, routing and scheduling are presented in [35, 36]. Lin et al. [35] proposed a distributed algorithm based on the greedy maximal weighted scheduling algorithm, and Wang et al. [36] proposed a heuristic algorithm where routes are chosen according to a routing metric that captures spatial and frequency reuse. Once a path is established, the channel assignment and link

scheduling are simultaneously determined.

3.4   Scheduling with Directional Antennas

The main advantage of using directional antennas is the reduced interference and the possibility of having parallel transmissions among neighbors with a consequent increase of spatial reuse. The use of directional antennas was proved to improve the asymptotic bound on throughput by a constant factor with respect to the results presented in [3]. The factor depends on the beamwidth of the antennas used for transmission and reception [5]. Many practical schemes have been proposed to attempt to approach this bound. We include here some relevant work.

Spyropoulus et al. [37] formulated the scheduling problem as a matching in a graph. A matching in a graph is a subset of edges (i.e., links in the network topology) that have no vertices in common. The scheduling process consists of finding a series of maximum-weight matchings. Each matching constitutes a set of edges which can be scheduled simultaneously. The allocation time for each matching is chosen according to the traffic flowing through the most congested edges of the matching.

Cain et al. [38] described the scheduling in wireless networks as a graph coloring problem. Each color represents a time slot. Given a set of links which need to be scheduled, the main idea is to assign a color to each link such that no node has more than one link colored with the same color. The objective, therefore, is the minimization of colors so that each link is colored. A distributed scheme is then proposed to solve the problem.

Capone et al. [39] presented an ILP for the joint routing and scheduling problem with directional antennas. The authors also proposed a heuristic based on column generation approach. The main concern of this approach, however, is the high com-

putational effort to solve the problem.

3.5 MPR - Theoretical Work

The multi-packet reception model was introduced in [40] by Ghez et al., where multiple simultaneous packet receptions can be inferred by a probabilistic model, as opposed to the classical methods in which a deterministic failure would be declared. Specifically, the authors proposed the multi-packet reception model given by Equation (2.9), which was extensively used in subsequent work.

In [41], Mergen et al. analyzed the performance of two MAC and routing protocol combinations in regular (grid) MPR networks. In the first scenario, the performance of a simple MAC protocol based on slotted aloha and optimal routing is analyzed, while in the second scenario, an optimal MAC protocol with a random walk routing protocol is evaluated. The authors concluded that the MAC protocol does not change the order of the network capacity, but the routing does change the order, and a poor routing protocol can significantly degrade the performance of large networks.

Garcia-Luna-Aceves et al. [6] showed that MPR increases the order of per-source throughput by a logarithmic factor with respect to the protocol model. An extension of this work was presented in [20], where the throughput is also showed to be improved with respect to the physical model.

Moraes et al. [42] presented an architecture that exploits the advantages of MUD, SIC, array antennas, CDMA and mobility to increase the per-source throughput on WMNs. The overall improvement in the network performance is obtained at a cost of considerable increased processing complexity in the nodes.

Summarizing, the theoretical work [6, 20, 42] exploring MPR clearly shows that architectures exploiting multi-packet reception can increase the order the throughput

capacity of wireless network. However, few practical schemes were already proposed; some of them are discussed in the next section.

3.6 MPR - Protocols and Architectures

Few MAC protocols, routing and scheduling schemes that exploit MPR capability have already been proposed. Zhao et al. [17] proposed the first MAC protocol designed explicitly for networks with MPR capability. The key idea of the protocol is to adaptively grant access to the channel to a number of users such that the expected number of successfully received packets is maximized. The protocol tries to avoid unnecessary empty slots for light traffic and excessive collisions for heavy traffic. The difficulty of the protocol, however, lies in its computational complexity which grows exponentially with the number of users in the network. To overcome this problem, in [18] the same authors proposed a simpler algorithm that achieves a comparable performance to the one in [17].

Wang et al. [16]. proposed a max-flow formulation that considers MPR capability, which results into an ILP. Due to the intractability of the problem (ILP is NP-hard, and the size of the problem increases exponentially with the number of links), the authors developed a centralized heuristic algorithm that jointly performs routing and scheduling. An interesting result that opens a research issue is the system bottleneck resulting from the fact that nodes cannot transmit and receive simultaneously.

Celik et al. [15] studied the behavior of legacy MAC protocols (i.e., similar to the 802.11 MAC protocol) in single-hop MPR networks. Their analytical and simulation results showed that the throughput reduction is very significant. The authors also devised a simple scheduling mechanism for MPR networks that leads to a considerable improving.

3.7   Summary

Table 3.1 presents a summary of the papers discussed in this chapter. The table indicates also whether a paper addresses routing and channel assignment or not. The columns *Dir. Antenna* and *MPR capability* indicate if directional antennas and MPR capability are considered. Column *Program. m.* refers to the programming model proposed (e.g., max-flow *linear program* (LP), integer linear program (ILP), etc.). Since many programming models result in intractable problems (e.g., integer linear programming), the column *Algorithm/Protocol* refers to the *practical* algorithm and or protocol used to solve the problem, and columns *Centralized* and *Distributed* indicate how they are implemented. The last column, *Int. model*, indicates the model of interference used in the corresponding paper.

Open Research Issues

Having surveyed previous work, we found several open research issues dealing with MPR. The following list points out some relevant work not considered in the literature:

1. Limitations of MPR networks. Theoretical work by Garcia-Luna-Aceves et al. [6] demonstrated that MPR increases the order of capacity of random wireless networks by a logarithmic factor with respect to the protocol model [3]. The same authors [20] demonstrated that throughput is also improved with respect to the physical model [3], and that MPR provides greater improvement than network coding. However, practical schemes such as [16] show that MPR *only* (i.e., without additional interface resources) may not improve the throughput substantially.

2. The use of directional antennas with multi-packet reception. There is no work

that considers the use of directional antennas with multi-packet reception. A reason may be the fact that MPR capability, intuitively, mitigates the inefficient spatial reuse of omni-directional antennas. However, the impact of directional antennas in MPR networks is a very important open research issue, which is worth to study.

3. The use of multiple transmit interfaces. Previous work attempted to improve the throughput in MPR network by increasing the MPR capability of nodes. However, as pointed out in item 1, this may not be enough to substantially improve throughput. We think that the number of transmit interfaces plays a key role in MPR networks, and it *must* be considered to fully exploit MPR capability.

4. Computational efficient schemes to solve the throughput optimization problem. From Table 3.1, the only computational scheme presented in previous work is an ILP [16], which is only useful for networks with a small number of nodes. Thus, this is a clear open research issue that has to be solved.

5. Distributed protocols. As seen in Section 3.6, a very limited number distributed protocols specially devised for MPR networks were proposed. The work by Celik et al. [15] clearly demonstrates that the use of legacy protocols in MPR networks leads to a very poor performance.

From the point of view of the protocol stack, two main layers directly involved in the throughput optimization problem are the routing and the MAC. Regarding these two layers, we can point out the following.

- Routing Layer

  Except for [16], there is no work dealing with routing for MPR networks. Furthermore, Garcia-Luna-Aveces et al. [16] proposed an ILP, which is intractable.

There is a need for new routing metrics for MPR networks, since previous approaches such as [8] focused on the minimization of *intraflow* interference. Since MPR mitigates the effect of this type of interference and helps in improving the spatial reuse, this may not be the main issue for MPR networks. Investigation of new routing schemes and metrics are needed.

- MAC Layer

Most scheduling protocols are based on the protocol model and the conflict graph. In this schemes, only one transmission is scheduled in the neighborhood of the sender node (its own transmission). For example, the IEEE 802.11 Distributed Coordination Function (DCF) adopts a backoff mechanism for which a node sensing the channel busy decreases its transmission probability. This becomes a very conservative approach for MPR networks, since multiple simultaneous transmissions may be achievable. New scheduling algorithms should take this fact into account to grant access to the channel to the optimal number of senders.

The joint routing and scheduling problem has only been considered in [16]. No distributed approach has been proposed yet for this problem. Furthermore, the results obtained in [16] open many question. Specifically, they showed that the bottleneck to further improve the performance is the fact that nodes cannot transmit and receive at the same time.

Table 3.1: Previous work summary.

Ref	Year	Routing	Channel assign.	Dir. antenna	MPR capability	Program. m.	Centralized	Distributed	Algorithm/Protocol.	Int. model
[23]	2006						x		Greedy scheduling	Physical
[24]	2006						x		Heuristic	Physical
[25]	2003							x	MAC 802.11 Ideal case	Protocol
[26]	2005							x	Heuristic approx. for clique enumeration	Protocol
[27]	2004							x	Heuristic	Protocol
[28]	2007							x	Heuristic based on Bellman-Ford algorithm	Protocol
[29]	2003					ILP	x		Column generation	Protocol
[10]	2003	x				Max-flow LP	x			Protocol
[30]	2005	x				Max-flow LP	x		Heuristic approximation algorithm	Protocol
[31]	2005	x				LP	x		Column generation	Protocol
[32]	2006	x				Max-flow LP/ILP	x		Heuristic based on Dijkstra and greedy scheduling	Protocol
[33]	2005	x	x			Max-flow LP/ILP	x		Heuristic approximation algorithm	Protocol
[34]	2006	x	x			Max-flow LP/ILP	x		Heuristic approximation algorithm	Protocol
[35]	2007	x	x					x	Greedy maximal weighted scheduling algorithm	Protocol
[36]	2008	x	x					x	Heuristic protocol	Protocol
[37]	2003	x		x		Maximal-weight matching		x	Dijkstra and maximal-weight matching	Protocol
[38]	2003	x		x		Graph coloring		x	Heuristic graph coloring algorithm	Protocol
[39]	2008	x	x	x		Max-flow ILP	x		Column generation	Physical
[31]	2003				x			x	Heuristic protocol	MPR Protocol
[31]	2004				x			x	Heuristic protocol	MPR Protocol
[16]	2008	x			x	Max-flow ILP	x		Heuristic protocol	MPR Protocol
[42]	2007	x			x			x	A very complex architecture (which may not be realizable) is proposed	MPR Protocol
This work	**2009**	**x**		**x**	**x**	**Max-flow LP**	**x**		**Combined LP, approximation and greedy algorithms**	**MPR Protocol and multi-access**

Chapter 4

Problem Formulation and Characterization

In this chapter, we present a mathematical generalized model for the throughput optimization problem in multi-hop wireless networks that support multi-packet reception capability. To model wireless interference, the formulation incorporates either MPR protocol model or multi-access channel model. The latter permits to accurately account for the achievable link capacities used by simultaneous transmissions. The problem is modeled as a joint routing and scheduling problem. The scheduling subproblem deals with finding optimal *schedulable sets*, which are defined as subsets of links that can be scheduled or activated simultaneously. As a main result, we demonstrate that any solution of the scheduling subproblem can be built with $|E| + 1$ or fewer schedulable sets, where $|E|$ is the number of links of the network. This result contrasts with the conjecture that states that a solution of the scheduling subproblem, in general, is composed of an exponential number of schedulable sets [10]. The model can be applied to a wide range of networks, such as half and full duplex systems, networks with directional or omni-directional antennas with one or multiple transmit antennas per node.

The chapter is organized as follows. Section 4.1 discusses the assumptions considered in the rest of the chapter. Section 4.2 presents the formulation of the throughput optimization in MPR-capable network. The problem is presented as a joint routing routing and scheduling optimization problem. Both the routing and scheduling sub-problems are discussed in 4.2.1 and 4.2.2 respectively. Finally, Section 4.3 characterizes the problem as a convex one, and presents two important theorems derived from the proposed formulation.

4.1   Assumptions

The assumptions considered in this chapter are:

1. The wireless network is MPR-capable. Thus, we use the models of interference presented in Section 2.3. Both models, MPR protocol model and multi-access channel model, state that the reception of all transmissions is achievable if the number of simultaneous transmissions in the receiver range R is less than or equal to K. The multi-access channel model imposes the additional constraint given by Equation (2.20). To avoid ambiguity, the specific model will be explicitly stated as needed.

2. Nodes are equipped with M transmit antennas. The transmission power is uniform for every node. We consider directional transmission and omni-directional reception. Directional transmission improves the spatial reuse, while omni-directional reception maximizes the benefits of MPR.

3. The radiation pattern of transmit antennas is modeled with the flap-top model given in Section 2.1.1, where β is beamwidth of the antennas.

4. Nodes are stationary.

We will use the notation (M, K, β)-network to refer to a network with M interfaces per node, where the receiver antenna can decode up to K packets simultaneously, and the transmit antennas have a beamwidth β. We use this notation to simplify the explanation. It is straightforward to generalize to networks where M, K and β are not the same at every node.

4.2 Problem Formulation

As in previous chapters, we represent a wireless network as a graph $G = (V, E)$, where V is the set of nodes and E the set of links; r_{ij} denotes the distance between two nodes i and j. There exists a link $e = (i, j) \in E$ from node $i \in V$ to node $j \in V$ if $r_{ij} \leq R$, where R is the receiver range. If the MPR protocol model is used to model interference, the capacity of a link (i, j) is denoted as c_{ij}, and is computed according to Equation (2.13). Note that this quantity is fixed. On the other hand, if the multi-access channel is used to model interference, the capacity of the link (i, j) is denoted as $c_{ij}(S)$, where S is the set of link simultaneously activated. This capacity must satisfy Equation (2.20).

The throughput optimization problem in wireless networks can be casted as a special max-flow problem. Let N be the set of end-to-end flows. Each flow is characterized by a 3-tuple (s_n, d_n, f_n), which denotes the source node, the destination node and the flow in bits per second (bps). Although a flow is characterized by (s_n, d_n, f_n), we will also use the term flow to informally refer to f_n. The feasible aggregated throughput, or simply throughput, is defined as follows.

Definition 4.1 *Feasible throughput. A throughput of $F = \sum_{n \in N} f_n$ bits per second for a set of flows N is said to be feasible if there is a scheme to schedule transmissions and choice of routes between sources and destinations, so that every flow $n \in N$*

can achieve a data transfer to its destination at the corresponding rate f_n. The scheme needs to specify, for each link, when it should be activated under the model of interference, and the amount of data it should send. Data can be delayed at intermediate nodes before reaching its destination.

The feasible throughput as defined above is considered the main performance metric used in this work. Thus, the goal of the routing and scheduling schemes discussed in the next sections is the maximization of this metric.

According to the definition of feasible throughput, the problem can be divided into two main subproblems:

- Routing, which attempts to maximize throughput by routing through (potentially) multiple paths connecting each source-destination pair, and may ignore the impact of wireless interference to simplify its formulation;

- Scheduling, which deals with finding sets of links that can be scheduled simultaneously and the fraction of time allocated to each set.

In order to formulate the problem succinctly, we first present the routing subproblem, followed by the scheduling subproblem. Then, we give the joint routing and scheduling problem.

4.2.1 Routing Subproblem

In the absent of wireless interference, the max-flow model attempts to optimize the throughput by routing through (likely) multiple paths connecting each source-destination pair. The routing problem formulation is shown in Figure 4.1. Equation (4.1) is the throughput to be optimized. Equation (4.2) represents the flow conservation constraint; for each flow $n \in N$, the amount of flow at each node other

$$\max F_{RT\text{-}LP} \;\; = \;\; \sum_{n \in N} f_n \tag{4.1}$$

$$\sum_{j:(i,j)\in E} x_{ij}^n - \sum_{j:(j,i)\in E} x_{ji}^n \;\; = \;\; \begin{cases} f_n; i = s_n \\ -f_n; i = d_n \quad n \in N \\ 0; \text{otherwise} \end{cases} \tag{4.2}$$

$$\sum_{n \in N} x_{ij}^n \;\; \leq \;\; \omega_{ij}; (i,j) \in E \tag{4.3}$$

$$f_n \;\; \geq \;\; 0; n \in N \tag{4.4}$$

$$x_{ij}^n \;\; \geq \;\; 0; n \in N, (i,j) \in E \tag{4.5}$$

Figure 4.1: Routing linear program (RT-LP).

than its own source or destination must be zero. Equation (4.3) states that the total amount of flow routed through a link (i,j) cannot exceed a capacity ω_{ij}. The actual value of the capacity depends on the model of interference. If the MPR protocol model is used, the capacity of a link is considered as a constant [6, 16]. On the other hand, if the multi-access channel model is used, the capacity of a link depends on the links simultaneously activated with that link. Because of the circular dependency between the routing and the scheduling subproblems, the approach in this work is to consider ω_{ij} as an upper bound on capacity, which should be revisited in the scheduling subproblem (as we shall see in Section 4.2.2). Equations (4.4) and (4.5) restrict the per-source throughput and the amount of flow on each link to be non-negative. We will refer to Equations (4.1)-(4.5) as *routing linear program* (RT-LP). The model given by RT-LP is sometimes called *sum multicommodity flow* model in the literature [43].

4.2.2 Scheduling Subproblem

In wireless networks, generally only some links may be *scheduled* or activated simultaneously. A *schedulable set* $S \subseteq E$ is a set of links which can operate at the same time. For example, in the network of Figure 4.2(a), if we assume that nodes have only one omnidirectional transmit antenna and links (a, b), (c, d) and (e, f) conflict with each other (i.e., they cannot be simultaneously scheduled) then only one link can be scheduled at any time. Thus, $S_1 = \{(a, b)\}$, $S_2 = \{(c, d)\}$ and $S_3 = \{(e, f)\}$ constitute the set of schedulable sets. The conflict graph corresponding to the network is shown in Figure 4.2(b).

Note that when constructing the conflict graph, we draw an edge between two vertices if the corresponding links conflict with each other. Thus, for this particular example, where the transmissions are omnidirectional and $M = K = 1$, a schedulable set $S \subseteq E$ must be an *independent set* in the conflict graph G_c. An independent set is a set of vertices, such that there is no edge between any two of the vertices. Referring to Figure 4.2, note that the three schedulable sets correspond to independent sets in the conflict graph of Figure 4.2(b).

Feasibility Conditions for Scheduling in (M, K, β)-networks

In general, for $M \geq 1$, $K \geq 1$ and when nodes can directionally transmit, a schedulable set S may be feasible even though it does not form an independent set in the conflict graph. The feasibility conditions for scheduling in (M, K, β)-networks depend on the model of interference. The MPR protocol model restricts the number of simultaneous transmissions around a receiver node. We start this section by presenting these constraints. Then, we consider the multi-access channel model and the additional constraints on the link capacities used by concurrent transmissions.

Let $S \subseteq E$ be a set of links which are simultaneously scheduled. For any $(i, j) \in S$,
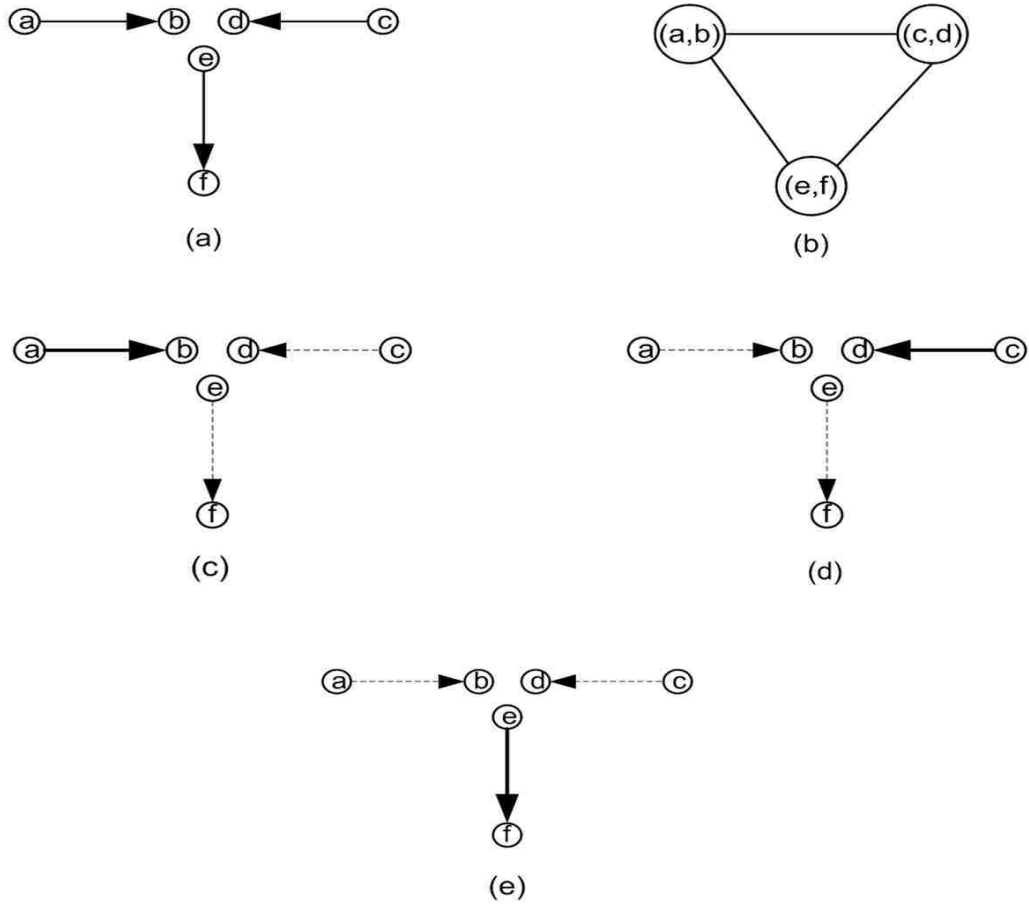
Figure 4.2: (a) A wireless network with three links conflicting with each other, and (b) corresponding conflict graph. (c), (d), (e) Schedulable sets under the protocol model: $S_1 = \{(a, b)\}, S_2 = \{(c, d)\}$, and $S_3 = \{(e, f)\}$.

$\mathcal{R}_i$, $\mathcal{T}_j$, and $\mathcal{T}'_j$ are defined by Equations (2.2), (2.16) and (2.21). Then, we have the following definition.

Definition 4.2 *Schedulable set under MPR protocol model. Given an (M, K, β)-network, a set $S \subseteq E$ is a schedulable set under the MPR protocol model iff $\forall$ $e = (i, j) \in S$:*

$$|\mathcal{R}_i| \leq M, \tag{4.6}$$

$$|\mathcal{T}'_j| \leq K, \tag{4.7}$$

The term on the left hand side of Equation (4.6) is the number of links having node i as transmitter, which must be less than or equal to M. Equation (4.7) states that the receiver node j can decode at most K packets. Note that a node cannot transmit and receive simultaneously with a *single* antenna, but through different interfaces. The use of directional antennas permit such a scheme, since transmit antennas radiate only to certain directions and minimize the interference at the location of the transmitter node. Furthermore, interference cancelation techniques allow to remove a known unwanted transmitted signal by subtracting it from the received signals.

Additional Feasibility Conditions for Multi-Access Channel Model

The multi-access channel model imposes additional constraints on the rates used to transmit simultaneous packets. As seen in Equation (2.20), the link capacities used by concurrent transmissions must lie inside the capacity region. Thus, for multi-access channels, we have the following definition.

Definition 4.3 *Schedulable set under multi-access channel model. Given an (M, K, β)-network, a set $S \subseteq E$ is a schedulable set under the multi-access channel model iff $\forall$ $(i, j) \in S$:*

$$|\mathcal{R}_i| \leq M, \tag{4.8}$$

$$|\mathcal{T}'_j| \leq K, \tag{4.9}$$

$$\sum_{i' \in T} c_{i'j}(S) \leq \varphi\left(\frac{\sum_{i' \in T} P_{i'j}}{\eta_j}\right), \forall T \subseteq \mathcal{T}_j. \tag{4.10}$$

While we focus on (M, K, β)-networks, in next sections we will also consider half-duplex (HD) networks for performance comparison purposes. Since Equations (4.6), (4.7), (4.8), and (4.9) model networks where nodes can send and receive simultaneously through different interfaces, they should be substituted for the following constraint in HD networks:

$$|\mathcal{R}_i| + \left\lceil \frac{|\mathcal{T}_i'|}{K} \right\rceil \leq 1, \tag{4.11}$$

for every node i scheduled in S as transmitter or a receiver.

As we shall see, the problem formulation presented in Section 4.2.3, and the schemes proposed in Chapter 5 are general and can be applied to both half-duplex and full-duplex networks.

Scheduling Constraints

Before extending RT-LP so that wireless interference is considered, we formally define a *schedule* as follows.

Definition 4.4 *Feasible Schedule. Let $G = (V, E)$ be an (M, K, β)-network, and $\Gamma = \{S_1, S_2, ..., S_{|\Gamma|}\}$ be the set of all feasible schedulable sets satisfying Definition 4.2 or Definition 4.3, according to the interference model used. A feasible schedule in $G = (V, E)$ is a set $\Gamma' = \{S_1, S_2, ..., S_{|\Gamma'|}\} \subseteq \Gamma$ of schedulable sets, and the fraction of time allocated to each schedulable set. The schedule is periodic with period 1. If $\lambda_k, 0 \leq \lambda_k \leq 1$ represents the fraction of time allocated to the schedulable set S_k, then the schedule interval $[0, 1]$ is $\cup_k[t_k, t_{k+1}]$, where links in S_k are activated for the activity period $t_{k+1} - t_k = \lambda_k$, $k \in \{1, 2, ..., |\Gamma'|\}$, $t_1 = 0$ and $t_{|\Gamma'|+1} = 1$.*

Having defined the concept of a schedule, we now proceed to mathematically formulate the scheduling constraints to incorporate to RT-LP. We will call the variable λ_k as the activity period variable corresponding to the schedulable set S_k. The time resource restriction in the scheduling subproblem can be written as:

$$\sum_{k=1}^{|\Gamma|} \lambda_k = 1. \tag{4.12}$$

Equation (4.12) can be interpreted as a resource allocation constraint, where the resource to be allocated is *time*. The total fraction of time allocated to all schedulable sets must be equal to one.

In the scheduling subproblem, links are scheduled according to the scheduling constraints. Since a link may be activated during multiple activity periods, the amount of flow routed through it must not exceed the sum of its capacity on those periods multiplied by the corresponding activity periods:

$$\sum_{n\in N} x_{ij}^n \leq \sum_{\forall k\in\{1,2,...,|\Gamma|\}|(i,j)\in S_k} \lambda_k c_{ij}(S_k), \tag{4.13}$$

where $c_{ij}(S_k)$ is the capacity of link (i,j) when the set S_k is scheduled. Note that for the MPR protocol model, this value is a constant, which may be equal to one [6, 16], or may be computed according to Equation (2.13). On the other hand, for the multi-access channel model, $c_{ij}(S_k)$ must lie inside the capacity region given by Equation (2.20).

4.2.3 Joint Routing and Scheduling Problem

In general, only a small subset $\Gamma' \subseteq \Gamma$ is needed to evaluate Equations (4.12) and (4.13), as we shall see in *Theorem 4.2*. By incorporating Equations (4.12) and (4.13) into RT-LP and optimizing not only over the variables given by Equations (4.4) and

(4.5) but also over all possible set $\Gamma' \subseteq \Gamma$ of schedulable sets, the formulation of the joint routing and scheduling problem is given in Figure. 4.3.

$$\max_{\Gamma' \subseteq \Gamma} F_{RTSCH\text{-}LP} \quad = \quad \sum_{n \in N} f_n \tag{4.14}$$

$$\sum_{j:(i,j) \in E} x_{ij}^n - \sum_{j:(j,i) \in E} x_{ji}^n \quad = \quad \begin{cases} f_n; \text{if } i = s_n \\ -f_n; \text{if } i = d_n \quad n \in N \\ 0; \text{otherwise} \end{cases} \tag{4.15}$$

$$\sum_{n \in N} x_{ij}^n \quad \leq \quad \sum_{\forall k \in \{1,2,...,|\Gamma'|\}|(i,j) \in S_k} \lambda_k c_{ij}(S_k); (i,j) \in E \tag{4.16}$$

$$\sum_{k=1}^{|\Gamma'|} \lambda_k \quad = \quad 1 \tag{4.17}$$

$$f_n \quad \geq \quad 0; n \in N \tag{4.18}$$

$$x_{ij}^n \quad \geq \quad 0; n \in N, (i,j) \in E \tag{4.19}$$

$$\lambda_k \quad \geq \quad 0; k \in \{1,2,...,|\Gamma'|\} \tag{4.20}$$

Figure 4.3: Routing and scheduling linear program (RTSCH-LP).

We will refer to this linear program as *routing and scheduling linear program* (RTSCH-LP). The reason of the hardness of RTSCH-LP is the exponentially large number of sets of schedulable sets. Potentially, there are $2^{|E|}$ distinct sets $\Gamma' \subseteq \Gamma$. To find the optimal set requires an exhaustive search, which would take exponential time. In the next section, we characterize RTSCH-LP and derive *Theorems 4.1* and *4.2*, which shed some lights on how to solve such a complex problem.

4.3 Characterization of the Throughput Optimization Problem

The complexity of the joint routing and scheduling problem is mainly determined by the scheduling subproblem. Thus, we will briefly discuss the complexity of the routing subproblem first, followed by the that of the scheduling subproblem.

Complexity of the Routing Subproblem

The routing subproblem is modeled by LP-RT, which is defined in Figure 4.1. This linear program is a max-flow problem. The number of flow conservation constraints (Equation (4.2)) is $|V| \cdot |N|$, because there is one constraint per node per flow. Similarly, the number of capacity constraints (Equation (4.3)) and flow variable constraints (Equations (4.4) and (4.5)) are $|E|$, $|N|$, and $|E| \cdot |N|$ respectively. Thus, the number of constraints and variables are polynomially bounded in $|E| \cdot |N|$, and can be solved by a polynomial time linear programming algorithm. For example, by using an interior point method, the running time of the algorithm to solve LP-RT is $O(|E|^3|N|^3)$ [22].

From an optimization perspective, LP-RT describes a *routing polytope*. This polytope is the collection of feasible points ignoring wireless interference, and is a simple structure on which a linear objective function can be *easily* optimized. For example, if the simplex algorithm is applied to RT-LP, it will find the optimal throughput in the following way: start from a vertex of the polytope, say the origin, where $x_{ij}^n = 0$ for all $n \in N, (i,j) \in E$, and then proceed to improve the solution (by moving along edges of the polytope from one polytope vertex to another) until reaching the polytope vertex corresponding to the optimal throughput. Since in practice simplex run in polynomial time, the solution will be found in polynomial

time [44].

Characterization of the Scheduling Subproblem

The complexity of the routing and scheduling linear program (RTSCH-LP) is mainly determined by the scheduling subproblem. Thus, a key issue is the characterization of it. We start by presenting some definitions.

Let $G = (V, E)$ be an (M, K, β)-network, where the set of links is ordered in an arbitrary manner $E = \{e_1, e_2, ..., e_{|E|}\}$. The *link space* $\{0, 1\}^{|E|}$ is the vector space over the 2-element field $\{0, 1\}$ of all function (scheduler) $E \rightarrow \{0, 1\}$. Every point of $\{0, 1\}^{|E|}$ corresponds naturally to a subset of E, the set of those links to which it assigns a one, and every subset of E is uniquely represented in $\{0, 1\}$ by its indicator function. We may thus think of $\{0, 1\}^{|E|}$ as the power set of E made into a vector space. Since $\{\{e_1\}, \{e_2\}, ..., \{e_{|E|}\}\}$ is a basis of $\{0, 1\}^{|E|}$, the dimension of the vector space is $|E|$. According to these definitions, a schedulable set can be characterized by a *schedulable vector* $\vec{S}$ of size $|E|$. The jth element of this vector is set to one if the link $e_j \in E$ is a member of $\vec{S}$, and to zero otherwise. Any schedulable vector $\vec{S}$ can be regarded as a point in $\{0, 1\}^{|E|}$, which also becomes a vertex of the the convex hull of the set of schedulable vectors. We call this this convex hull as *allocation polytope*, which is formally defined as follows.

Definition 4.5 *Allocation Polytope. Let $G = (V, E)$ be an (M, K, β)-network, and $\Gamma = \{S_1, S_2, ..., S_{|\Gamma|}\}$ be the set of all schedulable sets. Then, the allocation polytope is defined as the convex hull of all schedulable vectors $\vec{S_1}, \vec{S_2}, ..., \vec{S_{|\Gamma|}}$, and is denoted as $Co(\Gamma)$.*

The allocation polytope represents the region that tells whether a solution of the scheduling subproblem is feasible or not. Let $\vec{u} = (u_1, u_2, ..., u_{|E|})$ be an $|E|$-

dimensional *utilization vector*, where u_i is the utilization of link e_i, which indicates the total fraction of time allocated to link e_i. By regarding the utilization vector as a point in $\{0, 1\}^{|E|}$, we have the following theorem.

Theorem 4.1 *Feasible Schedule. A solution to the scheduling subproblem given by a set $\Gamma' = \{S_1, S_2, ..., S_{|\Gamma'|}\} \subseteq \Gamma$ with corresponding activity periods $\lambda_1, \lambda_2, ..., \lambda_{|\Gamma'|}$ is feasible iff the resulting utilization vector $\vec{u}$ lies within the allocation polytope.*

Proof:

$\Rightarrow$ Assume a feasible schedule (i.e., a schedule that satisfies *Definition 4.4*), with a set $\Gamma' = \{S_1, S_2, ..., S_{|\Gamma'|}\}$ and corresponding activity periods $\lambda_1, \lambda_2, ..., \lambda_{|\Gamma'|}$. Then $\vec{u}$ must be of the form:

$$\vec{u} = \sum_{i=1}^{|\Gamma'|} \lambda_i \vec{S_i}. \tag{4.21}$$

By definition, the allocation polytope is the set of all convex combinations of all possible schedulable vectors:

$$Co(\Gamma) \quad = \quad \{\theta_1 \vec{S_1} + ... + \theta_k \vec{S_k}, \text{ for all } S_i \in \Gamma, \theta_i \geq 0, \theta_1 + ... + \theta_k = 1\}. \tag{4.22}$$

Note that the utilization vector $\vec{u}$ given by Equation (4.21) is a convex combination of the schedulable vectors corresponding to the sets in Γ', where the *weights* are given by the activity periods $\lambda_1, \lambda_2, ..., \lambda_{|\Gamma'|}$. Since $\Gamma' \subseteq \Gamma$, $\vec{u}$ is a particular point that satisfies Equation (4.22) and therefore lies inside the allocation polytope.

$\Leftarrow$ Assume that $\vec{u}$ lies within the allocation polytope. Then, $\vec{u}$ can be expressed as a convex combination of a set of schedulable vectors, which have a corresponding set $\Gamma' = \{S_1, S_2, ..., S_{|\Gamma'|}\}$. By allocating λ_i seconds to $S_i \in \Gamma'$ (the schedulable set that has a corresponding schedulable vector $\vec{S_i}$), we can build a feasible schedulable, which implies that $\vec{u}$ is feasible.

Theorem 4.1 implies that the optimal schedule can be found by using linear programming, since the solution space is bounded by linear constraints. The hardness, however, arises because of the non-trivial procedure to build the solution space of the scheduling subproblem (i.e., the allocation polytope), since it may have an exponential number of vertices that can only be found by enumeration.

The following example illustrates the throughput optimization problem as an optimization problem, and the application of *Theorem 4.1*.
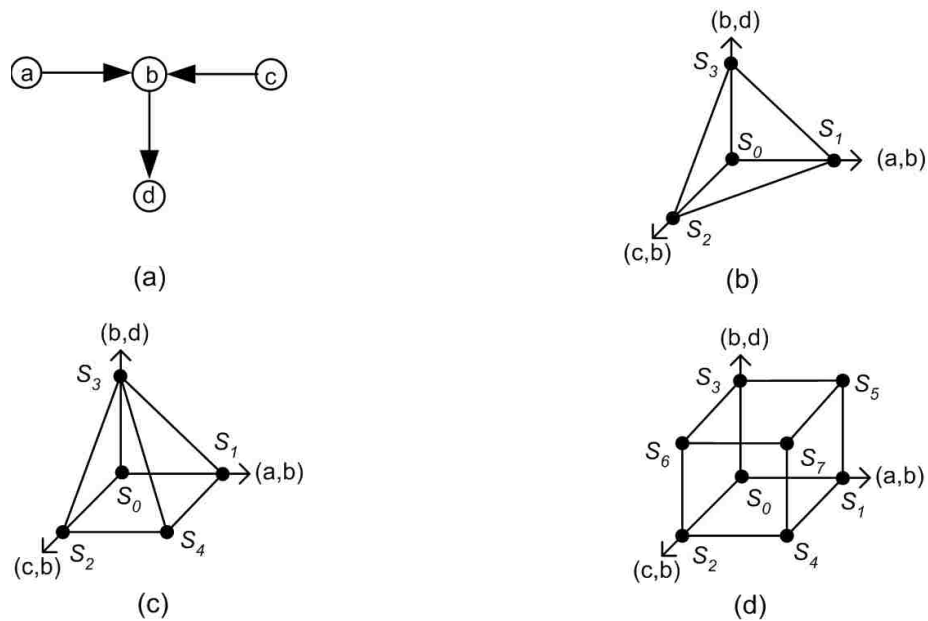

Figure 4.4: (a) Network topology with three links: (a, b), (c, b), and (b, d). (b) Allocation polytope, for $K = 1$ and half-duplex operation of network in (a). The schedulable vectors are: $\vec{S_0} = (0, 0, 0)$, $\vec{S_1} = (1, 0, 0)$, $\vec{S_2} = (0, 1, 0)$, and $\vec{S_3} = (0, 0, 1)$. (c) Allocation polytope, for $K = 2$, of network in (a). The schedulable vector $\vec{S_4} = (1, 1, 0)$ is included, since node b can simultaneously decode packets from nodes a and c. (d) Allocation polytope including all potential schedulable vectors of network in (a). The additional schedulable vectors are: $\vec{S_5} = (1, 0, 1)$, $\vec{S_6} = (0, 1, 1)$, and $\vec{S_7} = (1, 1, 1)$.

Example 4.1. Consider the network shown in Figure 4.4(a), and assume a half-duplex network with $K = 1$. The channel is an AWGN with variance η, and

wireless interference is modeled according to the multi-access channel model. Assume also the existence of two end-to-end flows: flow 1, from node a to node d routed through node b; and flow 2, from node c to node d routed through node b. The objective is the maximization of the aggregated throughput, namely $F = f_1 + f_2$. The flow conservation constraints (Equation (4.15)) state that the amount of flow at node b must be zero, while the amount of flow leaving nodes a and c must be maximized. The only set that may activate the three links is $\Gamma' = \{S_1, S_2, S_3\}$, where $S_1 = \{(a, b)\}$, $S_2 = \{(c, b)\}$, and $S_3 = \{(b, d)\}$. The corresponding link capacity constraints given by Equation (4.16) are:

$$x_{ab}^1 \leq \lambda_1 \varphi \left(\frac{P_{ab}}{\eta_b} \right), \tag{4.23}$$

$$x_{cb}^2 \leq \lambda_2 \varphi \left(\frac{P_{cb}}{\eta_b} \right), \tag{4.24}$$

$$x_{bd}^1 + x_{bd}^2 \leq \lambda_3 \varphi \left(\frac{P_{bd}}{\eta_d} \right), \tag{4.25}$$

where $\eta_b = \eta_d = \eta$. The scheduling constraint given by Equation (4.17) is expressed as:

$$\sum_{i=1}^{|\Gamma'|} \lambda_i = \lambda_1 + \lambda_2 + \lambda_3 = 1. \tag{4.26}$$

This equation requires the scheduling algorithm to allocate time to each schedulable set, such that the resulting utilization vector lies inside allocation polytope shown in Figure 4.4(b). Assume now a multi-access channel with $K = 2$, where node b can simultaneously decode transmissions from node a and c. The set $S_4 = \{(a, b), (c, b)\}$ is now a schedulable set, and the capacity of links (a, b) and (c, b) are restricted to lie inside the capacity region shown in Figure 4.5, where $\eta_b = \eta$. Let $\vec{c_2}$ be the operation point. By scheduling S_4 along with S_3 (i.e., $\Gamma' = \{S_3, S_4\}$), the constraints given by
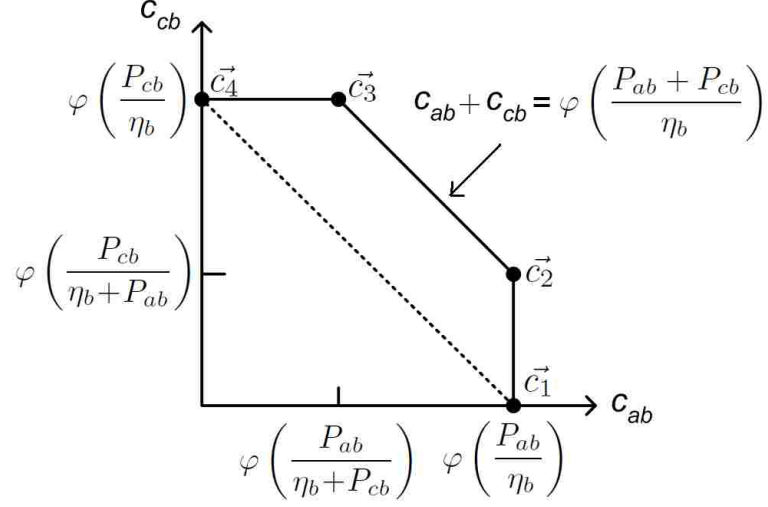
Figure 4.5: Capacity region for receiver node b in Figure 4.4(a).

Equation (4.16) are:

$$x_{ab}^1 \leq \lambda_4 \varphi\left(\frac{P_{ab}}{\eta_b}\right), \tag{4.27}$$

$$x_{cb}^2 \leq \lambda_4 \varphi\left(\frac{P_{cb}}{\eta_b + P_{ab}}\right), \tag{4.28}$$

$$x_{bd}^1 + x_{bd}^2 \leq \lambda_3 \varphi\left(\frac{P_{bd}}{\eta_d}\right), \tag{4.29}$$

$$\tag{4.30}$$

where $\eta_d = \eta$, and $\lambda_3 + \lambda_4 = 1$. Since S_4 is now a schedulable set, it is included as a vertex of the the allocation polytope shown in Figure 4.4(c). Finally, the use of directional antennas and full-duplex capability can further enlarge the allocation polytope, as shown in Figure 4.4(d).

From the previous example, we can see that links (a, b) and (c, b) are activated for λ_4 seconds, and link (b, d) for λ_3 seconds. In a general scheduling problem, we are interested on activating every link $e_i \in E$ for certain fraction of time u_i. The following proposition upper bounds the number of schedulable sets to achieve this.

Theorem 4.2 *Any utilization vector $\vec{u}$ can be represented as a convex combination of $|E| + 1$ or fewer schedulable vectors in $Co(\Gamma)$.*

Proof: *Theorem 4.2* can be demonstrated by applying Caratheodorys's theorem on convex sets [9]. Let $\Gamma_1 = \{S_1, S_2, ..., S_{|\Gamma_1|}\} \subseteq \Gamma$ be a schedule with corresponding allocation times $\lambda_1, \lambda_2, ..., \lambda_{|\Gamma_1|}$ greater than zero, and utilization vector $\vec{u} = (u_1, ..., u_{|E|})$. We will assume that $|\Gamma_1| > |E| + 1$, and show that there is solution Γ_2 that produces the same utilization vector with no more than $|E| + 1$ schedulable sets. Denote the ith scalar component of the schedulable vector $\vec{S_k}$ as S_{ki}. Then, for any $e_i \in E$, the component u_i of $\vec{u}$ is:

$$\sum_{k=1}^{|\Gamma_1|} \lambda_k S_{ki} = u_i; e_i \in E. \tag{4.31}$$

Now, we can formulate a linear program where the optimization variables are activity period variables $\lambda'_1, \lambda'_2, ..., \lambda'_{|\Gamma_1|}$, as shown in Figure 4.6. The fundamental theorem

$$\sum_{k=1}^{|\Gamma_1|} \lambda'_k S_{ki} = u_i; e_i \in E \tag{4.32}$$

$$\sum_{k=1}^{|\Gamma_1|} \lambda'_k = 1; \tag{4.33}$$

$$\lambda'_k \geq 0; k \in \{1, 2, ..., |\Gamma_1|\} \tag{4.34}$$

Figure 4.6: Linear program to obtain $\Gamma_2 = \{S_k | S_k \in \Gamma_1 \text{ and } \lambda'_k > 0\}$.

of linear programming states that every feasible linear program has a basic feasible solution. In a basic feasible solution, only the basic variables are nonzero. Here, we assume that the solution is a non-degenerate basic feasible solution. In a degenerate basic feasible solution, a basic variable can be zero. Referring back to Figure 4.6, the linear program has $|E| + 1$ basic variables (one per equality constraint). Thus, this

basic solution naturally corresponds to a set $\Gamma_2 = \{S_k | S_k \in \Gamma_1 \text{ and } \lambda'_k > 0\}$, which demonstrates *Theorem 4.2*.

Theorem 4.2 implies that any solution to the scheduling subproblem can be built no more than $|E| + 1$ schedulable sets, contradicting the conjecture that says that a solution is generally composed of an exponential number of schedulable sets [10]. *Theorem 4.2* encourages the design of new scheduling polynomial time algorithms to approximate to optimal solutions, instead of devising complex algorithms that search for an exponential number of schedulable sets [10]. Certainly, this is an open research topic that deserves close attention. The following example highlights this fact.

Example 4.2. Consider the network of Figure 4.4(a) and allocation polytope shown in Figure 4.4(d). Let $\Gamma'_1 = \{S_1, S_2, S_3, S_4, S_5, S_6\}$ be a schedule with corresponding allocation times $\lambda_i = \frac{1}{6}$ for all $i \in \{1, 2, ..., 6\}$. The schedule produces an utilization vector $\vec{u} = \sum_{i=1}^{6} \lambda_i \vec{S_i} = (\frac{1}{2}, \frac{1}{2}, \frac{1}{2})$, activating each link for $\frac{1}{2}$ seconds. According to *Theorem 4.2*, we can build a schedule with no more than $|E| + 1 = 4$ schedulable sets that produces the same utilization vector. A possible solution is the set $\Gamma'_2 = \{S_0, S_7\}$ with corresponding allocation times of $\lambda_0 = \lambda_7 = \frac{1}{2}$. The allocation of $\frac{1}{2}$ seconds to S_0 implies that the network is idle for half of the time. Notice also that $|\Gamma'_2| = 2 < |E| + 1$. In general, however, the number of schedulable sets we should expect is $|E| + 1$. For example, for the allocation polytope of Figure 4.4(b) and for an utilization vector $\vec{u} = (\frac{1}{4}, \frac{1}{4}, \frac{1}{4})$, the only set that produces the desired $\vec{u}$ is $\Gamma'_3 = \{S_0, S_1, S_2, S_3\}$ with corresponding allocation times $\lambda_i = \frac{1}{4}$ for $i \in \{0, 1, 2, 3\}$. Thus, $|\Gamma'_3| = |E| + 1$.

Complexity of the Scheduling Subproblem

The complexity of the routing and scheduling linear program (RTSCH-LP) is mainly determined by the scheduling subproblem. To find an optimal solution, the problem requires searching for a set of optimal schedulable vectors in $\{0,1\}^{|E|}$, which is exponentially large in $|E|$. The hardness of the problem, alternatively, can be proved by noting that the throughput optimization problem under the protocol model, for omni-directional antenna networks without MPR-capability [10], is a particular case of the of the joint routing and scheduling problem in an (M, K, β)-network (i.e., it can be reduced to RTSCH-LP). Since the former is an NP-hard problem, RTSCH-LP is also NP-hard.

4.4 Summary

In this chapter, we have presented a generalized problem formulation for the throughput optimization in MPR-capable networks. The flexibility of the formulation permits to model a wide range of networks, such as half and full duplex systems, or networks with directional and omni-directional antennas with one or multiple transmit antennas per node. Besides the MPR protocol model of interference, in which the unit of transmission is the packet, the formulation incorporates multi-access channel, which accurately accounts for the achievable link capacities used by simultaneous transmissions. We have further characterized the problem as a convex optimization. By using convex analysis, we have proved two fundamental theorems that may be relevant for future protocols and architecture designs for wireless networks.

Chapter 5

Joint Routing and Scheduling Schemes

In this chapter, we present polynomial time joint routing and scheduling (JRS) schemes based on a combination of greedy, approximation algorithm, and linear programming paradigms to solve the throughput optimization problem presented in Chapter 4. Because of the hardness of the problem, the proposed approaches decouple the routing and scheduling subproblems. The routing subproblem is solved by using linear programming. For the scheduling subproblem, we propose three different scheduling algorithms based on greedy and approximation algorithms.

The schemes consist of three steps:

1. Solve RT-LP.

2. Solve the scheduling subproblem. Create a set $\Gamma' \subseteq \Gamma$ by using an approximation or a greedy algorithm. To run in polynomial time, the scheduling algorithm guarantees that the number of schedulable sets found during the searching process is upper-bounded by $|E|$.

3. Solve RTSCH-LP, considering only the subset $\Gamma' \subseteq \Gamma$ found in step 2.

The remainder of this chapter is organized as follows. Section 5.1 discusses the first step, which solves the routing subproblem. Sections 5.2, 5.3, and 5.4 present three different scheduling algorithms to solve the scheduling subproblem. The first algorithm is a greedy approach which solves the scheduling subproblem under the MPR protocol model. The second algorithm is an approximation algorithm which guarantees that, for certain type of networks, its schedule period is at most two times the schedule period of the the optimal scheduler. This algorithm also solves the scheduling subproblem under the MPR protocol model. The third algorithm is another greedy approach which solves the scheduling subproblem under the multi-access channel model. The algorithm schedules link so that they operate at max-capacity. Finally, Section 5.6 presents a linear program to solve step 3, and discusses upper and lower bounds on throughput as well as the complexity of the overall scheme.

5.1 Routing Linear Program

This step consists of solving RT-LP. The procedure is intended to identify multiple paths for each flow, such that the throughput is maximized. In the absence of wireless interference (e.g., on a wired network), finding the maximum achievable throughput between the source and the destination, given the flexibility of using multiple paths, is formulated as the max-flow problem given by RT-LP in Figure 5.1.

The output of the step 1 is the set of links which are assigned a positive flow value by RT-LP, namely $E_{RT\text{-}LP} = \{(i,j) \in E | \sum_{n \in N} x_{ij}^n > 0\}$, where the variables $x_{ij}^{n}{}'$s are the optimization variables of RT-LP given by Equation (5.5).

The main and key issue regarding LP-RT is the link capacity ω_{ij} used in Equation

$$\max F_{RT\text{-}LP} \;=\; \sum_{n \in N} f_n \tag{5.1}$$

$$\sum_{j:(i,j)\in E} x_{ij}^n - \sum_{j:(j,i)\in E} x_{ji}^n \;=\; \begin{cases} f_n; i = s_n \\ -f_n; i = d_n \quad n \in N \\ 0; \text{otherwise} \end{cases} \tag{5.2}$$

$$\sum_{n \in N} x_{ij}^n \;\leq\; \omega_{ij}; (i,j) \in E \tag{5.3}$$

$$f_n \;\geq\; 0; n \in N \tag{5.4}$$

$$x_{ij}^n \;\geq\; 0; n \in N, (i,j) \in E \tag{5.5}$$

Figure 5.1: Routing linear program (RT-LP).

(5.3), for all $(i,j) \in E$. If this quantity is considered as a constant as proposed in [3, 6, 16] (e.g., unit link capacity [16]), then RT-LP can be easily solved. This simplification permits to find suboptimal solutions in a polynomial time. At the same time, the simplification is compatible with the MPR protocol model, where a link capacity is given by Equation (2.13)). On the other hand, if the multi-access channel model is used, then any link capacity may be affected by all links simultaneously activated in the network, and must lie inside the capacity region given by Equation (2.20). The difficulty of evaluating Equation (2.20) arises from the dependency between the routing and the scheduling subproblems. To accurately find the capacity of a link (i,j), the routing subproblem must know which links are simultaneously scheduled with link (i,j). On the other hand, the scheduling subproblem schedules the link (i,j) according to the flow routed through it, which is assigned by the routing process. Thus, to decouple this circular dependency, the right-hand side of Equation (5.3) is just considered as an upper bound in step 1. The value of the upper bound is given by:

$$\omega_{ij} = \varphi\left(\zeta r_{ij}^{-\gamma}\right), \tag{5.6}$$

where:

$$\zeta = \begin{cases} 1, & \text{under the the MPR protocol model;} \\ \frac{P_{ij}}{\eta}, & \text{under the multi-access channel model.} \end{cases} \tag{5.7}$$

P_{ij} is given by Equation (2.15). It is the power of the signal transmitted by node i at receiver node j, and η the variance of the AWGN channel. Clearly, ω_{ij} is an upper bound, since the total noise at receiver node j is given by η only. When solving the scheduling subproblem, the actual link capacity will be revisited, so that the noise at receiver node j takes the value given by Equation (2.18).

RT-LP is a linear program bounded in size. According to Equation (5.4), there are $|N|$ flow variables. Similarly, there are $|N| \cdot |E|$ variables used to indicate the amount of flow routed by each link, as seen in Equation (5.5). The number of flow conservation constraints given by Equation (5.2) is $|N| \cdot |V|$, and the number of links capacity constraints given by Equation (5.3) is $|E|$. Thus, the number of variables and constraints are $O(|N| \cdot |E|)$, and can be solved by a polynomial time linear programming algorithm [22].

5.2 Greedy Scheduler Under MPR Protocol Model

Step 2 processes the set $E_{RT\text{-}LP} = \{(i,j) \in E | \sum_{n \in N} x_{ij}^n > 0\}$ given by step 1. The scheduling algorithm schedules all the links in that set, such that every link (i,j) can send the amount of flow $\sum_{n \in N} x_{ij}^n$ during a schedule period. In this section, we present a greedy scheduler under the MPR protocol model.

Algorithm Description

The scheduling algorithm partitions the set $E_{RT\text{-}LP} = \{(i,j) \in E \mid \sum_{n \in N} x_{ij}^n > 0\}$ in maximal disjoint schedulable sets, and tries to minimize the number of such sets. A maximal set S is defined as a schedulable set (*Definition 4.2*), such that, when all links in S are activated, no more links can be activated without violating the scheduling constraints. The algorithm proceeds by always choosing the next link with maximum link utilization. The utilization of a link (i,j) defined in Section 4.3 can be expressed as:

$$u_{ij} = \frac{\text{total number of bits routed through link } (i,j)}{\text{capacity of link } (i,j)} \tag{5.8}$$

$$= \frac{\sum_{n \in N} x_{ij}^n}{c_{ij}}, \tag{5.9}$$

where $\sum_{n \in N} x_{ij}^n$ is the flow through link (i,j) resulting from step 1. Note that the utilization u_{ij} is the fraction of time link (i,j) must be activated, so that $\sum_{n \in N} x_{ij}^n$ bits can be sent through it during a schedule period. The detailed process is shown in Figure 5.3. The *Greedy Scheduler I* (GSI) creates sets $S_1, S_2, ..., S_{|\Gamma_{GSI}|}$, where every link of each set satisfies the feasibility conditions given by *Definition 4.2*. In line 9, a link is greedily chosen to belong to the set S_k according to the link utilization. The greedy selection attempts to group links with similar utilizations in the same set.

Throughput Performance of GSI

The output of GSI is $\Gamma_{GSI} = \{S_1, S_2, ..., S_{|\Gamma_{GSI}|}\}$ only. The algorithm is not intended to allocate corresponding allocation times, which is done in step 3. However, we may easily find a feasible solution for RTSCH-LP at this step, which may be used as a lower bound to the solution produced by step 3 (as we shall see in Section 5.6). To this end, consider the following allocation policy. Let τ_k be the fraction of time

---

Greedy Scheduler I (GSI)

1: INPUT: $E_{RT\text{-}LP}$, $G(V, E)$
2: OUTPUT: Set Γ_{GSI} of schedulable sets.
3: $\Gamma_{GSI} = \{\}$;
4: $k = 0$;
5: **while** $(E_{RT\text{-}LP} \neq \{\})$ **do**
6:     $k = k + 1$;
7:     $S_k = \{\}$;
8:     **while** $\exists\ (i, j) \in E_{RT\text{-}LP}|\mathcal{E}(S_k \cup \{(i, j)\})$ **do**
9:       $(i, j) = \arg \max\{u_{ij}|(i, j)E_{RT\text{-}LP} \text{ and } \mathcal{E}(S_k \cup \{(i, j)\}))\}$;
10:       $S_k = S_k \cup \{(i, j)\}$;
11:       $E_{RT\text{-}LP} = E_{RT\text{-}LP} - \{(i, j)\}$;
12:     **end while**
13:     $\tau_k = \max\{u_{ij}|(i, j) \in S_k\}$;
14:     $\Gamma_{GSI} = \Gamma_{GSI} \cup S_k$;
15: **end while**
16: **return** Γ_{GSI};

Figure 5.2: Greedy Scheduler I (GSI). $\mathcal{E}(S)$ stands for the event $\mathcal{E}(S) = \{$Equations (4.6) and (4.7) are satisfied for all $(i, j) \in S\}$.

allocated to the set S_k:

$$\tau_k = \max\{u_{ij}|(i, j) \in S_k\}. \tag{5.10}$$

τ_k is equal to the maximum link utilization among all links in S_k. Define τ_{GSI} as the period of the schedule produced by the algorithm; i.e.,

$$\tau_{GSI} = \sum_{k=1}^{|\Gamma_{GSI}|} \tau_k. \tag{5.11}$$

Clearly, a link $(i, j) \in S_k$ is allocated enough time, such that the flow $\sum_{n \in N} x_{ij}^n$ routed through it can be sent during a schedule period. Thus, the throughput produced by this allocation policy is:

$$F_{GSI} = \frac{\text{end-to-end bits transmitted during a schedule period}}{\text{schedule period}} \tag{5.12}$$

$$= \frac{F_{RT\text{-}LP}}{\tau_{GSI}} \tag{5.13}$$

According to the *Definition 4.4*, the above allocation policy may not produce a feasible schedule, since the period τ may be greater than 1. However, the solution provided by the above allocation policy can be slightly modified with the following allocation times:

$$\lambda_k = \frac{\tau_k}{\tau_{GSI}}, \tag{5.14}$$

for all schedulable set $S_k \in \Gamma_{GSI}$. Thus,

$$\text{schedule period} = \sum_{k=1}^{\Gamma_{GSI}} \lambda_k = \sum_{k=1}^{\Gamma_{GSI}} \frac{\tau_k}{\tau_{GSI}} = 1, \tag{5.15}$$

which satisfies *Definition 4.4*. Moreover, the throughput given by Equation (5.13) still holds. The following example illustrates the operation of GSI.

Example 5.1. Consider the three links of Figure 5.3(a) with the respective link utilizations: $u_{ab} = 0.8$, $u_{cd} = 0.6$, and $u_{ef} = 0.5$. The operation of the scheduling algorithm is shown in Figure 5.3(b). Assume that links conflict with each other, and that nodes can decode at most two packets at the same time (i.e., $K = 2$). Thus, at most two links can be simultaneously scheduled. The algorithm starts by scheduling (a, b) and (c, d), which constitute a maximal set S_1. According to the allocation policy discussed above and line 13, the algorithm allocates $\tau_1 = 0.8$ seconds to the set S_1. This fraction of time is enough to satisfy the link utilization of all links in S_1.
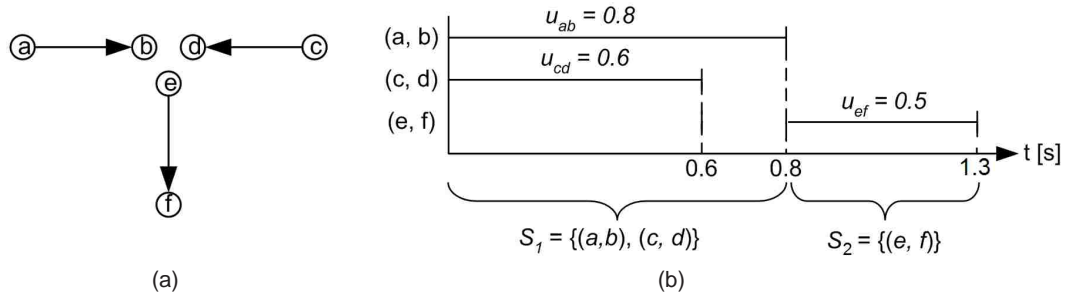
Figure 5.3: (a) Network topology, where links $(a, b), (c, d)$, and (e, f) are to be scheduled. (b) Operation of GSI, assuming that at most two links can be simultaneously scheduled at any time. The times allocated to S_1 and S_2 are $\tau_1 = 0.8$ and $\tau_2 = 0.5$.

At $t = 0.8$, a new maximal set S_2 is created with those links that were not scheduled yet, namely link (e, f). The fraction of time allocated to S_2 is $\tau_2 = 0.5$ seconds.

GSI constitutes the first algorithm designed for scheduling in (M, K, β)-networks. In the following section, we will present an approximation algorithm which is based on GSI.

5.3 Approximation-based Scheduler Under MPR Protocol Model

In this section, we present an *Approximation-based Scheduler* (AS), a variant of GSI proposed in Section 5.2. While the schedulable sets $S_1, S_2, ... S_{|\Gamma_{GSI}|}$ built by GSI are disjoints (i.e., $S_i \cap S_j = \{\}$, for all $i \neq j$, $i, j \in \{1, 2, ..., |\Gamma_{GSI}|\}$), AS constructs schedulable sets which may have common links.

Before describing AS, we will give the definition of an approximation algorithm for the scheduling subproblem in wireless networks. The objective of the subproblem is the minimization of the schedule period, such that every link $(i, j) \in E_{RT\text{-}LP}$ is scheduled for at least a fraction of time u_{ij} given by Equation (5.9). We will denote

the schedule period produced by the optimal scheduler as τ_{OPT}. An approximation algorithm is one that produces a feasible solution whose schedule period is *close* to the optimal; by close we mean within a guaranteed factor of optimality. Thus, we say that AS is an κ-factor approximation algorithm if the expected period of its solution is $\tau_{AS} \leq \kappa \cdot \tau_{OPT}$, for $\kappa > 1$.

Algorithm Description

AS schedules all the links in $E_{RT\text{-}LP}$ by finding maximal schedulable sets. Consider again the utilization of a link (i, j) given by Equation (5.9):

$$
\begin{aligned}
u_{ij} &= \frac{\text{total number of bits routed through link } (i, j)}{\text{capacity of link } (i, j)} \\
&= \frac{\sum_{n \in N} x_{ij}^n}{\omega_{ij}},
\end{aligned}
\tag{5.16}
$$

where $\sum_{n \in N} x_{ij}^n$ is the flow through link (i, j) resulting from step 1. The scheduling algorithm schedules links in such a way that every link (i, j) can send the amount of flow $\sum_{n \in N} x_{ij}^n$ during a schedule period. AS schedules links one by one, in an arbitrary order, until a maximal set S_1 is obtained. The fraction of time allocated to S_1 is equal to the minimum link utilization among all links in S_1, i.e.,

$$
\tau_1 = \min\{u_{ij} | (i, j) \in S_1\}.
\tag{5.17}
$$

Let $l = \text{argmin } \{u_{ij} | (i, j) \in S_1\}$. Note that by scheduling S_1 for τ_1 seconds, link l can send $u_{ij} \cdot c_{ij} = \sum_{n \in N} x_{ij}^n$ bits during this period. Thus, l is then removed from S_1, and is not considered for any subsequent set. The remaining links form a new set S_2, which becomes maximal by adding new links not scheduled yet. Successive sets are found iteratively in a similar way. Consider a general iteration when S_k is
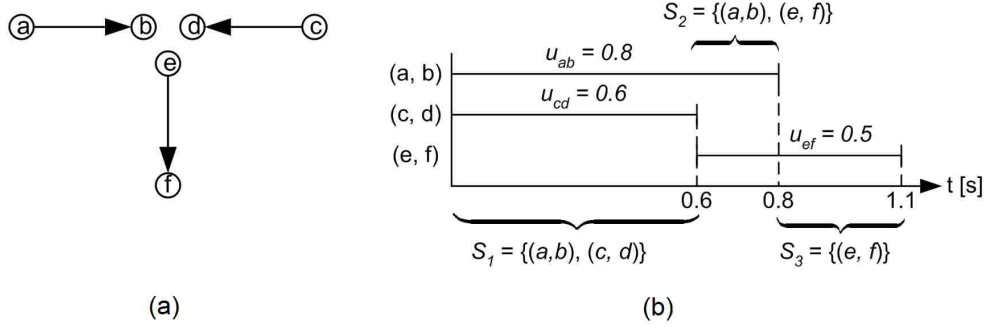
Figure 5.4: (a) Network topology, where links $(a, b), (c, d)$ and (e, f) are to be scheduled. (b) Operation of the approximation algorithm scheduler, assuming that at most two links can be simultaneously scheduled at any time. The times allocated to $S_1, S_2,$ and S_3 are $\tau_1 = 0.6$, $\tau_2 = 0.2$ and $\tau_3 = 0.3$.

being created, and sets $S_1, ..., S_{k-1}$ have already been built. Define the residual link utilization of a link (i, j) as:

$$u'_{ij} = u_{ij} - \sum_{\forall k' \in \{1,2,...,k-1\}|(i,j) \in S_{k'}} \tau_{k'}. \tag{5.18}$$

For a general iteration k, Equation (5.17) can be rewritten as:

$$\tau_k = \min\{u'_{ij}|(i, j) \in S_k\}. \tag{5.19}$$

The process is repeated until all link $(i, j) \in E_{LP1}$ has been scheduled for a fraction of time u_{ij}. The operation of the algorithm is illustrated with the following example.

Example 5.2. Consider the three links of Figure 5.4(a) with the respective link utilizations: $u_{ab} = 0.8$, $u_{cd} = 0.6$ and $u_{ef} = 0.5$. Assume that links interferer with each other, and $K = 2$ (i.e., at most 2 links can be scheduled simultaneously). The operation of the scheduling algorithm is shown in Figure 5.4(b). AS starts by scheduling (a, b) and (c, d), which constitute S_1. At $t = 0.6$, link (c, d) is removed from S_1. The time allocated to S_1 is $\tau_1 = 0.6$. The algorithm then schedules link

---

Approximation-based Scheduler (AS)

1: INPUT: $E_{RT\text{-}LP}$, $G(V, E)$
2: OUTPUT: Set Γ_{AS} of schedulable sets.

3: $u'_{ij} = u_{ij}, \forall (i, j) \in E_{RT\text{-}LP}$;
4: $\Gamma_{AS} = \{\}$; $S_0 = \{\}$; $t = 0$; $k = 0$;
5: **while** $(\exists\, (i, j)| u'_{ij} > 0)$ **do**
6:     $k = k + 1$;
7:     $S_k = S_{k-1}$;
8:     **while** $\exists\, (i, j) \in E_{RT\text{-}LP}| \mathcal{E}(S_k \cup \{(i, j)\})$ **do**
9:         $S_k = S_k \cup \{(i, j)\}$;
10:         $E_{RT\text{-}LP} = E_{RT\text{-}LP} - \{(i, j)\}$;
11:     **end while**
12:     $\Gamma_{AS} = \Gamma_{AS} \cup S_k$;
13:     $e = \mathrm{argmin}\{u'_e| e \in S_k\}$;
14:     $\tau_k = u'_e$;
15:     $u'_{ij} = u'_{ij} - u'_e, \forall (i, j) \in S_k$;
16:     $S_k = S_k - \{e\}$;
17: **end while**
18: **return** Γ_{AS};

Figure 5.5: Approximation-based Scheduler (AS). $\mathcal{E}(S)$ stands for the event $\mathcal{E}(S) =$ {Equations (4.6) and (4.7) are satisfied for all $(i, j) \in S$}.

(e, f), so that $S_2 = \{(a, b), (e, f)\}$. At time 0.8, (a, b) is removed from S_2 and $\tau_2 = 0.2$ by applying Equation (5.19). Similarly, S_3 is allocated $\tau_3 = 0.3$ seconds.

The pseudo-code of AS is shown in Figure 5.5. In lines 7-11, links are added one by one until a maximal set is created. In line 16, the link with minimum residual utilization is removed from S_k, so that a new maximal set is created in the next iteration.

Throughput Performance of AS

To find the throughput produced AS, we can do a similar analysis to reach to the expression given by Equation (5.13). Specifically, let

$$\tau_{AS} = \sum_{k=1}^{|\Gamma_{AS}|} \tau_k \tag{5.20}$$

be the schedule period, where τ_k is the fraction of time allocated to set S_k and is given by Equation (5.19). Then, the throughput is:

$$F_{AS} = \frac{\text{end-to-end bits transmitted during a schedule period}}{\text{schedule period}} \tag{5.21}$$

$$= \frac{F_{RT\text{-}LP}}{\tau_{AS}}. \tag{5.22}$$

From scheduling theory, AS can be seen as an approximation algorithm for the *minimum makespan scheduling problem* (MMSP) [43]. In the context of wireless scheduling, MMSP can be stated as follows: given processing times (link utilizations) of $|E_{RT\text{-}LP}|$ jobs (links), find an scheduling order of the jobs (links) so that the completion time, also called makespan, is minimized. AS may be considered as a factor two optimal scheduler under certain conditions, as stated in *Theorem 5.1*.

Theorem 5.1 *Factor two optimality of AS. Let $E' = \{e_1, e_2, ..., e_{|E'|}\}$ be the set of links to be scheduled by AS, and $u_1, u_2, ..., u_{|E'|}$ be the corresponding link utilizations. In a fully-connected $(M, K, 2\pi)$-network with $M \geq K$, and in a single-hop MPR-capable network where the transmissions are directed to a central node (e.g., a base station), the schedule period is guaranteed to be factor two optimal.*

Proof:
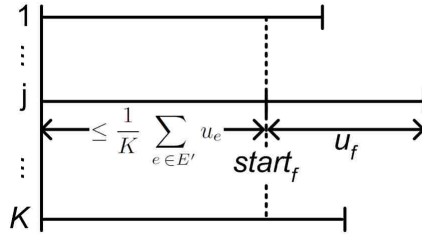For the two types of network topologies referred in the theorem, K links can be

Figure 5.6: Operation of the scheduling algorithm. Since the algorithm creates maximal schedulable sets, K links are always active until at $t = start_f$, the time the link with larger completion time is scheduled. This implies that $start_f \leq \frac{1}{K} \sum_{e \in E'} u_e$.

simultaneously scheduled. This is illustrated in Figure 5.6, where there is a *timeline* for each scheduled link. Let e_f be the link with the larger completion time (i.e., link e_f is scheduled until the completion time of the whole schedule), and $start_f$ be the time e_f is scheduled. Since the algorithm creates maximal sets, all the timelines are *busy* until $start_f$ (otherwise, the schedulable set prior to $start_f$ would not be maximal, and the algorithm would have already scheduled e_f). From this observation, it follows that $start_f$ is less than or equal to the *average timeline*:

$$start_f \leq \frac{1}{K} \sum_{e \in E'} u_e. \tag{5.23}$$

The average timeline, on the other hand, can be considered as a lower bound of any schedule period; i.e., the optimal schedule period τ_{OPT} is at least the total duration of all link utilizations divided by K. In addition, τ_{OPT} is at least equal to the largest link utilization. These two lower bounds can be expressed as:

$$\frac{1}{K} \sum_{e \in E'} u_e \leq \tau_{OPT}, \tag{5.24}$$

$$\max_{e \in E'}\{u_e\} \leq \tau_{OPT}. \tag{5.25}$$

By combining Equations (5.24) and (5.25) with Equation (5.23), we can express the schedule period τ_{AS} of the algorithm as:

$$\tau_{AS} = start_f + u_f \leq 2\tau_{OPT},$$

<div align="right">(5.26)</div>

which proves *Theorem 5.1*.

As for GSI, AS may not produce a feasible schedule as defined in *Definition 4.4*. However, by modifying the allocation times as

$$\lambda_k = \frac{\tau_k}{\tau_{AS}},$$

<div align="right">(5.27)</div>

we have that *Definition 4.4* is satisfied and the throughput given by Equation (5.22) holds.

5.4 Greedy Scheduler Under Multi-Access Channel Model

In Sections 5.2 and 5.3, we presented two scheduling algorithms that satisfy the feasibility conditions for scheduling under the MPR protocol model, as stated in *Definition 4.2*. In this section, we present a scheduling algorithm that satisfies the additional constraint imposed by multi-access channel, namely Equation (4.10).

Algorithm Description

The algorithm, called *Greedy Scheduler II* (GSII), not only creates schedulable sets according to *Definition 4.3*, but also computes link capacities that lie inside the capacity region of the corresponding receiver nodes. GSII is shown in Figure 5.7.

Greedy Scheduler II (GSII)

1: INPUT: $E_{RT\text{-}LP}$, $G(V, E)$;
2: OUTPUT: $\Gamma_{GSII} = \{S_1, S_2, ..., S_{|\Gamma_{GSII}|}\}$, $c_{ij}(S)$, $\forall (i,j) \in S, \forall S \in \Gamma_{GSII}$;
3: $\Gamma_{GSII} = \{\}$; $k = 0$;
4: $nt_j = |\{i|(i,j) \in E_{LP-RT}\}|$; $\forall j \in V$;
5: **while** $E_{LP-RT} \neq \{\}$ **do**
6: $\quad k = k + 1$; $S_k = \{\}$;
7: $\quad$ **while** $\exists (i,j) \in E_{RT\text{-}LP}$ and $\mathcal{E}(S_k \cup \{i,j\})$ **do**
8: $\quad\quad j = \arg\max\{nt_j | \exists (i,j) \in E_{RT\text{-}LP}$ and $\mathcal{E}(S_k \cup \{i,j\})\}$;
9: $\quad\quad \Psi_j = \{i'|(i',j') \in S_k, j \neq j'$, and $\frac{-\beta}{2} \leq \alpha_{i'j} \leq \frac{\beta}{2}\}$;
10: $\quad\quad \eta_j = \eta + \sum_{i' \in \Psi_j} P_{i'j}$;
11: $\quad\quad$ **while** $\exists (i,j) \in E_{RT\text{-}LP}$ and $\mathcal{E}(S_k \cup \{i,j\})$ **do**
12: $\quad\quad\quad (i,j) = \arg\max\{r_{ij} | \exists (i,j) \in E_{RT\text{-}LP}$ and $\mathcal{E}(S_k \cup \{i,j\})\}$;
13: $\quad\quad\quad S_k = S_k \cup \{(i,j)\}$; $E_{RT\text{-}LP} = E_{RT\text{-}LP} - \{(i,j)\}$; $nt_j = nt_j - 1$;
14: $\quad\quad\quad \eta_{ij} = \eta_j + \sum_{t:(t,j) \in S_k} P_{tj}$;
15: $\quad\quad\quad c_{ij}(S_k) = \varphi\left(\frac{P_{ij}}{\eta_{ij}}\right)$;
16: $\quad\quad\quad$ **for all** $(i',j') \in S_k | j \neq j'$ and $\frac{-\beta}{2} \leq \alpha_{ij'} \leq \frac{\beta}{2}$ **do**
17: $\quad\quad\quad\quad \eta_{i'j'} = \eta_{i'j'} + P_{ij'}$; // link (i,j) adds noise to (i',j')
18: $\quad\quad\quad\quad c_{i'j'}(S_k) = \varphi\left(\frac{P_{i'j'}}{\eta_{i'j'}}\right)$;
19: $\quad\quad\quad$ **end for**
20: $\quad\quad$ **end while**
21: $\quad$ **end while**
22: $\quad \Gamma_{GSII} = \Gamma_{GSII} \cup S_k$;
23: **end while**

Figure 5.7: Scheduling algorithm. $\mathcal{E}(S)$ stands for the event $\mathcal{E}(S) = \{$Equations (4.8) and (4.9) are satisfied for all $(i,j) \in S\}$.

The algorithm schedules, one by one, all links in $E_{RT\text{-}LP}$ until a maximal set is created. Once the set becomes maximal, GSII creates a new schedulable set with those links not scheduled yet in previous sets. Line 8 selects the receiver node, denoted by j, with the largest number of transmitters to that node. Then, lines 11-20 schedule as many links with node j as receiver as possible, so that the multi-access channel at node j is fully exploited. At line 12, a link (i,j) is chosen in decreasing order of distance between nodes i and j, to compensate the inferior capacity of the link (first links to be scheduled experience less interference, as explained below). The

noise η_{ij} experienced by a link (i,j) is computed in line 14 and consists of destructive interference (the first term, which is given by Equation (2.18)) and constructive interference (the second term). The latter refers to the power from the links previously scheduled to the same schedulable set, which also have node j as receiver. Finally, line 15 computes the capacity $c_{ij}(S_k)$ the link (i,j) will operate at.

A key question regarding GSII is whether the link capacity assigned at line 15 is achievable. The following theorem shows that links operate at max-capacity, and therefore the capacities are achievable.

Theorem 5.2 *Let $(i_1, j), (i_2, j), ..., (i_H, j)$ be a set of $H \leq K$ links scheduled by GSII in this order, which belong to the same schedulable set. Then, they operate at max-capacity.*

Proof: The proof is by induction. Since all links belong to the same schedulable set, we will omit the identifier of the set.

Basis step: assume that links $(i_1, j), (i_2, j)$ are scheduled in this order. The capacity of the links are (line 15):

$$
\begin{aligned}
c_{i_1 j} &= \varphi\left(\frac{P_{i_1 j}}{\eta_{i_1 j}}\right) = \varphi\left(\frac{P_{i_1 j}}{\eta_j}\right), \\
c_{i_2 j} &= \varphi\left(\frac{P_{i_2 j}}{\eta_{i_2 j}}\right) = \varphi\left(\frac{P_{i_2 j}}{\eta_j + P_{i_1 j}}\right)
\end{aligned}
$$

where $\eta_j = \eta + \sum_{t \in \Psi_j} P_{tj}$ represents the destructive interference. By adding the capacity of the two links we obtain:

$$
\begin{aligned}
c_{i_1 j} + c_{i_2 j} &= W \log_2\left(\frac{n_j + P_{i_1 j}}{n_j} \cdot \frac{n_j + P_{i_1 j} + P_{i_2 j}}{n_j + P_{i_1 j}}\right), \\
&= W \log_2\left(1 + \frac{P_{i_1 j} + P_{i_2 j}}{n_j}\right),
\end{aligned}
$$

which proves that links (i_1, j) and (i_2, j) operate at max-capacity.

Extension step: assume that links $(i_1, j), (i_2, j), ..., (i_{H-1}, j)$ were already scheduled by GSII and operate at max-capacity:

$$\sum_{h=1}^{H-1} c_{i_h j} = W \log_2 \left(1 + \frac{\sum_{h=1}^{H-1} P_{i_h j}}{\eta_j} \right).$$

GSII then schedules the Hth link having node j as receiver, with a capacity assigned in line 15 as:

$$c_{i_H j} = \varphi \left(\frac{P_{i_H j}}{\eta_{i_H j}} \right) = W \log_2 \left(1 + \frac{P_{i_H j}}{\eta_j + \sum_{h=1}^{H-1} P_{i_h j}} \right).$$

The sum of the capacity of the links is:

$$
\begin{aligned}
\sum_{h=1}^{H} c_{i_h j} &= c_{i_H j} + \sum_{h=1}^{H-1} c_{i_h j} = W \log_2 \left(1 + \frac{P_{i_H j}}{\eta_j + \sum_{h=1}^{H-1} P_{i_h j}} \right) + \\
&\quad W \log_2 \left(1 + \frac{\sum_{h=1}^{H-1} P_{i_h j}}{\eta_j} \right) \\
&= W \log_2 \left(\frac{\eta_j + \sum_{h=1}^{H-1} P_{i_h j} + P_{i_H j}}{\eta_j + \sum_{h=1}^{H-1} P_{i_h j}} \cdot \frac{\eta_j + \sum_{h=1}^{H-1} P_{i_h j}}{n_j} \right) \\
&= W \log_2 \left(1 + \frac{\sum_{h=1}^{H} P_{i_h j}}{n_j} \right),
\end{aligned}
$$

which demonstrates *Theorem 5.2.*

For a given receiver node j, *Theorem 5.2* guarantees that the capacity of the links having node j as receiver is one of the $H!$ vertices of the capacity region in the positive quadrant. Those capacities are therefore achievable with SIC and CDMA.

Since the link capacity vector is a vertex of the capacity region, it is achievable. Thus, we have the following corollary.

Corollary 5.1 *Let $(i_1, j), (i_2, j), ..., (i_H, j)$ be a set of $H \leq K$ links scheduled by GSII in this order, which belong to the same schedulable set. Then, the associated link capacity vector lies inside the capacity region of the multi-access channel of receiver node j.*

Throughput Performance of GSII

In order to compute an achievable throughput of GSII, consider the following allocation policy. Let τ_k be the fraction of time allocated to the schedulable set S_k, $k \in \{1, 2, ..., |\Gamma_{GSII}|\}$, which is given by the following equation:

$$\tau_k = \max \left\{ \frac{\sum_{n \in N} x_{ij}^n}{c_{ij}(S_k)} \right\}, \tag{5.28}$$

where $\sum_{n \in N} x_{ij}^n$ is the flow through link (i, j) assigned by RT-LP, and $c_{ij}(S_k)$ is the capacity of the link (i, j) when scheduled in S_k. Define the period of the schedule produced by GSII as:

$$\tau_{GSII} = \sum_{k=1}^{|\Gamma_{GSII}|} \tau_k. \tag{5.29}$$

From Equation (5.28), we can conclude that GSII guarantees that every link can send at least $\sum_{n \in N} x_{ij}^n$ bits during a schedule period. Consequently, the corresponding throughput is:

$$F_{GSII} = \frac{\text{end-to-end bits transmitted during a schedule period}}{\text{schedule period}} \tag{5.30}$$

$$= \frac{F_{RT-LP}}{\tau_{GSII}}. \tag{5.31}$$

As for GSI and AS, GSII may not produce a feasible schedule as defined in *Definition 4.4*. However, by modifying the allocation times as

$$\lambda_k = \frac{\tau_k}{\tau_{GSII}}, \tag{5.32}$$

we have that *Definition 4.4* is satisfied and the throughput given by Equation (5.31) holds.

5.5   Optimality of GSI, AS, and GSII

The solution obtained by GSI, AS, and GSII are feasible schedules and constitute solutions for the joint routing and scheduling problem. However, they do not guarantee optimality with respect to the schedulable sets they find. For example, suppose Γ_{GSI} is the set of schedulable sets found by GSI. Then, the allocation times τ_1, τ_2, ..., $\tau_{|\Gamma_{GSI}|}$ may not be optimal with respect to Γ_{GSI} (i.e., there may be a better allocation time policy that only uses the same set of schedulable sets). To find such an optimal solution, we need to apply step 3, which is presented in next section.

5.6   Joint Routing and Scheduling Linear Program

In the previous section, we presented three scheduling algorithms which produce feasible solutions for the joint routing and scheduling problem, where the corresponding throughput are given by Equations (5.13), (5.22), and (5.31). For a compact presentation, let F_A and Γ_A be the throughput and the set of schedulable sets found in step 2, where A refers to the scheduling algorithm GSI, AS, or GSII; i.e.,

$$
F_A \;=\; \begin{cases} F_{GSI} = \frac{F_{RT-LP}}{\tau_{GSI}}; & \text{if GSI is used in step 2;} \\[2mm] F_{AS} = \frac{F_{RT-LP}}{\tau_{AS}}; & \text{if AS is used in step 2;} \\[2mm] F_{GSII} = \frac{F_{RT-LP}}{\tau_{GSII}}; & \text{if GSII is used in step 2;} \end{cases} \tag{5.33}
$$

$$
\Gamma_A \;=\; \begin{cases} \Gamma_{GSI}; & \text{if GSI is used in step 2;} \\[2mm] \Gamma_{AS}; & \text{if GSI is used in step 2;} \\[2mm] \Gamma_{GSII}; & \text{if GSII is used in step 2.} \end{cases} \tag{5.34}
$$

The throughput F_A may not optimal with respect to Γ_A. The optimal allocation time policy which produces F_{OPT} that uses the same set Γ_A may be found by solving a variant of RTSCH-LP. The linear program is shown in Figure 5.8.

$$\max_{\Gamma' \subseteq \Gamma_A} F_{RTSCH\text{-}LP} \quad = \quad \sum_{n \in N} f_n \tag{5.35}$$

$$\sum_{j:(i,j) \in E} x_{ij}^n - \sum_{j:(j,i) \in E} x_{ji}^n \quad = \quad \begin{cases} f_n; \text{if } i = s_n \\ -f_n; \text{if } i = d_n \quad n \in N \\ 0; \text{otherwise} \end{cases} \tag{5.36}$$

$$\sum_{n \in N} x_{ij}^n \quad \leq \quad \sum_{\forall k \in \{1,2,...,|\Gamma_A|\}|(i,j) \in S_k} \lambda_k c_{ij}(S_k); (i,j) \in E \tag{5.37}$$

$$\sum_{k=1}^{|\Gamma_A|} \lambda_k \quad = \quad 1 \tag{5.38}$$

$$f_n \quad \geq \quad 0; n \in N \tag{5.39}$$

$$x_{ij}^n \quad \geq \quad 0; n \in N, (i,j) \in E \tag{5.40}$$

$$\lambda_k \quad \geq \quad 0; k \in \{1, 2, ..., |\Gamma_A|\} \tag{5.41}$$

Figure 5.8: Joint routing and scheduling linear program used in step 3.

Note the difference between the linear programs in Figures 4.3 and 5.8. While the former is optimized over all set $\Gamma' \subseteq \Gamma$, the latter is only optimized over all set $\Gamma' \subseteq \Gamma_A$. Since Γ is the set of all schedulable sets, its size is exponentially large on the number of links, i.e., $|\Gamma| = \Theta(2^{|E|})$, and the problem in Figure 4.3 is NP-hard. On the other hand, $|\Gamma_A| = \Theta(|E|)$, and the problem in Figure 5.8 can be solved in polynomial time. As a result, we have the following theorem.

Theorem 5.3 *Optimality of the proposed scheme. The solution obtained from the linear program shown in Figure 5.1 is better than any other schedule that only uses the schedulable sets in Γ_A.*

The proof is straightforward. Assuming that the problem is non-degenerate, then there is a unique global optimal solution, which can be found by a linear programming algorithm. This solution is guaranteed to be optimal. *Theorem 5.3* permits to obtain a lower bound on throughput, as presented below.

Upper and Lower Bounds on Throughput

As a consequence of *Theorem 5.3*, the throughput $F_{RTSCH\text{-}LP}$ given by Equation (5.35) is lower bounded by the throughput produced by the scheduling algorithm, F_A. At the same time, $F_{RTSCH\text{-}LP}$ is clearly upper bounded by F_{RT-LP}, which is the throughput obtained by the routing linear program. These bounds are expressed as:

$$F_A = \frac{F_{RT\text{-}LP}}{\tau_A} \leq F_{RTSCH\text{-}LP} \leq F_{RT\text{-}LP}, \tag{5.42}$$

where A refers to GSI, AS, or GSII, depending of the scheduling algorithm used in step 2. In Chapter 6 we will see some numerical examples, showing how close to the upper bound the throughput obtained by the proposed scheme is.

5.7 Complexity Analysis

To demonstrate that the heuristic has a polynomial running time, we will show that the running time and the size (number of variables and constraints) of steps 1 and 3 are bounded (step 2 is either a greedy approach or an approximation algorithm, which obviously run in polynomial time). Step 1 is a linear program (Figure 5.1), with $|N| + |N| \cdot |E|$ total positive flow variables (Equations (5.4) and (5.5)). The number of flow conservation (Equation (5.2)) and link capacity (Equation (5.3)) constraints are $|N| \cdot |V|$ and $|E|$ respectively. Thus, the number of variables and constraints are polynomially bounded in $|N| \cdot |E|$ and can be solved by a polynomial time linear programming algorithm. The linear program of step 3 (Figure 5.8) is similar to LP-RT, except that one additional constraint is added, namely Equation (5.38), and $O(|E|)$ additional variables (i.e., the activity period variables). Therefore, the running time of step 1 and step 2 using an interior-point method is $O(|E|^3|N|^3)$ [22].

5.8 Summary

In this chapter, we have presented polynomial time schemes based on a combination of greedy, approximation algorithm, and linear programming paradigms to solve the joint routing and scheduling problem in MPR-capable networks. We have discussed how the routing subproblem can be solved by using linear programming. For the scheduling subproblem, we have firstly devised a simple greedy algorithm. Then, we have presented an approximation algorithm, which was shown to produce a factor two optimal schedule period under certain conditions. For multi-access channels, we have further proposed a greedy algorithm that not only creates schedulable sets but also computes rates or link capacities that lie inside the capacity regions of the corresponding receiver nodes. Finally, we have discussed how to solve the joint routing and scheduling problem by using only the schedulable sets found by the scheduling algorithms. In the next chapter, we will see numerical examples and their resolutions according to the schemes presented in this chapter.

Chapter 6

Performance Studies

In this chapter, we present numerical examples based on the schemes presented in Chapter 5. The algorithms were implemented as a solver in C language. To solve linear programs, the solver incorporates the library LP-solve [45]. This library is a source code written in ANSI C, which implements the Simplex algorithm for linear programming as well as branch and bound algorithms for mixed integer linear programming.

We have conducted performance studies using the JRS schemes presented in Chapter 5. According to the scheduling algorithm used in step 2, there can be three variants of JRS. The first variant uses the GSI algorithm presented in Section 5.2. Similarly, the second and third variants use AS and GSII algorithms presented in Sections 5.3 and 5.4 respectively.

The chapter starts by presenting numerical results using JRS with GSI as scheduler in Section 6.1. We apply this scheme to solve the throughput optimization problem under the MPR protocol model; i.e., interference is modeled according to the MPR protocol model presented in Section 2.3.1. Then, Section 6.2 shows numerical results using JRS with GSII as scheduler. In the latter, the interference is

modeled according to the multi-access channel presented in Section 2.3.2.

6.1 Performance Studies Under the MPR Protocol Model

All the examples shown in this section were obtained with the same parameter values. Referring back to Equations (2.12) and (2.13), we set $W = 1$, and a link capacity $c_{ij} = 10$ units when the distance r_{ij} between nodes i and j is equal to R (maximum distance from which a node can decode a packet). The path loss exponent γ was set to 4, which corresponds to the two-ray model. Having set these values, any link capacity can be computed according to Equations (2.12) and (2.13).

The results were evaluated in terms of $F_{RTSCH\text{-}LP}$, the objective function of the joint routing and scheduling problem (Equation (5.35)), and normalized to the upper bound $F_{RT\text{-}LP-RT}$ (Equation (5.1)); i.e.,

$$\text{Normalized throughput} = \frac{F_{RTSCH\text{-}LP}}{F_{RT\text{-}LP}}. \tag{6.1}$$

We simulated grid and random topologies. For the first topology, we included the results produced by JRS with GSI as scheduling algorithm (JRS-GSI), and by the shortest path (SP) approach. The results from JRS-GSI are denoted as JRS, since there is no name ambiguity. This comparison permits to visualize the improvement with respect to current routing protocols used in wireless networks [8], which are based on SP. For the second topology, we only analyze the results of the JRS approach. We include results for both (M, K, β)-networks and half-duplex networks. This comparison shows the gain obtained by the former type of networks with respect to the latter, which was proposed in previous work [16].

Grid Topology

We start with an illustrative example in the 16-node grid topology shown in Figure 6.1. R was set to $\sqrt{2}D$, where D is defined in Figure 6.1. Node 0 is the source node, and node 15 the destination. If all the links were scheduled simultaneously, an optimal solution would route the flow through 3 different paths, which may be the paths shown in Figure 6.1. A shortest path approach, on the other hand, only uses path 1. In this example, we use the max-flow min-cut theorem to find an upper bound (UB) on throughput. The capacity of the source cut is limited by the number of transmit antennas. The three links incident to node 0 may be simultaneously scheduled only if node 0 has 3 transmit antennas. Similarly, the capacity of the
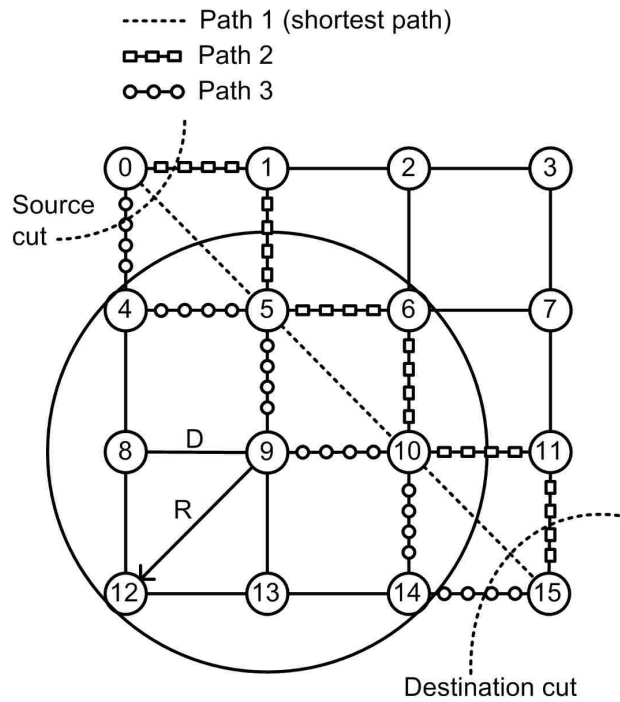
Figure 6.1: Grid topology.

destination cut is limited by the number of incident links to node 15 simultaneously scheduled. To schedule those links at the same time, K should be equal or greater than 3. A cut capacity involving other nodes depends on K and M as well.

Impact of the Number of Transmit Antennas

Figure 6.2 shows the numerical results for nodes endowed with directional antennas, with $\beta = \frac{\pi}{3}$. Table 6.1 shows the schedulable sets and allocated time for different
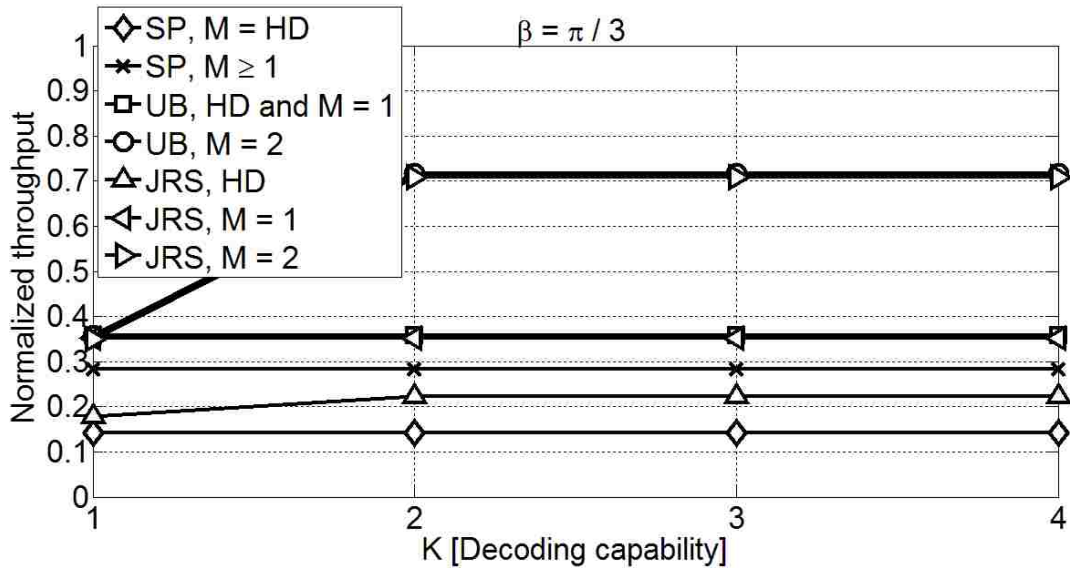
Figure 6.2: Throughput vs K, for $\beta = \frac{\pi}{3}$.

values of M and K. For half-duplex (HD) systems, the SP approach, which routes packets through path 1, needs two schedulable sets to route the flow and to produce a throughput of 0.14. JRS routes through paths 2 and 3, and schedules four sets to achieve a throughput of about 0.17.

For $M = 1$ (i.e., one exclusive transmit antenna), SP doubles its throughput to 0.28 by scheduling the three links in only one set. Note that, because of the use of directional antennas, links do not interfere with each other. Additionally,

Table 6.1. Schedulable sets and allocated time, for $\beta = \frac{\pi}{3}$.

	Sets and corresponding allocated times
SP, HD	$S_1 = \{(0,5),(10,15)\}, S_2 = \{(5,10)\}, \lambda_1 = \lambda_2 = 0.5$
SP, $M \geq 1$	$S_1 = \{(0,5),(5,10),(10,15)\}, \lambda_1 = 1$
JRS, HD, $K = 1$	$S_1 = \{(0,1),(4,5),(6,10),(11,15)\}$ $S_2 = \{(0,4),(1,5),(9,10),(14,15)\}$ $S_3 = \{(5,6),(10,11)\}$ $S_4 = \{(5,9),(10,14)\}$ $\lambda_1 = \lambda_2 = \lambda_3 = \lambda_4 = 0.25$
JRS, $M = 1$, $K = 1$, ..., 5	$S_1 = \{(0, 4), (4, 5), (5, 9), (9, 10)\ (10, 14), (14, 15)\}, \lambda_1 = 1$
JRS, $M = 2$, $K = 1$	$S_1 = \{(0, 4), (4, 5), (5, 9), (9, 10)\ (10, 14), (14, 15)\}, \lambda_1 = 1$
JRS, $M = 2$, $K > 1$	$S_1 = \{(0, 1), (0, 4), (1, 5), (4, 5), (5, 6), (5, 9), (6, 10), (9, 10), (10, 11), (10, 14), (11, 15), (14, 15)\ \}, \lambda_1 = 1$

incrementing K above 2 does not have any impact. The performance of JRS is also improved to optimal performance by routing through path 2 and scheduling all the links of the route in only one set (see Figure 6.3). Note that the upper bound UB is achieved, which is independent of K because the throughput cannot be further improved with only one transmit antenna per node (i.e., the source node cannot simultaneously send to more than one neighbor at the same time). Note also that JRS routes through path 3 instead of path 1, since we modeled link capacities such that shorter transmission distance implies a higher link capacity. For $M = 2$ (two transmit antennas) and $K = 1$, JRS produces the same solution as for $M = 1$. However, in this case, the limitation is not the number of transmit antennas but the number of incident links simultaneously scheduled to the destination, which is equal to K. For $K > 2$, JRS uses paths 2 and 3 simultaneously, which doubles the throughput to achieve the optimal.
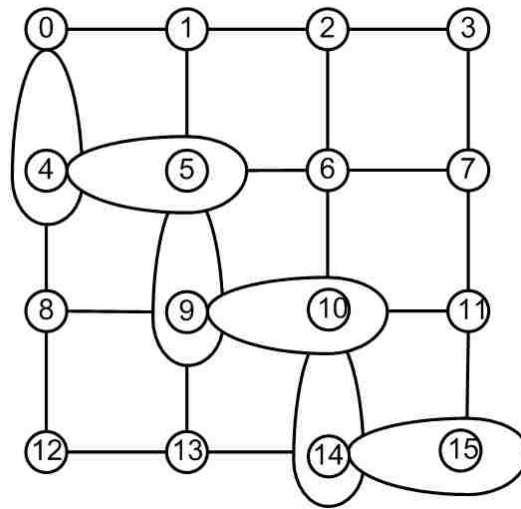
Figure 6.3: Optimal schedule for one transmit antenna with $\beta = \frac{\pi}{3}$.

Impact of the Beamwidth

Figure 6.4 shows the throughput results, for $M = 2$. For $\beta = \frac{\pi}{3}$, the directional transmission permits JRS to achieve the min-cut upper bound. For example, consider
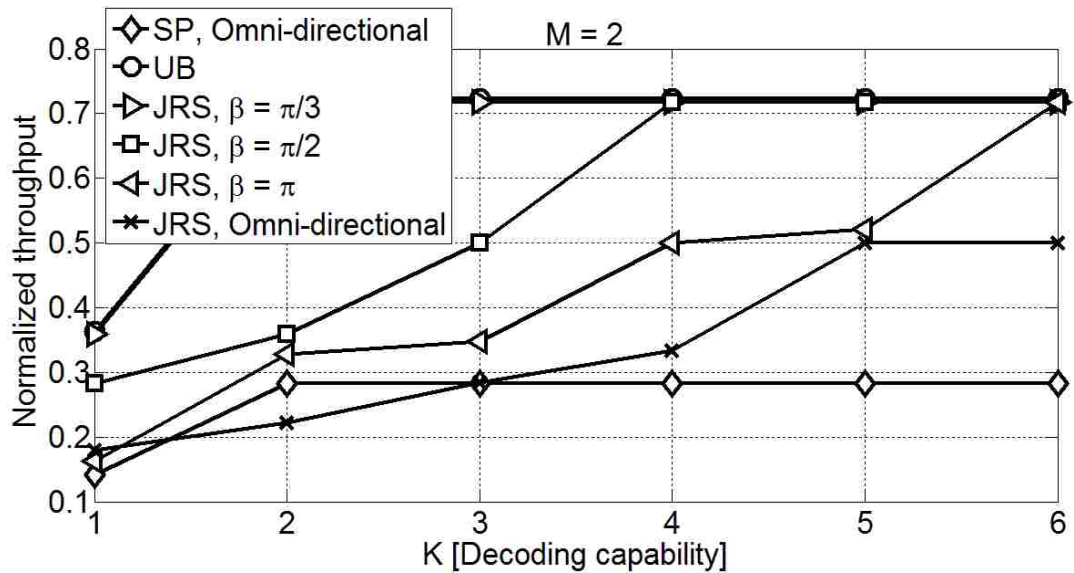

Figure 6.4: Throughput vs K, for $M = 2$, $R = 200$.

the case of K = 1. The optimal solution found with $\beta = \frac{\pi}{3}$ is shown in Figure 6.3. For $\beta \geq \frac{\pi}{2}$, the above solution is not feasible anymore, since transmissions along the path interfere with each other; e.g., the transmission of node 0 (intended for node 4) affects also node 5, which should receive from node 4. The increment in decoding capability, however, permits to approach to optimal throughput with wider beamwidth antennas. For $\beta = \frac{\pi}{2}$ and π, optimal performance is achieved with K $\geq$ 4 and K $\geq$ 6 respectively.

Random Topology
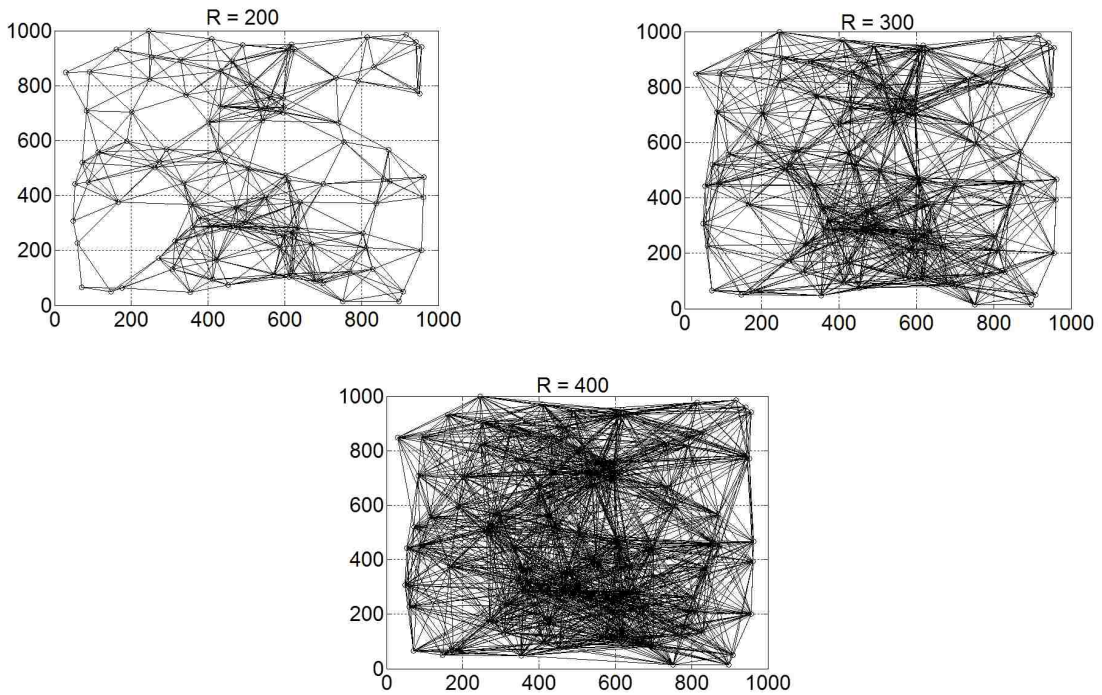
Figure 6.5: Random topology.

We obtained numerical results for the random topologies shown in Figure 6.5. Nodes were uniformly distributed over a 1000 x 1000 square-meter area, where 10 flows were created. The source and destination of each flow were randomly selected.

The path loss exponent and link capacity were set as in the Grid topology. We evaluated the impact of some design parameters, for which several scenarios with different values of β, K, M and R were considered. We only consider the results provided by the JRS.

Impact of the Number of Transmit Antennas

Figure 6.6 shows the throughput as a function of K, for different number of antennas
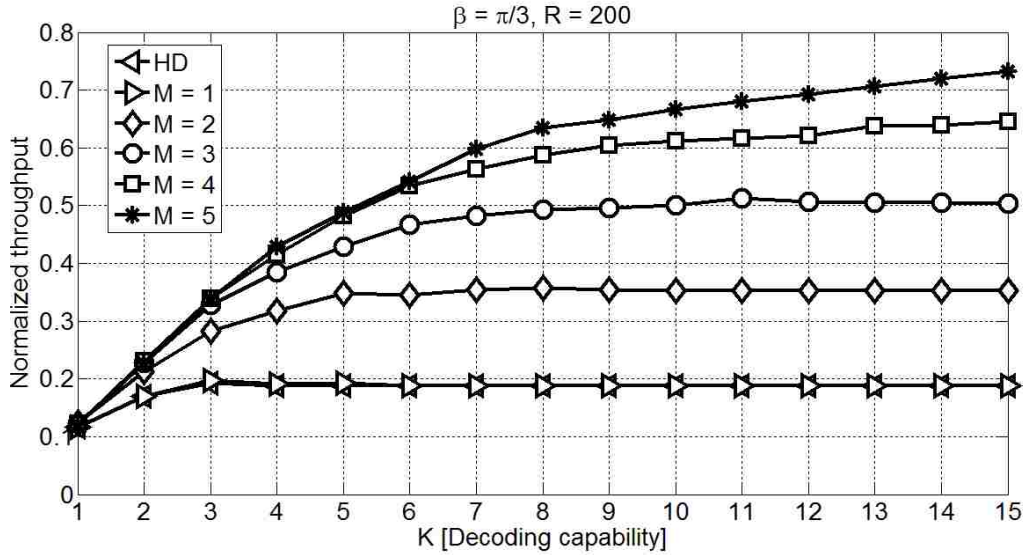
Figure 6.6: Throughput vs K, for $\beta = \frac{\pi}{3}$, $R = 200$.

with $\beta = \frac{\pi}{3}$. Note that the throughput for HD and $M = 1$ increases monotonically until $K = 3$, and that further increments of K have no impact. The corresponding curves are almost overlapped because they have the same bottleneck: only one interface can operate in transmit mode. By adding more transmit antennas, the MPR capability is better exploited and the throughput is increased. Note also that the throughput increases approximately linearly until K equals the number of transmit antennas.

Impact of the Beamwidth

Figure 6.7 shows the curves of throughput vs K, for HD and different values of β.
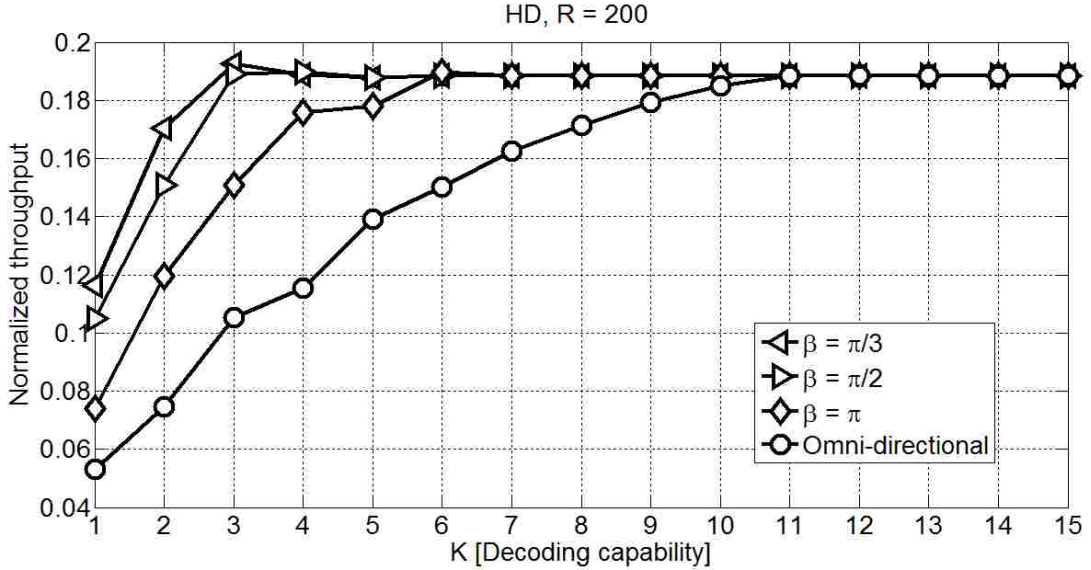
Figure 6.7: Throughput vs K, for $M = HD$, $R = 200$.

The best performance is obtained with the minimum beamwidth value $(\beta = \frac{\pi}{3})$, due to a better spatial reuse. However, the disadvantage of having wider beamwidth antennas can be compensated by increasing the MPR capability; for $M \geq 11$, even the use of omni-directional antennas produces an optimal performance. The effect of using two transmit antennas per node is shown in Figure 6.8: the maximum throughput increases from about 0.19 to 0.35. Note also that, for both, HD and $M = 2$, and for a given value of K, say 5, a beamwidth $\beta = \frac{\pi}{2}$ produces about the same result as a beamwidth $\beta = \frac{\pi}{3}$ (i.e., a beamwidth of $\frac{\pi}{2}$ is narrow enough for optimal performance, and narrower beamwidths would not produce significant improvement). This is better highlighted in Figure 6.9.
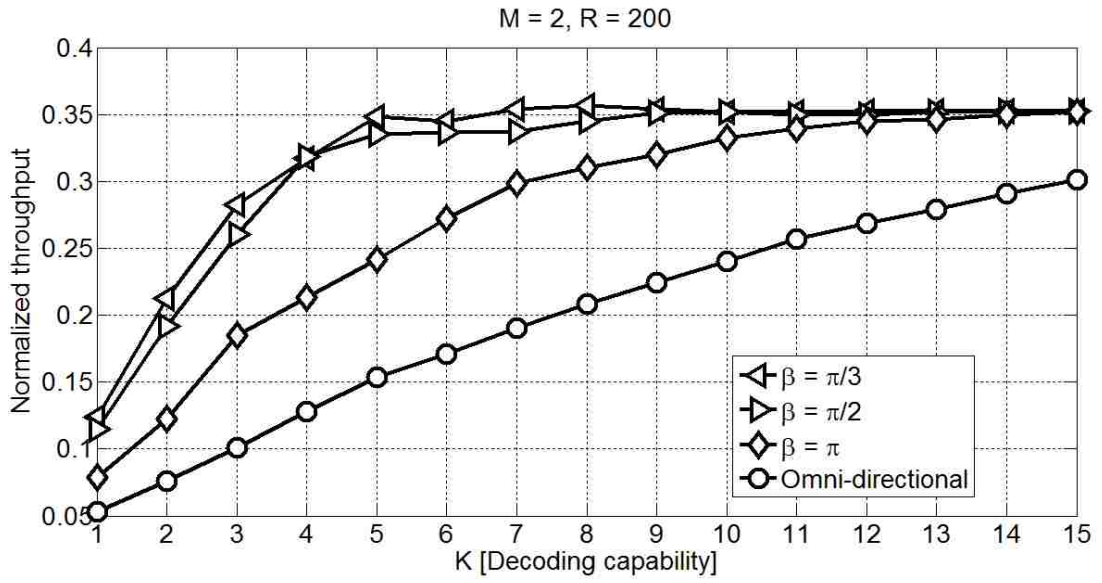
Figure 6.8: Throughput vs K, for $M = 2, R = 200$.

Impact of the Receiver Range R

Figure 6.10 shows, for HD, the normalized throughput $F_{RTSCH\text{-}LP}/F_{RT\text{-}LP}{}'$, where
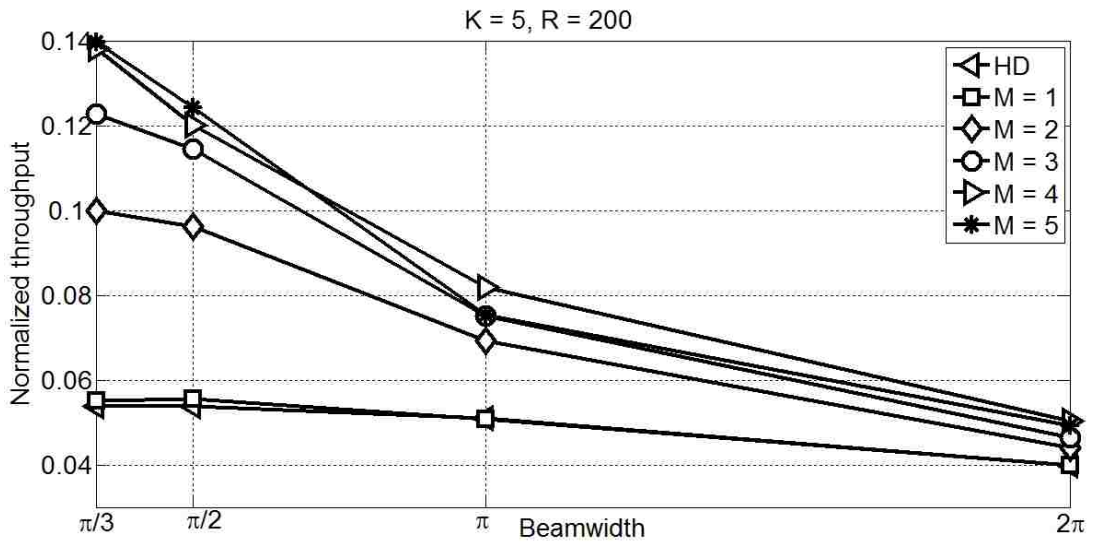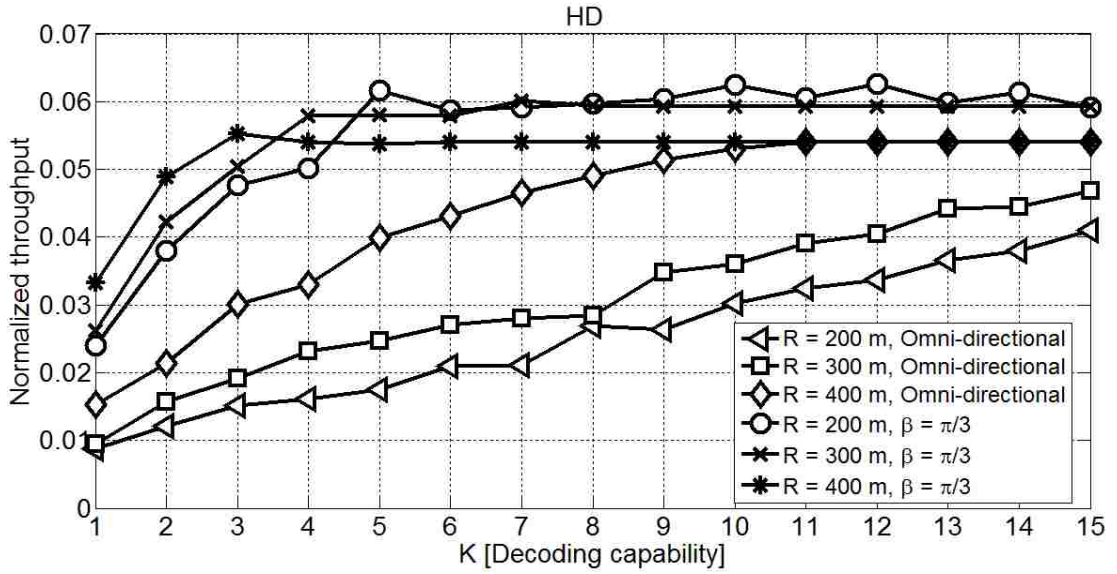

Figure 6.9: Throughput vs beamwidth, for $K = 5, R = 200$.

Figure 6.10: Throughput vs K, for $M = HD$.

$F_{RT\text{-}LP}{}'$ is the flow value when $R = 400$. RT-LP produces the maximum upper bound on throughput when R increases, because of a higher connectivity (the average node degrees for $R = 200$, 300 and 400 meters (m) were 10.26, 21.92 and 35.7 respectively). For omni-directional transmit antennas, the best performance is obtained when $R = 400$; the throughput monotonically increases until 0.054 at $K = 11$, and higher values of K do not produce any improvement. For small values of K, and $R = 200$ or $R = 300$, increments in K produce smaller improvement than for the case of $R = 400$. Similarly, for $\beta = \frac{\pi}{3}$ and $K \leq 3$, the best performance is obtained when $R = 400$. On the other hand, for $K > 4$, higher throughput is obtained when $R = 200$. These results allow us to infer the following: i) for high values of R, the high connectivity permits the routing of flows through short paths in term of hops. Thus, *few links* are needed to be scheduled, which can be achieved with small values of K. For higher values of K, the improvement in throughput is not significant because of two bottlenecks: the large number of conflicting links due to the high connectivity, and the limited number of transmit antennas; ii) for small values of R,

the increments of K have more impact than for the case of high values of R, because more links can be simultaneously scheduled due to the lower connectivity. This last item agrees with the results of the protocol model of Gupta and Kumar [3], where for optimal performance, R should be as small as possible. However, to guarantee connectivity, this value cannot be arbitrarily minimized. Similar conclusions can be obtained by using two transmit antennas per node, as shown in Figure 6.11.
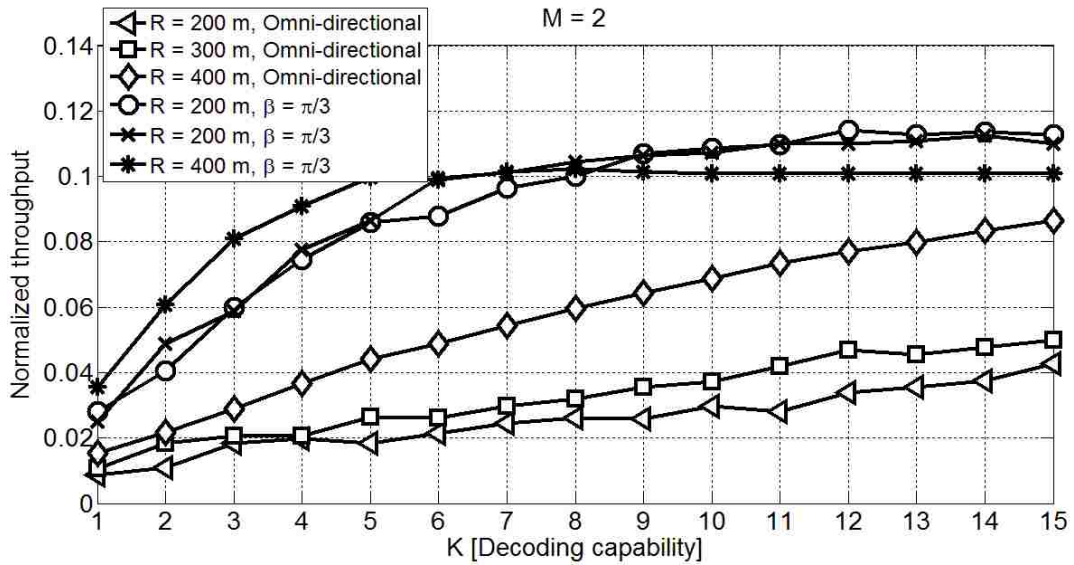

Figure 6.11: Throughput vs K, for $M = 2$.

6.2 Performance Studies Under the Multi-Access Channel Model

In this section, we present a numerical example based on the JRS with GSII as scheduling algorithm. We will refer to this scheme simply as JRS, since there is no name ambiguity. We assume an AWGN multi-access channel, where the rates at which simultaneous packets are sent must lie inside the capacity region given by

Equation (2.20). As shown in Theorem 5.2, JRS guarantees this. For this scenario, we will analyze the impact of decoding capability, beamwidth, and number of transmit antennas on multi-hop networks. While corresponding to a particular instance of the problem, the results illustrate how topological properties such as average node degree should be considered for proper network designs. This conclusion holds for any instance of the joint routing and scheduling problem.

We set the channel bandwidth $W = 1$ MHz, transmission power $P_0 = 100$ mW, receiver range $R = 30$ meters, path loss exponent $\gamma = 3$, and channel noise $\eta = -10$ dB. We generated 4 random flows such that all links of a 30-node random network shown in Figure 6.12 were scheduled by JRS. The average node degree of the network
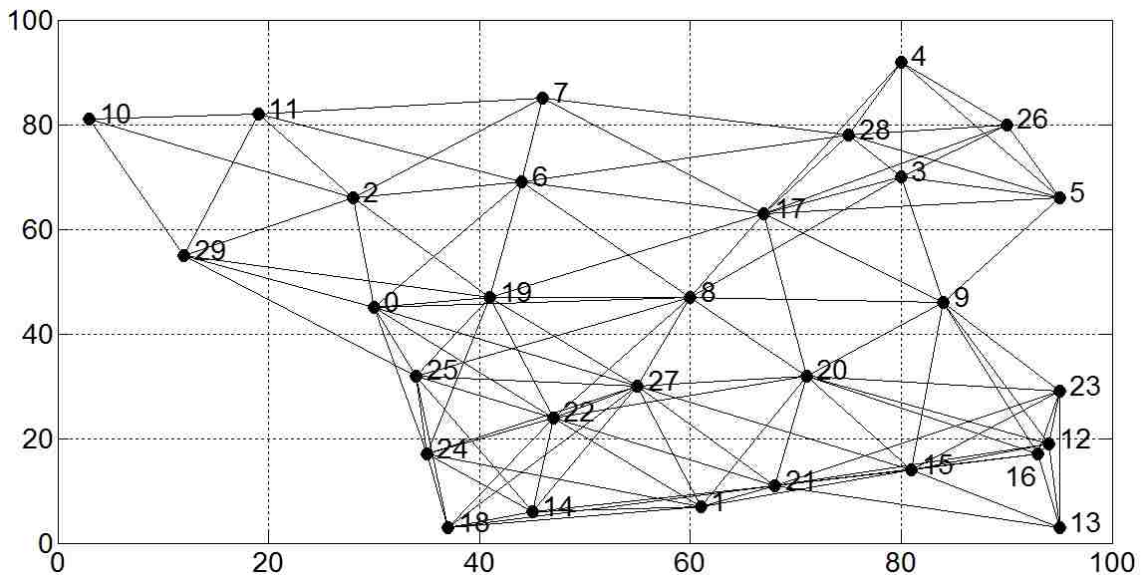

Figure 6.12: A 30-node random network. There is a link (solid line) between two nodes if the distance between them is less than or equal to $R = 30$ meters.

topology was 7.6.

In the numerical examples, we will show the impact of different parameters on the *average node degree of the schedulable sets* found by JRS, which is denoted as

$g(M, K, \beta)$. It is defined as the number of links per node activated on average:

$$g(M, K, \beta) = \frac{1}{|V|} \sum_{i=1}^{|\Gamma_{GSII}|} \lambda_i |S_i|. \tag{6.2}$$

Note that $g(M, K, \beta)$ is a linear combination of the size of the size of schedulable sets, where the weights are given by the allocation times. Thus, it may also be considered as the time-averaged node degree of the network.

Impact of the Number of Transmit Antennas

Figures 6.13 and 6.14 show the throughput obtained with two different values of
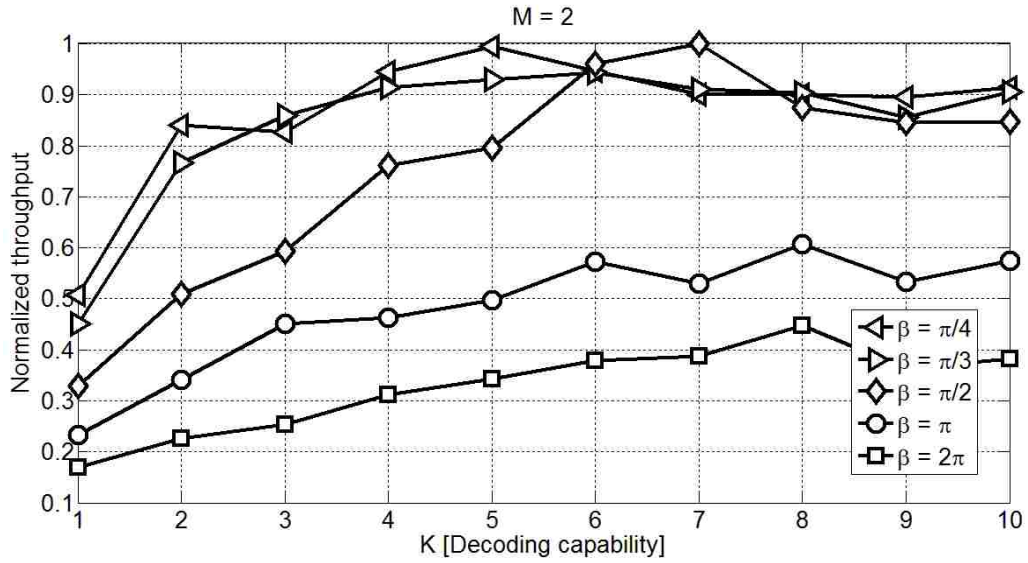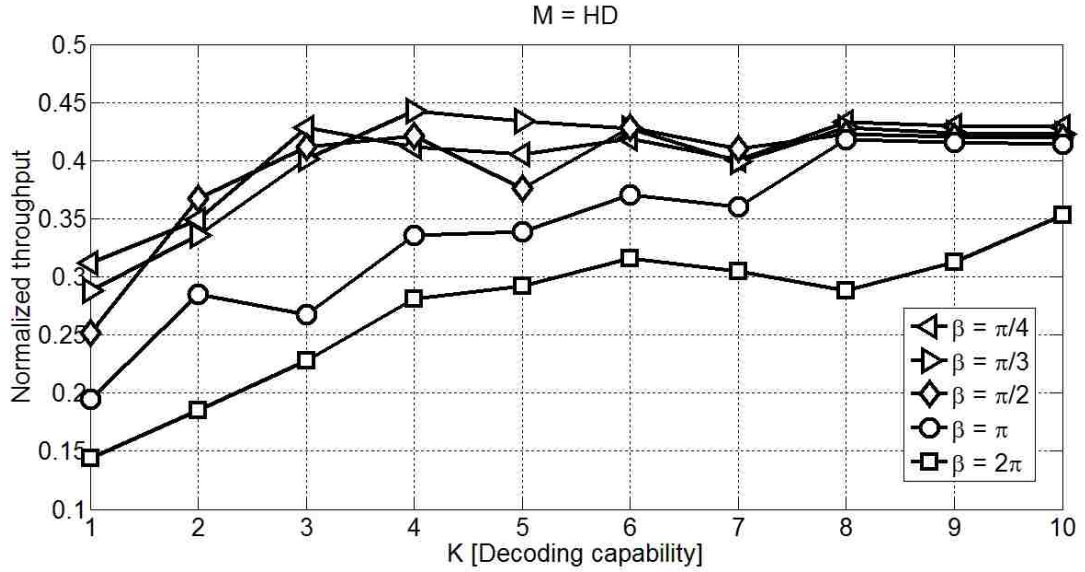

Figure 6.13: Throughput vs K, for $M = 2$.

M. For comparison purposes, the results in both figures are normalized to the maximum throughput found by JRS, which is obtained when $M = 2, K = 5, \beta = \frac{\pi}{4}$. As expected, the throughput increases with K. However, for high values of K, the throughput remains approximately constant and does not improve any further,

Figure 6.14: Throughput vs K, for $M = HD$.

independently of the beamwidth. The number of links simultaneously scheduled at any time is limited by the number of transmit antennas. This constitutes a *transmission-oriented bottleneck*; as K increases, transmitting nodes cannot generate enough transmissions to exploit the decoding capability. This fact is illustrated in Figures 6.15 and 6.16, where the average node degrees for $M = 2$ and $M = HD$ approach 1.5 and 0.53 as K increases. The size of schedulable sets cannot get larger, unless M is increased.

Impact of Beamwidth

Referring back to Figures 6.13 and 6.14, the best performances are obtained with narrower beamwidths, because of better spatial reuse. Note that for both $H = 2$ and $H = HD$, and for high values of K, the results obtained with $\beta = \frac{\pi}{4}$, $\beta = \frac{\pi}{3}$, and $\beta = \frac{\pi}{2}$ converge to the same throughput. The disadvantage of having wider beamwidth antennas may be compensated by increasing the decoding capability. However, we
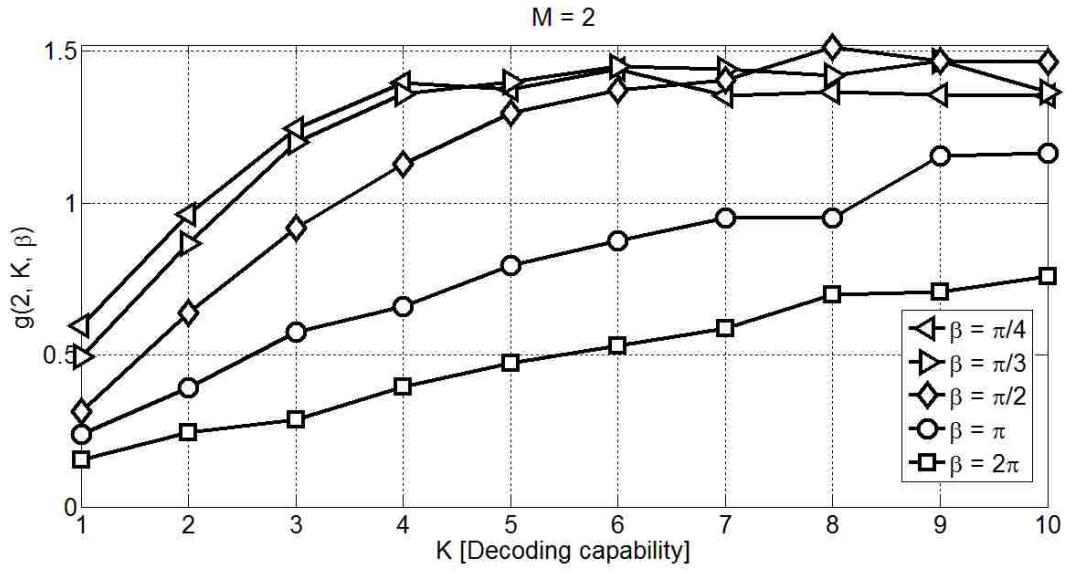
Figure 6.15: Average node degree vs K, for $M = 2$.

should also highlight the impact of omnidirectional transmissions. Consider the results of Figures 6.14 and 6.16 for $\beta = 2\pi$. For $K \geq 9$, even though the average node
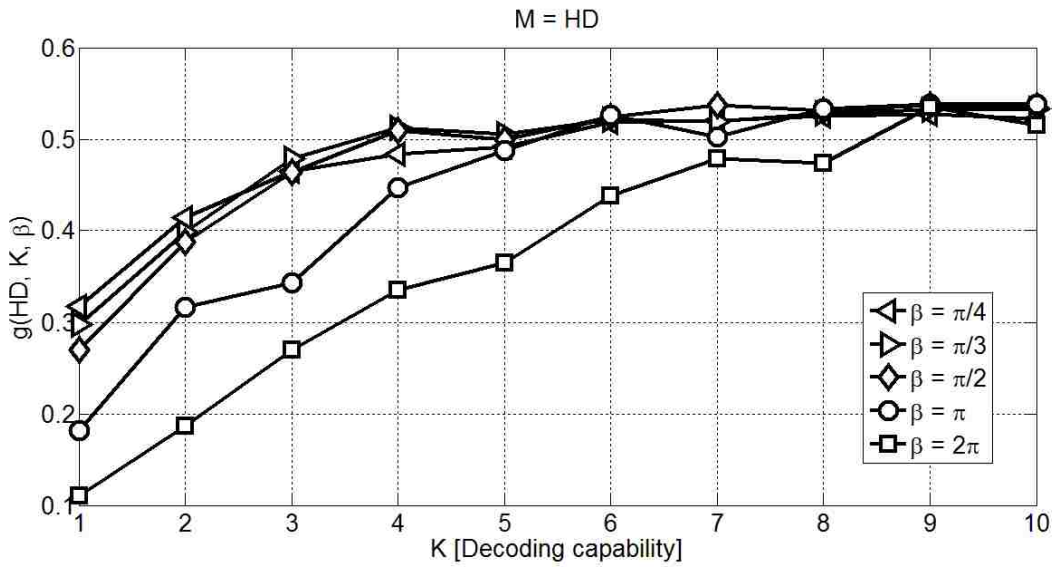

Figure 6.16: Average node degree vs K, for $M = HD$.

95

degree is about the same for all β, the throughput with omnidirectional antennas is notoriously inferior. A reason of this poor performance is the cumulative noise experienced at any receiver node; all transmissions not directed to a given receiver represent additional noise to that receiver. Figures 6.17 and 6.18 compare the
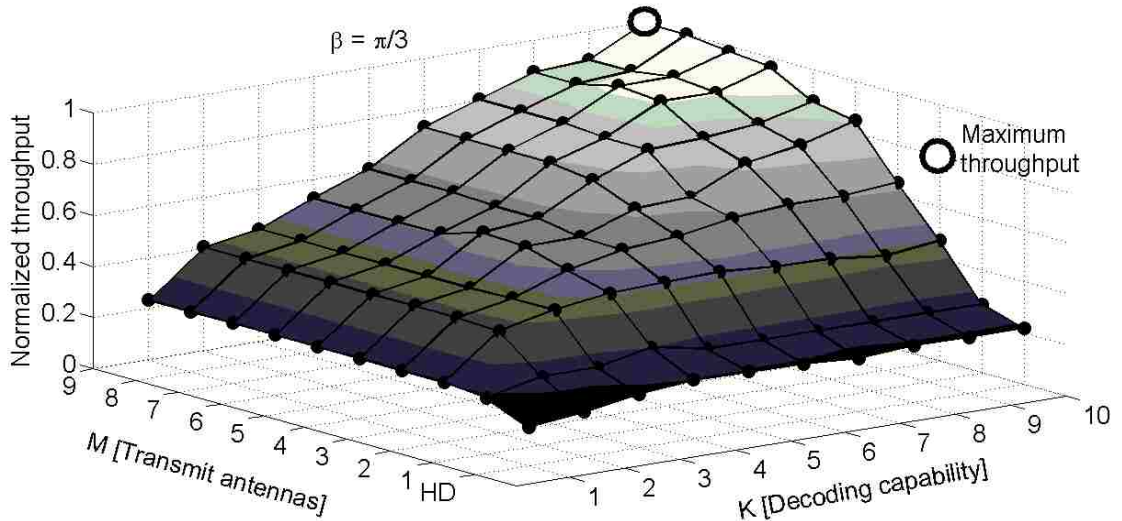

Figure 6.17: Throughput vs (K, M), for $\beta = \frac{\pi}{3}$.

performance of networks with $\beta = \frac{\pi}{3}$ and $\beta = 2\pi$. The results are normalized to the maximum throughput, obtained with $M = 9, K = 10, \beta = \frac{\pi}{3}$. An interesting observation is that, with $\beta = \frac{\pi}{3}$, the throughput clearly increases with both K and M. On the other hand, with $\beta = 2\pi$, increments in M only do not lead to significant improvement. The better spatial reuse when $\beta = \frac{\pi}{3}$ leads to larger schedulable sets than those obtained with $\beta = 2\pi$. Consequently, larger average node degrees are obtained with the former, as shown in Figure 6.19. For $K < 6$ and $M > 1$, $g(M, K, \frac{\pi}{3})$ is more than 3 times $g(M, K, 2\pi)$.
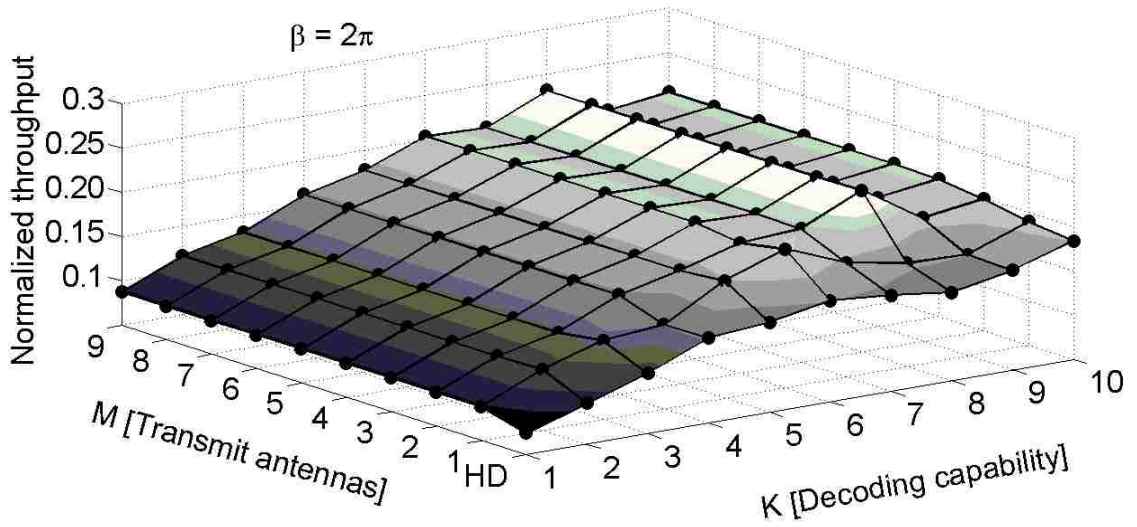
Figure 6.18: Throughput vs (K, M), for $\beta = 2\pi$.

Impact of Decoding Capability

Increasing K clearly improves throughput. However, independently of β and for a fixed value of K, increments on M may not result on better performances because of
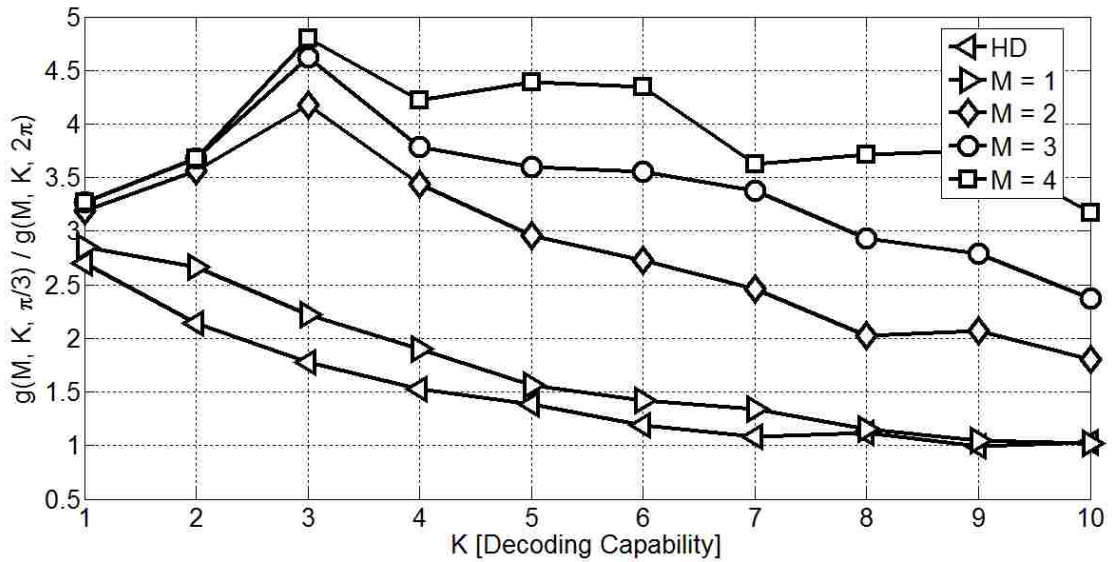

Figure 6.19: $g\left(M, K, \frac{\pi}{3}\right) \div g\left(M, K, 2\pi\right)$.

a *receiver-oriented bottleneck*; i.e., receiver nodes cannot decode more than K simultaneous transmissions, even though transmitting nodes may increase the number of transmissions. For a typical decoding capability, e.g., $K = 4$ [15], Figure 6.20 shows the throughput as a function of β and M, normalized to the throughput obtained
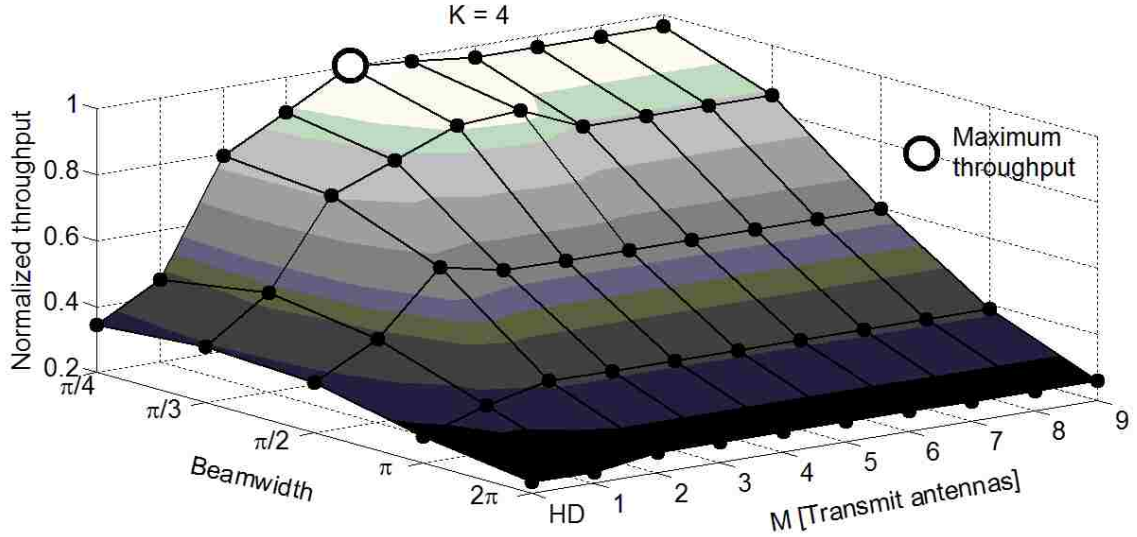

Figure 6.20: Throughput vs (M, β), for $K = 4$.

with $M = 5, K = 4, \beta = \frac{\pi}{4}$. For any value of β and small values of M, say $M \leq 4$, the throughput increases almost monotonically. On the other hand, incrementing M beyond 5 does not affect the performance. To quantify the throughput gain produced by a unitary increment on the number of transmit antennas, define throughput improvement (TI) as:

$$TI(M2, M1) = \frac{F_{RTSCH-LP}(M2) - F_{RTSCH-LP}(M1)}{F_{RTSCH-LP}(M1)},$$

where $F_{RTSCH-LP}(M)$ is the throughput obtained with M transmit antennas. Figure 6.21 shows that, for any beamwidth, incrementing the number of transmit antennas from HD to 1 implies a throughput improvement of at least 20%. However, an increment on M has more impact when combined with narrower beamwidths; for example,
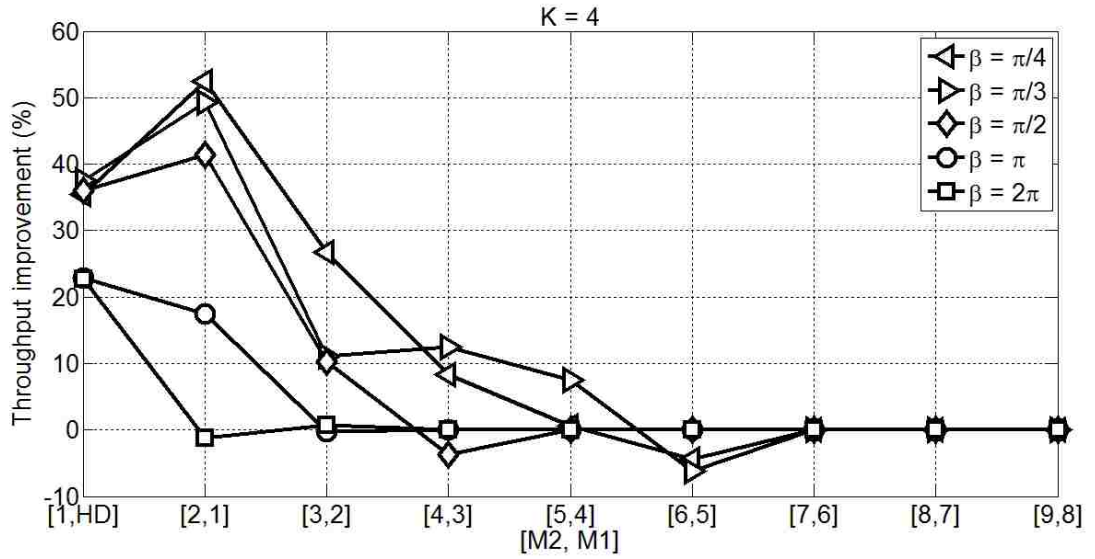
Figure 6.21: Throughput improvement as a function of unitary increment on M, for $K = 4$.

increasing M from 1 to 2 has no impact when $\beta = 2\pi$. On the other hand, an improvement of at least 40% is obtained when $\beta \geq \frac{\pi}{2}$. A receiver-oriented limitation is clearly noted as M increases beyond 5, where no improvement is obtained.

6.3 Summary

In this chapter, we have presented numerical examples of the throughput optimization problem in wireless networks. We have applied the proposed JRS scheme to solve the problem under both MPR protocol model and multi-access channel model. Moreover, the flexibility of the scheme permits to evaluate the throughput performance of networks with directional and omnidirectional antennas, half and full duplex operational modes, and single and multiple transmit antennas per node.

The results showed that to fully exploit MPR capability, nodes may need to

be endowed with multiple transmit antennas. For both the MPR protocol model and multi-access channel, we found that the three parameters, decoding capability, number of transmit antennas and beamwidth, play important and complementary roles on the throughput improvement. The numerical examples clearly illustrated that, if any of them is not carefully selected, the network may experience either transmitter or receiver oriented bottleneck.

As an open research issue, we think that the design of distributed algorithms based on interior point methods for convex optimization may be an interesting research direction; since the throughput optimization problem can be characterized as a convex problem (as seen in Chapter 4), a natural approach to solve it is by applying convex optimization techniques.

Chapter 7

Conclusion

In this dissertation, we have presented a novel model for throughput optimization problem in multi-hop wireless networks with MPR-capability. While this may be considered as the main contribution, the present work has several innovative features not included in previous works, which are listed below.

1. We have presented a generalized model for the throughput optimization problem in wireless networks. To the best of our knowledge, this is the first work that simultaneously considers multiple transmit interfaces, generalized antenna model and multi-packet reception [46].

2. To solve the proposed model, we have presented a polynomial time heuristic based on a combination of greedy and linear programming paradigms [46].

3. We have extended the proposed scheme presented in [46] to an approximation scheme, which guarantees that, for certain type of networks, the schedule period of the scheduling algorithm is at most two times the schedule period of the optimal scheduler [47].

4. We have characterized the throughput optimization problem in multi-hop wireless as a convex optimization. The advantages of addressing the problem as a convex optimization include the application of well-known techniques and theorems for this kind of problem [46, 47].

5. The main theoretical result obtained in this work has been given by *Theorem 4.2.*, which demonstrates that any solution of the scheduling subproblem can be built with $|E| + 1$ or fewer schedulable sets. This result is general, valid for any wireless network (e.g., single or multi-hop networks, with single or multi-packet reception, with directional or omni-directional antennas). The result contradicts the conjecture that says that a solution is generally composed of an exponential number of schedulable sets. *Theorem 4.2* may have impact in future scheduling schemes, since it encourages the design of new polynomial time algorithms to approximate to optimal solutions, instead of devising complex algorithms that search for an exponential number of schedulable sets [48].

6. Using information theoretic results, we have also incorporated the multi-access channel into the model. To the best of our knowledge, the proposed model is the first joint routing and scheduling formulation that considers the capacity region of the multi-access channel in a network. It accurately accounts for the capacity of the links used by simultaneous transmissions to a single receiver [49].

7. We have devised a greedy scheduling algorithm that exploits the multi-access channel in a network. We have demonstrated that the algorithm guarantees the operation of links at max-capacity, where the sum of the capacity of the links is maximized and the multi-access channel is fully exploited [49].

8. We have studied the impact of directional antennas in MPR networks. There is no previous work considering the use of directional antennas with multi-packet reception. A reason may be the fact that MPR capability, intuitively,

mitigates the inefficient spatial reuse of omni-directional antennas. However, as numerical results showed, the benefit of combining these two technologies deserves further investigation and should not be neglected [46, 47, 48, 49].

As future work, an interesting research direction is the incorporation of MIMO and power control in our model. Additionally, our approach to characterize the problem as a convex optimization is suitable for optical networks. Thus, beyond wireless networks, we believe that the results obtained in this work can be easily extended to that type of networks. Finally, the devise of distributed protocols that exploit multi-packet reception capability is an open research issue that should be studied.

References

[1] C. Siva Ram Murthy and B. S. Manoj. *Ad Hoc Wireless Networks: Architectures and Protocols.* Prentice Hall, 2004.

[2] Ian F. Akyildiz, Xudong Wang, and Weilin Wang. Wireless mesh networks: a survey. *Comput. Netw. ISDN Syst.*, 47(4):445–487, 2005.

[3] P. Gupta and P.R. Kumar. The capacity of wireless networks. *Information Theory, IEEE Transactions on*, 46(2):388–404, Mar 2000.

[4] Junning Liu, D. Goeckel, and D. Towsley. Bounds on the gain of network coding and broadcasting in wireless networks. *INFOCOM 2007. 26th IEEE International Conference on Computer Communications. IEEE*, pages 724–732, May 2007.

[5] S. Yi, Y. Pei, and S. Kalyanaraman. On the capacity improvement of ad hoc wireless networks using directional antennas. In *MobiHoc '03: Proceedings of the 4th ACM international symposium on Mobile ad hoc networking & computing*, pages 108–116, New York, 2003.

[6] J. J. Garcia-Luna-Aceves, H. Sadjadpour, and Z. Wang. Challenges: towards truly scalable ad hoc networks. In *MobiCom '07: Proceedings of the 13th annual ACM international conference on Mobile computing and networking*, pages 207–214, 2007.

[7] Ieee std. 802.11, wireless lan medium access control (mac) and physical layer (phy) specifications. 1999.

[8] Richard Draves, Jitendra Padhye, and Brian Zill. Routing in multi-radio, multi-hop wireless mesh networks. In *MobiCom '04: Proceedings of the 10th annual international conference on Mobile computing and networking*, pages 114–128. ACM Press, 2004.

References

[9] Thomas M. Cover and Joy A. Thomas. *Elements of Information Theory.* October 2001.

[10] Kamal Jain, Jitendra Padhye, Venkata N. Padmanabhan, and Lili Qiu. Impact of interference on multi-hop wireless network performance. In *MobiCom '03: Proceedings of the 9th annual international conference on Mobile computing and networking*, pages 66–80, New York, NY, USA, 2003. ACM.

[11] C. A. Balanis. *Antenna theory, Analysis and Design.* John Wiley, 2005.

[12] Hongning Dai, Kam-Wing Ng, and Min-You Wu. An overview of mac protocols with directional antennas in wireless ad hoc networks. In *ICCGI '06: Proceedings of the International Multi-Conference on Computing in the Global Information Technology*, page 84, Washington, DC, USA, 2006. IEEE Computer Society.

[13] S. Karande, Z. Wang, H. Sadjadpour, and J.J. Garcia-Luna-Aceves. Capacity of wireless ad-hoc networks under multipacket transmission and reception. In *Signals, Systems and Computers, 2008 42nd Asilomar Conference on*, pages 2115–2119, Oct. 2008.

[14] S. Ghez, S. Verdu, and S.C. Schwartz. Stability properties of slotted aloha with multipacket reception capability. *Automatic Control, IEEE Transactions on*, 33(7):640–649, Jul 1988.

[15] G.D. Celik, G. Zussman, W.F. Khan, and E. Modiano. Mac for networks with multipacket reception capability and spatially distributed nodes. *INFOCOM 2008. The 27th Conference on Computer Communications. IEEE*, pages 1436–1444, April 2008.

[16] X. Wang and J.J. Garcia-Luna-Aceves. Embracing interference in ad hoc networks using joint routing and scheduling with multiple packet reception. *INFOCOM 2008. The 27th Conference on Computer Communications. IEEE*, pages 843–851, April 2008.

[17] Q. Zhao and L. Tong. A multiqueue service room mac protocol for wireless networks with multipacket reception. *Networking, IEEE/ACM Transactions on*, 11(1):125–137, Feb 2003.

[18] Q. Zhao and L. Tong. A dynamic queue protocol for multiaccess wireless networks with multipacket reception. *IEEE Transactions on Wireless Communications*, 3:2221–2231, 2001.

[19] Hongqiang Zhai and Yuguang Fang. Impact of routing metrics on path capacity in multirate and multihop wireless ad hoc networks. *Network Protocols, IEEE International Conference on*, 0:86–95, 2006.

References

[20] J. J. Garcia-Luna-Aceves, H. Sadjadpour, and Z. Wang. Extending the capacity of ad hoc networks beyond network coding. In *IWCMC '07: Proceedings of the 2007 international conference on Wireless communications and mobile computing*, pages 91–96, 2007.

[21] Z. Wang, H. Sadjadpour, and J. J. Garcia-Luna-Aceves. The capacity and energy efficiency of wireless ad hoc networks with multi-packet reception. In *MobiHoc '08: Proceedings of the 9th ACM international symposium on Mobile ad hoc networking and computing*, pages 179–188, 2008.

[22] S. Boyd and L. Vandenberghe. *Convex Optimization*. Cambridge University Press, 2004.

[23] G. Brar, D. Blough, and P. Santi. Computationally efficient scheduling with the physical interference model for throughput improvement in wireless mesh networks. In *MobiCom '06: Proceedings of the 12th annual international conference on Mobile computing and networking*, pages 2–13, 2006.

[24] T. Moscibroda and R. Wattenhofer. The complexity of connectivity in wireless networks. *INFOCOM 2006. 25th IEEE International Conference on Computer Communications. Proceedings*, pages 1–13, April 2006.

[25] Jangeun Jun and M.L. Sichitiu. The nominal capacity of wireless mesh networks. volume 10, pages 8–14, Oct 2003.

[26] Naouel Ben Salem and Jean-Pierre Hubaux. A Fair Scheduling for Wireless Mesh Networks. In *The First IEEE Workshop on Wireless Mesh Networks (WiMesh)*, 2005.

[27] T. Salonidis and L. Tassiulas. Distributed on-line schedule adaptation for balanced slot allocation in wireless ad hoc networks. *Quality of Service, 2004. IWQOS 2004. Twelfth IEEE International Workshop on*, pages 20–29, June 2004.

[28] P. Djukic and S. Valaee. Distributed link scheduling for tdma mesh networks. *Communications, 2007. ICC '07. IEEE International Conference on*, pages 3823–3828, June 2007.

[29] P. Bjorklund, P. Varbrand, and Di Yuan. Resource optimization of spatial tdma in ad hoc radio networks: a column generation approach. *INFOCOM 2003. Twenty-Second Annual Joint Conference of the IEEE Computer and Communications Societies. IEEE*, 2:818–824 vol.2, March-3 April 2003.

References

[30] M. Kodialam and T. Nandagopal. Characterizing achievable rates in multihop wireless mesh networks with orthogonal channels. *Networking, IEEE/ACM Transactions on*, 13(4):868–880, Aug. 2005.

[31] J. Zhang, H. Wu, and B. Li Q. Zhang. Joint routing and scheduling in multi-radio multi-channel multi-hop wireless networks. In *Broadnets 2005*, 2005.

[32] Z. Wu, S. Ganu, and D. Raychaudhuri. Irma: integrated routing and mac scheduling in multihop wireless mesh networks. In *WiMesh 2006*, 2006.

[33] Murali Kodialam and Thyaga Nandagopal. Characterizing the capacity region in multi-radio multi-channel wireless mesh networks. In *MobiCom '05: Proceedings of the 11th annual international conference on Mobile computing and networking*, pages 73–87, New York, NY, USA, 2005. ACM Press.

[34] Mansoor Alicherry, Randeep Bhatia, and Li (Erran) Li. Joint channel assignment and routing for throughput optimization in multi-radio wireless mesh networks. In *MobiCom '05: Proceedings of the 11th annual international conference on Mobile computing and networking*, pages 58–72, New York, NY, USA, 2005. ACM.

[35] Xiaojun Lin and S. Rasool. A distributed joint channel-assignment, scheduling and routing algorithm for multi-channel ad-hoc wireless networks. *INFOCOM 2007. 26th IEEE International Conference on Computer Communications. IEEE*, pages 1118–1126, May 2007.

[36] Xin Wang and J. J. Garcia-Luna-Aceves. Distributed joint channel assignment, routing and scheduling for wireless mesh networks. *Comput. Commun.*, 31(7):1436–1446, 2008.

[37] A. Spyropoulos and C.S. Raghavendra. Energy efficient communications in ad hoc networks using directional antennas. *INFOCOM 2002. Twenty-First Annual Joint Conference of the IEEE Computer and Communications Societies. Proceedings. IEEE*, 1:220–228 vol.1, 2002.

[38] J.B. Cain, T. Billhartz, L. Foore, E. Althouse, and J. Schlorff. A link scheduling and ad hoc networking approach using directional antennas. *Military Communications Conference, 2003. MILCOM 2003. IEEE*, 1:643–648 Vol.1, Oct. 2003.

[39] A. Capone, I. Filippini, and F. Martignon. Joint routing and scheduling optimization in wireless mesh networks with directional antennas. *Communications, 2008. ICC '08. IEEE International Conference on*, pages 2951–2957, May 2008.

References

[40] S. Schwartz S. Ghez, S. Verdu. Stability properties of slotted aloha with multi-packet reception capability. *Automatic Control, IEEE Transactions on*, 33(7), July 1988.

[41] G. Mergen and L. Tong. Stability and capacity of regular wireless networks. *Information Theory, IEEE Transactions on*, 51(6):1938–1953, June 2005.

[42] R.M. de Moraes, H.R. Sadjadpour, and J.J. Garcia-Luna-Aceves. Many-to-many communication: A new approach for collaboration in manets. *INFO-COM 2007. 26th IEEE International Conference on Computer Communications. IEEE*, pages 1829–1837, May 2007.

[43] Vijay V. Vazirani. *Approximation Algorithms.* Springer, March 2004.

[44] David Luenberger. *Linear and Nonlinear Programming.* Springer, 2003.

[45] M. Berkelaar. Lp-solve, a public domain milp solver, available at http://lpsolve.sourceforge.net/5.5/.

[46] J. Crichigno, M. Y. Wu, and W. Shu. Throughput optimization in wireless networks with multi-packet reception and directional antennas. *WCNC 2009. IEEE Wireless Communications and Networking Conference*, April 2009.

[47] J. Crichigno, M. Y. Wu, J. Khoury, and W. Shu. A joint routing and scheduling scheme for wireless networks with multi-packet reception and directional antennas. *IEEE International Symposium on a World of Wireless, Mobile and Multimedia Networks*, June 2009.

[48] J. Crichigno, M. Y. Wu, S. K. Jayaweera, and W. Shu. Exploiting multi-packet reception and directional antennas in multi-hop wireless networks. *Submitted to IEEE Transactions on Parallel and Distributed Systems*, 2009.

[49] J. Crichigno, M. Y. Wu, S. K. Jayaweera, and W. Shu. Exploiting the multi-access channel in multi-hop wireless networks. *Infocom 2010. IEEE Conference on Computer Communications. Submitted*, March 2010.